

学位論文

Physiological analysis of stomatal responses
as controlled by the mesophyll

(葉肉組織による気孔開閉制御に関する生理学的解析)

平成 27 年 12 月博士 (理学) 申請

東京大学大学院理学系研究科

生物科学専攻

藤田 貴志

Abstract

Stomata are the microscopic pores on the epidermes in the aerial parts of most terrestrial plants, and act as the valves that control the gas exchange between the intercellular space and the air. It has been pointed out that the stomatal movements were controlled not only by the autonomous regulation of the turgor pressure in the guard cells, but also by the mesophyll. However, the roles of the mesophyll in the stomatal responses have not been elucidated.

In chapter 2, I constructed a system to control the environment of the leaf segments or the epidermal strips of *Commelina communis* and microscopically observed stomatal responses to CO₂ (100 ppm or 700 ppm). With the buffer-containing gels instead of aqueous buffers, I could observe the stomatal responses in a reasonably physiological state for a long time. I compared the stomatal responses in the leaf segments, the epidermal strips and the epidermal strips placed on the mesophyll segments, in red light or white light. The present results clearly indicated that mesophyll was important for both stomatal opening and closure, supporting the existence of ‘mesophyll signals’, the signals which have been proposed in previous studies (e.g. Lee & Bowling, 1992, 1993, 1995; Mott *et al.*, 2008).

In chapter 3, I analyzed the characteristics of the mesophyll signals. With the inhibitor of photosynthetic electron transport, I analyzed the dependency of stomatal responses on photosynthesis. The results showed that the stomatal opening was strongly dependent on photosynthesis, whereas the stomatal closure was not. Thus, the opening signals would be different from the closure signals. To investigate whether the mesophyll signals were aqueous, the polyethylene of the cellophane spacers were inserted between the epidermal strips and the mesophyll segments. It was suggested that the mesophyll signals related to stomatal opening and closure were both aqueous. Subsequently, the molecular size of the mesophyll signals was estimated by inserting the dialysis membranes between the epidermal strips and the mesophyll segments. The molecular sizes of the mesophyll signals were estimated to be less than 500 D for the stomatal opening whereas those for the stomatal closure ranged from 100 D to 1,000 D. The metabolites in the epidermal strips were quantified to narrow down the opening signals. Malate, citrate, fumarate and cis-aconitate were listed as the candidate metabolites. In particular, citrate was the potent organic acid to induce the stomatal opening in the epidermal strips of *C.*

benghalensis.

In chapter 4, I further confirmed the presence of mesophyll signals. The dark-treated epidermal strips were placed on the mesophyll segments pretreated in the dark or in the light. I confirmed the presence of mesophyll signals inducing the stomatal opening at ambient CO₂ and inhibiting the stomatal opening at high CO₂.

In chapter 5, I developed the immunocytochemical staining method to analyze the phosphorylation level of the plasma membrane H⁺-ATPase in *C. communis*. This method enable to detect the presence of mesophyll signals with high sensitivity.

In chapter 6, I discussed the results in chapters 2–5, and explained the future prospects.

Contents

Abbreviations	1
 Chapter 1: General introduction	
1-1. What are stomata?	3
1-2. Stomatal responses to light	5
1-3. Stomatal responses to CO ₂	6
1-4. Comparison of the stomatal responses between isolated epidermes and leaves	9
1-5. Substances controlling stomatal movements in guard cells	10
1-6. Objectives	13
1-7. Figure	15
 Chapter 2: The effects of the mesophyll that control the stomatal responses to light and CO₂	
2-1. Introduction	16
2-2. Materials and Methods	17
2-3. Results	21
2-4. Discussion	24
2-5. Tables	28
2-6. Figures	31
 Chapter 3: Analysis on the characteristics of the mesophyll signals	
3-1. Introduction	43
3-2. Materials and Methods	44
3-3. Results	46
3-4. Discussion	50
3-5. Tables	55
3-6. Figures	58

Chapter 4: Re-examination for the presence of the mesophyll signals	
4-1. Introduction	65
4-2. Materials and Methods	66
4-3. Results	68
4-4. Discussion	69
4-5. Table	74
4-6. Figures	75
Chapter 5: Methodology: Detection of the phosphorylation of the plasma membrane H⁺-ATPase in <i>Commelina communis</i>	
5-1. Introduction	82
5-2. Materials and Methods	83
5-3. Results	87
5-4. Discussion	89
5-5. Figures	93
Chapter 6: General discussion	97
References	103
Acknowledgements	116

Abbreviations

ABA	abscisic acid
ABCB14	ABC transporter B family member 14
AHA	Arabidopsis plasma membrane H ⁺ -ATPase
AL	actinic light
ALMT	aluminum activated malate transporter
ATP	adenosine triphosphate
BL	blue light
CA	carbonic anhydrase
[Ca ²⁺] _{cyt}	calcium ion concentration in cytosol
CE-MS	capillary electrophoresis-mass spectrometry
chl	chlorophyll
DCMU	3-(3,4-dichlorophenyl)-1,1-dimethylurea
DK	dark
DMSO	dimethyl sulfoxide
DTT	dithiothreitol
EDTA	2,2',2'',2'''-(ethane-1,2-diyl)dinitrilo)tetraacetic acid
FW	fresh weight
GCAC1	guard cell anion channel 1
GCP	guard cell protoplast
HRP	horseradish peroxidase
HT1	high temperature 1
HXK	hexokinase
IRGA	infrared gas analyser
MATE	multidrug and toxic compound extrusion
MeS	L-methionine sulfone
MES	2-(<i>N</i> -morpholino)ethanesulfonic acid
MFC	mass flow controller
ML	measuring light
MOPS	3-morpholinopropanesulfonic acid

M.W.	molecular weight
MWCO	molecular weight cut off
NADP	nicotinamide adenine dinucleotide phosphate
OST1	open stomata 1
PBS	phosphate buffered saline
PEPC	phosphoenolpyruvate carboxylase
PFA	paraformaldehyde
PGA	phosphoglyceric acid
PIPES	1,4-piperazine diethane sulfonic acid
PMSF	phenylmethanesulfonyl fluoride
PP2C	protein phosphatase 2C
PPFD	photosynthetically active photon flux density
QUAC1	quick-activating anion channel 1
RHC1	resistant to high CO ₂ 1
RL	red light
RO	reverse osmosis
Rubisco	ribulose 1,5-bisphosphate carboxylase/oxygenase
RuBP	ribulose 1,5-bisphosphoric acid
SD	standard deviation
SDH2-2	succinate dehydrogenase 2-2
SDS	sodium dodecyl sulfate
SDS-PAGE	sodium dodecyl sulfate-polyacrylamide gel electrophoresis
SEM	standard error of mean
SP	saturation pulse
TCA	tricarboxylic acid
Tris	tris(hydroxymethyl)aminomethane
Triton X-100	<i>t</i> -octylphenoxypoly-ethoxyethanol
WL	white light
WT	wild type
YFP	yellow fluorescent protein
Φ _{II}	photochemical quantum yield of photosystem II

Chapter 1

General introduction

1-1. What are stomata?

Stomatal functions

Stomata are microscopic pores found in the aerial parts of most terrestrial plants except for liverworts. A stoma is surrounded by a pair of specialized cells, 'guard cells'. Stomata can open and close to regulate gas exchange between the plant and the atmosphere. Thus, they act as the valves controlling the entry of CO₂ for photosynthesis into the leaf and the exit of H₂O from the transpiration flow (Zeiger, 1983; Willmer & Fricker, 1996). In addition, when stomata open, leaves are cooled by heat of vaporization. The differences in the leaf temperature are utilized for the isolation of the mutant plants related to stomatal responses (e.g. Hashimoto *et al.*, 2006).

Anatomy and morphology of specialized epidermal cells

Guard cells

From the morphological viewpoint, guard cells are classified into two groups; kidney-shaped and dumb-bell-shaped guard cells. The dumb-bell-shaped guard cells are found only in monocotyledons. In kidney-shaped guard cells, the cell walls facing the stoma are thicker than the cell walls juxtaposed to neighboring cells. When water enters a pair of kidney-shaped guard cells, the guard cells swell and bend away from each other, thereby opening the stoma (Fig. 1-1a). There are no plasmodesmata between mature guard cells and neighboring epidermal cells (Wille & Lucas, 1984). Hence, before entering the guard cell, the substances delivered to the guard cells should be released to the outside the plasma membrane, called 'apoplast'.

Most plants have functional chloroplasts in guard cells (Willmer & Fricker, 1996). Unlike mesophyll cells, guard cell chloroplasts tend to accumulate starch in the dark. The stomatal aperture generally increases with the decrease of the starch content in the chloroplasts (Outlaw & Manchester, 1979). Compared with mesophyll cells, the number of chloroplasts per cell, the size of chloroplasts and the volume of the granal stacking are also small in guard cells (e.g. Willmer & Fricker, 1996). The activity of photosystem I in guard cell chloroplasts would be higher than that in mesophyll chloroplasts, because of their higher chlorophyll (chl) a/b ratio

and enhanced cyclic phosphorylation mediated by phenazine methosulfate (Lurie, 1977). The linear electron transport in guard cells has been also investigated (Hipkins *et al.*, 1983; Shimazaki & Zeiger, 1985; Cardon & Berry, 1992; Lawson *et al.*, 2002, 2003). In *Commelina communis*, analysis of the quantum yield of photosystem II (Φ_{II}) revealed that the activity of the linear photosynthetic electron transport in guard cell chloroplasts was lower than that in mesophyll chloroplasts by 20–30%, however, both chloroplasts responded to light and CO₂ in a similar manner (Lawson *et al.*, 2002, 2003). In guard cells, ¹⁴CO₂ was incorporated into 3-phosphoglyceric acid (3-PGA) and ribulose 1,5-bisphosphoric acid (RuBP) (Gotow *et al.*, 1988). Contrary to this study, it has been shown that ¹⁴CO₂ is incorporated into malate, indicating the involvement of phosphoenolpyruvate carboxylase (PEPC) and malate dehydrogenase (Willmer & Dittrich, 1974; Raschke & Dittrich, 1977). Also the activities of ribulose 1,5-bisphosphate carboxylase/oxygenase (Rubisco) and Calvin cycle enzymes per cell basis tended to be lower in the guard cells than in mesophyll cells for *Pisum sativum*, *Vicia faba*, and so on (Outlaw *et al.*, 1982; Reckmann *et al.*, 1990). In spite of the numerous studies about guard cell chloroplasts, the roles of chloroplasts in stomatal movements are still unclear and further investigations are required.

There are numerous mitochondria in guard cells and the ratio of the number of mitochondria to that of chloroplasts is higher in guard cells than in mesophyll cells (Allaway & Setterfield, 1972). It was suggested that mitochondria in guard cells were main generators of ATP for stomatal movements. For example, in epidermal strips of *V. faba* and *C. communis*, stomatal light responses, especially to blue light, were severely inhibited by the addition of KCN, an inhibitor of the respiratory electron transport (Schwartz & Zeiger, 1984).

Subsidiary cells

Subsidiary cells, adjacent to guard cells, are different in shape and size from other epidermal cells (Fig. 1-1a). Subsidiary cells do not usually contain chloroplasts, anthocyanins and crystalline substances. Subsidiary cells function as water storage tanks for guard cells. Therefore, when stomata are opening, the volume of the guard cell increases, while the volume of the subsidiary cell dramatically decreases (Franks & Farquhar, 2007).

Hydroactive and hydropassive stomatal movements

Hydroactive stomatal movements are promoted via metabolic processes in guard cells. Therefore, when the hydroactive movements occur, water and ions such as K^+ and Cl^- are transported from other epidermal cells to guard cells. On the other hand, in hydropassive stomatal movements, metabolic processes are not involved. Hydropassive movements are influenced by the changes in the turgor relations in the stomatal complexes. Hence, when the epidermal cells shrink due to drying or high salinity, hydropassive stomatal opening may occur. Abscisic acid is one of the stress hormones in response to the drying (e.g. Zeevaart & Creelman, 1988). Stomata in lycophyte and ferns do not close in response to abscisic acid (ABA), but respond to the drying only in the hydropassive manner (Brodribb & McAdam, 2011; McAdam & Brodribb, 2012).

1-2. Stomatal responses to light

Stomata exhibit at least two types of responses to light (Kuiper, 1964; Sharkey & Raschke, 1981; Zeiger, 1983). One type is termed the blue-light response, for which the action spectrum peaks at around 450 nm. Blue light is efficient in the stomatal opening (Hsiao & Allaway, 1973; Iino *et al.*, 1985). Blue light induces H^+ extrusion from the guard cells, and thereby the membrane potential of a guard cell is hyperpolarized (Assmann *et al.*, 1985; Shimazaki *et al.*, 1986; Roelfsema *et al.*, 2001). It has been well established that phototropins, the blue-light receptors, absorb blue light in guard cells and induce stomatal opening by sequentially causing the following events; activation of the plasma membrane H^+ -ATPases, hyperpolarization of the plasma membrane and activation K^+ uptake channels (Kinoshita & Shimazaki, 1999; Kinoshita *et al.*, 2001; Shimazaki *et al.*, 2007). In addition to the regulation of H^+ -ATPases, blue light inhibits S-type anion channels (Marten *et al.*, 2007). It was also shown that stomata opened in green light even when the photosynthesis was inhibited (Wang *et al.*, 2011). Because the green light used in Wang *et al.* (2011) would not be absorbed by phototropins, some light receptors other than phototropins, possibly cryptochromes, might be responsible for the stomatal opening in green light.

The second type of stomatal response is termed the red-light response. The action spectrum of which resembles that of photosynthesis (e.g. Kuiper, 1964; Lawson, 2009). The red-light response is strongly inhibited by 3-(3,4-dichlorophenyl)-1,1-dimethylurea (DCMU),

which is a potent inhibitor of photosynthesis. Also, there is a strong correlation between stomatal conductance and the photosynthetic rate in red light. Accordingly, it is widely believed that photosynthesis is involved in the red-light response (e.g. Sharkey & Raschke; 1981; Messinger *et al.*, 2006; Wang *et al.*, 2011). Red light also inhibits S-type anion channels when red light is projected on a large area of the leaf (Roelfsema *et al.*, 2002). It has been also shown that illumination of a single stomatal complex with red beam is insufficient to induce stomatal opening (Mott *et al.*, 2008). From the genetic analysis using *Arabidopsis thaliana*, Matrosova *et al.* (2015) showed that the protein kinase HIGH TEMPERATURE 1 (HT1) was a component involved in the stomatal opening in red light. The information about HT1 kinase is described in the next section.

1-3. Stomatal responses to CO₂

CO₂ is an important environmental variable that regulates stomatal responses (e.g. Willmer, 1988). In general, stomata close at high CO₂ and open at low CO₂. When stomata open, plants can take up CO₂ for photosynthesis from outside the leaf and simultaneously lose water from inside the leaf. Thus, plants have a dilemma between CO₂ uptake and water loss. With the increase in the ambient CO₂, the photosynthetic rate increases and attains the CO₂-saturated rate (e.g. Lambers *et al.*, 2008). In this situation, it is not necessary for plants to open their stomata widely, and thereby stomata closure would be induced.

By several studies, it was shown that guard cells in isolated epidermes or guard cell protoplasts (GCPs) have the ability to respond to environmental stimuli, including CO₂. It is widely believed that guard cells have the sensor to the environmental stimuli and a series of the signaling components (e.g. Fitzsimons & Weyers, 1983; Weyers *et al.*, 1983; Webb *et al.*, 1996; Brearley *et al.*, 1997; Hu *et al.*, 2010). Several CO₂ signaling components in the guard cells have been identified by the molecular genetics using *A. thaliana* (e.g. Hashimoto *et al.*, 2006; Negi *et al.*, 2008; Vahisalu *et al.*, 2008; Hu *et al.*, 2010; Xue *et al.*, 2011).

Convergence of CO₂ signaling and ABA signaling in guard cells

It has been shown that ABA promotes the stomatal closure in response to CO₂ (Raschke, 1975). The mutants firstly isolated as those defective in stomatal CO₂ signaling were the dominant ABA-insensitive protein phosphatase 2C (PP2C) mutants *abi1-1* and *abi2-1*

(Koornneef *et al.*, 1984; Roelfsema & Prins, 1995). These mutants conditionally showed CO₂ insensitivity (Webb & Hetherington, 1997; Leymarie *et al.*, 1998). The ABA signaling, mediated by the ABA receptors PYR/RCARs, partially participates in the stomatal responses to high CO₂ (Merilo *et al.*, 2013, Chater *et al.*, 2015). Since the stomatal responses to CO₂ are suppressed by the defects in the ABA signaling, it was suggested that CO₂ signaling in a guard cell converged with ABA signaling.

Roles of carbonic anhydrases (CAs) in CO₂ signaling in guard cells

Carbonic anhydrases are grouped into three families, α , β , and γ -CA (Moroney *et al.*, 2001). It has been shown that β -CAs, especially CA1 and CA4 in guard cells are important for the rapid stomatal closure at high CO₂ (Hu *et al.*, 2010). CA1 is mainly localized in chloroplasts and CA4 is localized in the plasma membrane (Fabre *et al.*, 2007; Hu *et al.*, 2010). Expression of yellow fluorescent protein (YFP) -tagged CA1 in the guard cell chloroplasts or YFP-tagged CA4 in the plasma membrane in the *calca4* double mutant is sufficient to restore the wild type (WT)-like stomatal responses to CO₂ (Hu *et al.*, 2015). Azoulay-Shemer *et al.* (2015) generated the GC-Chlase Δ N transgenic plants that were deficient in chlorophyll specifically in their guard cells by the guard-cell specific over-expression of the N-terminal truncated form of *Citrus sinensis* chlorophyllase. The stomata of GC-Chlase Δ N transgenic plants that lacks chlorophyll in guard cell chloroplasts close in response to CO₂ (Azoulay-Shemer *et al.*, 2015). Hence, it was indicated that the role of CA1 in CO₂ signaling was not related to photosynthesis in the guard cell. Neither the roles of α -CAs nor those of γ -CAs in CO₂ signaling have been determined. Expressing a mammalian carbonic anhydrase in guard cells of *calca4* double-mutants restored the stomatal responses to CO₂ (Hu *et al.*, 2010). In this study, it was suggested that the CAs provided bicarbonate and/or protons as possible second messengers involved in CO₂ signaling in the guard cells. Xue *et al.*, (2011) pointed out an important role of bicarbonate in stomatal responses, using the patch-clamp technique. The activation of anion channels in guard cells is required for stomatal closure. This event is induced by the elevation in the cytoplasmic bicarbonate concentration (Xue *et al.*, 2011). From a recent study, a MULTIDRUG AND TOXIC COMPOUND EXTRUSION (MATE) transporter-like protein, RESISTANT TO HIGH CO₂ 1 (RHC1), was suggested to be a bicarbonate sensor in guard cells (Tian *et al.*, 2015).

Roles of protein kinases in guard cells

Recently, thermal imaging becomes the common tool for isolation of the mutants defective in stomatal responses. In *A. thaliana*, the *high temperature 1*; *ht1-1* and *ht1-2* (*ht1*) mutants involved in stomatal responses to CO₂ were the mutants found by the thermal imaging (Hashimoto *et al.*, 2006). HT1 encodes a protein kinase, and the guard cells in *ht1-2* mutant constitutively showed the responses to high CO₂. Namely, the stomatal conductance of *ht1-2* mutant was low and the leaf temperature was elevated even when the ambient CO₂ was low. Interestingly, *ht1* plants showed the normal responses to blue light, fusicoccin and ABA (Hashimoto *et al.*, 2006). Thus, HT1 protein was considered to specifically inhibit the stomatal closure in response to CO₂. OPEN STOMATA 1 (OST1) protein kinase is one of the important components in stomatal CO₂ signaling (Xue *et al.*, 2011). Two models for the relationship between HT1 protein and OST1 protein were considered: (i) HT1 protein phosphorylates OST1 protein, thus deactivating OST1 (Tian *et al.*, 2015); or (ii) HT1 is epistatic to OST1 in the CO₂ signaling (Matrosova *et al.*, 2015). Further studies are required to reveal the relationship between HT1 protein and OST1 protein.

Roles of calcium

Several studies have shown the role of calcium as the secondary messenger of CO₂ signaling in guard cells (Schwartz 1985; Schwartz *et al.*, 1988; Webb *et al.*, 1996; Young *et al.*, 2006; Hubbard *et al.*, 2012). It has been reported that the frequency of [Ca²⁺]_{cyt} (calcium ion concentration in cytosol) spiking increases with the hyperpolarization of the membrane potential (Grabov & Blatt, 1998; Klüsener *et al.*, 2002; Siegel *et al.*, 2009). *growth controlled by abscisic acid 2* (*gca2*) mutant in *A. thaliana* is known as ABA-insensitive (Allen *et al.*, 2001; Young *et al.*, 2006). In WT plants, the frequency of [Ca²⁺]_{cyt} spiking decreased in response to high CO₂. In *gca2* mutant plants, however, the frequency of [Ca²⁺]_{cyt} spiking did not decrease and the stomata hardly closed. Also, in *gca2* mutant plants, the pattern of [Ca²⁺]_{cyt} spiking was altered by ABA (Allen *et al.*, 2001). Hence, GCA2 protein would function in the downstream of CO₂ and ABA signaling and repress the [Ca²⁺]_{cyt} spiking due to the depolarization in guard cells.

1-4. Comparison of the stomatal responses between isolated epidermes and leaves

Several studies have pointed out the close relationship between the photosynthetic rate and the stomatal conductance, which was observed under various conditions. Thus, it has been suggested that mesophyll should control stomatal responses. Photosynthetic metabolites have been proposed to be the signals that regulate the stomatal responses and maintain the balance between photosynthetic electron transport (ribulose 1,5-bisphosphoric acid (RuBP) regeneration) and RuBP carboxylation limitations (Wong *et al.*, 1979; Grantz & Schwartz, 1988; Messinger *et al.*, 2006). The roles of mesophyll in controlling the stomatal responses were analyzed by comparing stomatal responses between epidermal strips and leaves. Stomatal responses in epidermal strips are generally much slower than those in the leaves (Lee & Bowling, 1992; Olsen *et al.*, 2002; Mott *et al.*, 2008). It was reported that stomata in the epidermal strips hardly responded to red light (Lee & Bowling, 1992; Roelfsema *et al.*, 2002).

In several studies, the role of photosynthesis in guard cells was indicated to be minor in the stomatal responses to red light (e.g. Schwartz & Zeiger, 1984; Tominaga *et al.*, 2001). For example, the stomatal guard cells of *Paphiopedilum leeanum* leaves have no chloroplasts. However, the stomata in the intact leaves opened in response to red light (Nelson & Mayo, 1975). Furthermore, in *Chlorophytum comosum*, the stomatal opening in red light requires the mesophyll with active chloroplasts. The stomata over the chloroplast-less mesophyll do not respond to red light (Roelfsema *et al.*, 2006).

In Mott *et al.* (2008), the stomata in the epidermal strips exhibited a limited response to light and CO₂, whereas those in epidermal strips placed on a mesophyll responded to light and CO₂ in a manner similar to those in leaf segments. On the basis of these experiments, Mott *et al.* (2008) suggested that signals produced in mesophyll controlled stomatal responses. In addition, it was indicated that the mesophyll signals were common substances irrespective of the species. Their work was pioneering and highly suggestive in that they showed the importance of the mesophyll in stomatal responses in a very straightforward manner. However, in the experiment by Mott *et al.* (2008), the stomata in the epidermal strips might have widely opened in a hydropassive manner, since the stomata in the epidermal strips did not respond to environmental stimuli such as light and CO₂ but kept opening. Therefore, it remains unclear whether stomatal responses in the epidermal strips are comparable to those in leaves.

Sibbersen & Mott (2010) found that stomatal opening declined when various liquids were injected into the intercellular spaces of leaves, and suggested that mesophyll signals were gaseous. In the subsequent study, they suggested that the mesophyll signals were vapor phase ions, since stomata could respond to the voltage changes applied by an electrode placed below an epidermal strip (Mott *et al.*, 2013).

In contrast, Lee & Bowling (1993, 1995) showed that stomata responded to light when epidermal strips were floated on the solution that had been illuminated with mesophyll cells or chloroplasts. When the epidermal strips were floated on the same buffer without mesophyll cells or chloroplasts, the stomata did not open in the light (Lee & Bowling, 1992, 1995). Stomatal opening was also observed when the epidermal strips were floated on the supernatant of the solution that had been illuminated with mesophyll cells (Lee & Bowling, 1992). The authors also observed that the guard cell protoplasts swelled when suspended in the supernatant (Lee & Bowling, 1993). Therefore, it was suggested that the unknown soluble signals from mesophyll, named 'stomatin', controlled stomatal responses (Lee & Bowling, 1992). These studies indicated that mesophyll signals were aqueous. 'Stomatin' is also called 'mesophyll signals' (Mott *et al.*, 2008). Chloroplastic ATP, zeaxanthin, NADPH and RuBP have been proposed to be the possible candidates of mesophyll signals (Wong *et al.*, 1979; Farquhar & Wong, 1984; Lee & Bowling, 1992; Zeiger & Zhu, 1998; Tominaga *et al.*, 2001; Buckley *et al.*, 2003). Recently, Busch (2014) suggested that the redox state of the photosynthetic electron transport chain should be reflected to stomatal responses. However, the mesophyll signals have not been identified yet.

1-5. Substances controlling stomatal movements in guard cells

Possible major osmolytes in guard cells

Although stomatal responses are controlled by various environmental stimuli, the stomatal movements are brought about by changes in osmotic potential, due to the accumulation of solutes in or the release of solutes from the guard cell, and the subsequent water movement.

Starch in the guard cells degrades in the light period and accumulates in the dark period and there was a negative correlation between the stomatal aperture and the starch concentration in guard cell chloroplasts (Tallman & Zeiger, 1988). Hence, it was proposed that the sugars generated by the degradation of starch at dawn was the major osmolytes for stomatal opening.

It was also suggested that several organic acids, such as malate, derived from starch should promote stomatal opening (Outlaw & Lowry, 1977; Schnabl, 1980, 1981). In *V. faba*, stomatal opening in the light was prevented by the inhibition of malate synthesis in guard cells with an inhibitor of PEPC (Asai *et al.*, 2000). This study strongly supported that the malate, produced in guard cells, was an important osmoticum in stomatal opening. After the discovery of the strong correlation between the stomatal aperture and the accumulation of K⁺ with Cl⁻ and/or malate in the guard cells, the sugars derived from starch were not considered to be the major osmoticums in the guard cells (e.g. Outlaw & Lowry, 1977; Shimada *et al.*, 1979; Asai *et al.*, 2000). However, since the cumulated concentration of K⁺ and malate was not sufficient for the maintenance of the osmotic potential for stomatal opening, the sugars derived from the starch in the guard cells was focused again as the osmoticums (MacRobbie & Lettau, 1980a, b; Talbott & Zeiger, 1993). The decrease in the K⁺ concentration in guard cells starts around midday, accompanied by the increase in the sucrose concentration. This phenomenon raised the hypothesis that K⁺ was a major osmolyte in the morning while sucrose was more important from midday (Amodeo *et al.*, 1996; Talbott & Zeiger, 1998).

Contrary to these studies, it has been also reported that the stomatal aperture hardly correlated with the sucrose concentration in the epidermal strips (Pearson, 1973). Several studies suggested that sucrose, released from mesophyll and accumulated in the guard cells, controlled the stomatal responses (Lu *et al.*, 1995, 1997; Outlaw & De Vlieghere-He, 2001; Kang *et al.*, 2007; Kelly *et al.*, 2013). The major osmolytes in guard cells would be changed dependent on the circadian clock or by the several environmental stimuli.

Sucrose derived from mesophyll

Several sucrose and hexose transporters have been identified in the guard cells (Stadler *et al.*, 2003; Weise *et al.*, 2008; Bates *et al.*, 2012). It has been shown that sucrose released from the mesophyll is accumulated in the guard cell apoplast and transported into guard cells (Lu *et al.*, 1995, 1997; Outlaw & De Vlieghere-He, 2001). It was suggested that sugars accumulated in the guard cell apoplast 'osmotically' close stomata (Ewert *et al.*, 2000; Outlaw & De Vlieghere-He, 2001; Kang *et al.*, 2007).

Besides this hypothesis, it was also proposed that the sugars released from mesophyll evoked the signaling for the stomatal closure. Hexokinase (HXK) is known as an enzyme

catalyzing the phosphorylation of hexose (Granot *et al.*, 2013). It is well accepted that HXK works as a glucose sensor, coordinating the glucose concentration and the photosynthetic rate (Moore *et al.*, 2003; Rolland *et al.*, 2006). In *Solanum lycopersicum* and *A. thaliana*, stomatal opening was repressed by the overexpression of HXK in the whole plants or specifically in guard cells (Kelly *et al.*, 2012, 2013). It was proposed that sucrose transported from mesophyll to guard cells was cleaved into glucose and fructose. Then, HXK in the guard cell sensed the glucose and induced stomatal closure (Kelly *et al.*, 2013). It has also been shown that HXK evokes the ABA signaling in the guard cells and thereby induces the stomatal closure (Kelly *et al.*, 2013).

Malate derived from mesophyll

Malate would act as a regulator of stomatal movements in response to external CO₂ concentration (Hedrich & Marten, 1993; Hedrich *et al.*, 1994). Malate would also coordinate stomatal movements with mesophyll photosynthesis (Roelfsema *et al.*, 2002; Lee *et al.*, 2008; Fernie & Martinoia, 2009; Araújo *et al.*, 2011, 2013). In *S. lycopersicum*, the role of malate derived from mesophyll in stomatal movements was analyzed with the antisense transgenic plants with reduced expression of *SUCCINATE DEHYDROGENASE2-2 (SDH2-2)* gene which encoded the iron sulfur subunit of the succinate dehydrogenase protein complex (Araújo *et al.*, 2011). Succinate dehydrogenase catalyzes the oxidation of succinate to fumarate in the tricarboxylic acid (TCA) cycle, and therefore the concentrations of TCA metabolites including malate and fumarate were reduced in the antisense plants. The antisense plants exhibited the enhanced photosynthetic rate and stomatal conductance. When the succinate dehydrogenase was repressed in a guard cell-specific manner, however, the photosynthetic rate and stomatal conductance were unchanged. These results suggested that malate produced in the TCA cycle in the mesophyll was important in the stomatal closure.

Malate-sensitive anion channel GUARD CELL ANION CHANNEL 1 (GCAC1) works as an anion efflux channel and regulates the malate concentration in guard cell apoplast (Hedrich & Marten, 1993). GCAC1 is also named as QUICK-ACTIVATING ANION CHANNEL 1 (QUAC1) or *Arabidopsis thaliana* ALUMINUM-ACTIVATED MALATE TRANSPORTER 12 (AtALMT12) (Meyer *et al.*, 2010). It has been shown that the increase in the ambient CO₂ concentration activates the anion-efflux channel in a voltage dependent

manner and the apoplastic malate promotes stomatal closure (Hedrich & Marten, 1993; Hedrich *et al.*, 1994).

In contrast, it has been also shown that malate induces the stomatal opening. There are malate-influx transporters in guard cells, such as *Arabidopsis thaliana* ABC TRANSPORTER B FAMILY MEMBER 14 (AtABCB14) (Lee *et al.*, 2008). AtABCB14 imports malate from apoplast and induces stomatal opening with the increase in the osmotic pressure in the guard cell (Lee *et al.*, 2008). In this study, malate in the guard cell would act as an osmoticum and directly contribute to stomatal opening. Malate in guard cell cytosol also plays an important role in the distribution of chloride ion (De Angeli *et al.*, 2013). AtALMT9 functions as a vacuolar chloride channel and is activated by the increase in the malate concentration in the guard cell cytosol. Stomatal conductance was repressed by the knockout of AtALMT9 (De Angeli *et al.*, 2013). These results suggested that malate in the guard cell cytosol mediated the chloride accumulation in the vacuole via At ALMT9 and thereby promoted the stomatal opening.

1-6. Objectives

In this study, based on the preceding study by Mott *et al.* (2008), I developed a novel method to microscopically observe stomatal responses under physiologically more natural conditions. By placing epidermal strips on buffer-containing gels, rather than on a solution, I prevented the epidermal strips from being subject to extreme desiccation or hydration for up to 8 h. With this novel method, I aimed at clarifying whether the mesophyll plays an important role in stomatal responses to CO₂ by comparing the stomatal responses of the leaf segments, epidermal strips and epidermal strips placed on mesophyll segments. I used red light, as well as white light containing a blue light component. I also investigated how photosynthesis regulates stomatal responses, using the inhibitor of photosynthetic electron transport.

Whether the mesophyll signals move to the epidermis via aqueous phase in the apoplast was further examined by inserting polyethylene or cellophane films having the square holes between the epidermal strips and the mesophyll segments. Subsequently, the molecular size of mesophyll signals was estimated by inserting dialysis membranes instead of the films. In order to narrow down the candidates of mesophyll signals, the metabolites in epidermal strips were quantified by capillary electrophoresis-mass spectrometry (CE-MS). In this quantification,

several organic acids were detected and considered to be the possible mesophyll signals. Thus, I analyzed the stomatal responses to these organic acids.

To ensure the presence of mesophyll signals, I modified the method of Mott *et al.* (2008) as described above. I noticed, however, that the method might be insufficient to confirm the presence of mesophyll signals, and therefore further developed a novel method to confirm the presence of mesophyll signals. I examined whether the mesophyll, treated in advance with various environmental stimuli, could influence stomatal responses.

Stomatal responses in the epidermal strips are generally dull. When the condition changes, the stomatal aperture changes with half time in the order of hours. Moreover, stomatal aperture varies greatly from stoma to stoma even in the same epidermal strip. For the sensitive detection of mesophyll signals, I modified the method of Hayashi *et al.* (2011) for detecting phosphorylation of plasma membrane H⁺-ATPase to make it suitable for *C. communis*.

1-7. Figure

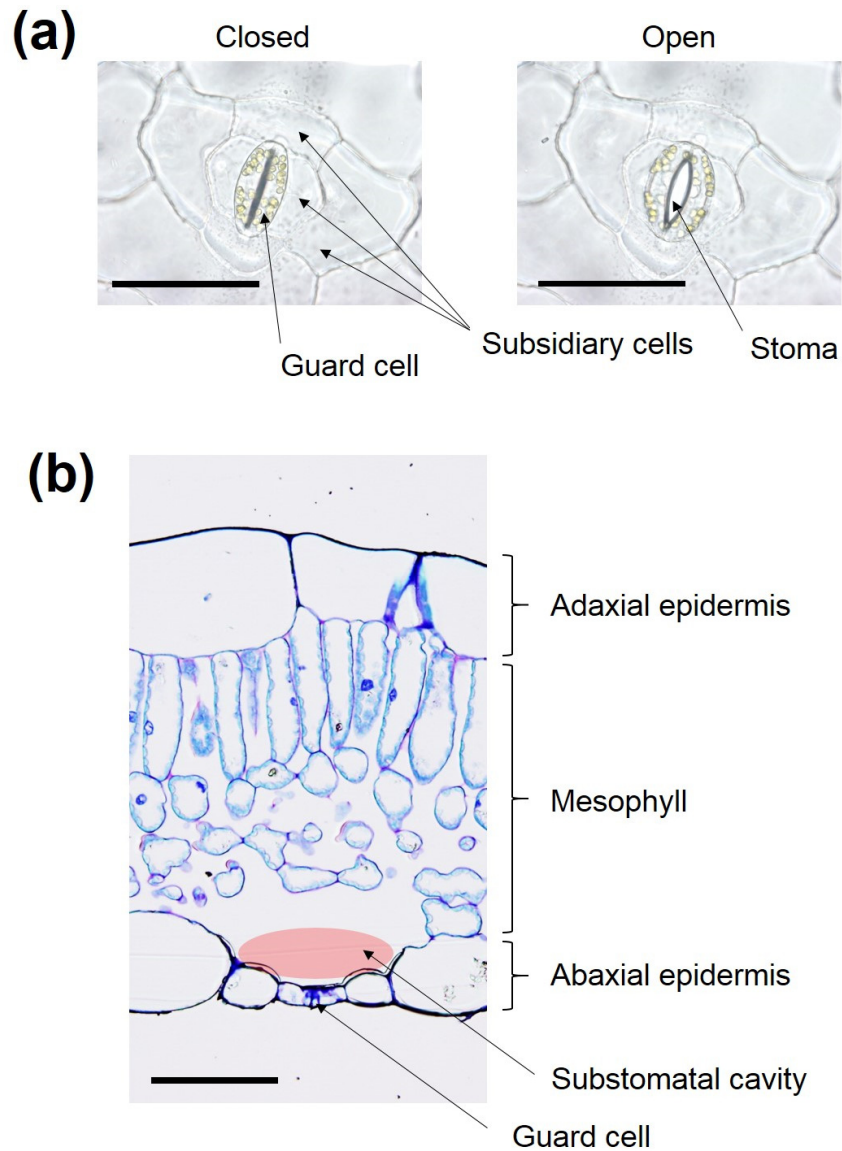


Fig. 1-1. Closed and open stomata (a), and a cross section of a leaf (b) in *C. communis*. A pair of guard cells are surrounded by six subsidiary cells (a, Left). A single stoma is surrounded by a pair of guard cells (a, Right). Substomatal cavity is the intracellular space at the vicinity of a stoma and shown as the red elliptical shape (b). Bars = 100 μm .

Chapter 2

The effects of the mesophyll that control the stomatal responses to light and CO₂

2-1. Introduction

Many studies used epidermal strips and isolated epidermes to evaluate stomatal responses to light and/or CO₂. However, some studies indicated that stomata in epidermal strips responded to light and/or CO₂ much less than those in intact leaves (Lee & Bowling, 1992, 1995; Mott *et al.*, 2008). Moreover, several studies indicated that the role of photosynthesis in guard cells in controlling stomatal responses to red light was minor (e.g. Schwartz & Zeiger, 1984; Tominaga *et al.*, 2001). For example, the guard cells of *Paphiopedilum leeanum* leaves have no chloroplasts; however, the stomata in the intact leaves opened in response to red light (Nelson & Mayo, 1975). Furthermore, in *Chlorophytum comosum*, stomatal opening in red light requires the mesophyll with the active chloroplasts. The stomata over the chloroplast-less mesophyll do not respond to red light (Roelfsema *et al.*, 2006). In Mott *et al.* (2008), the stomata in epidermal strips exhibited a limited response to light or CO₂, whereas those in epidermal strips placed on a mesophyll layer responded to light and CO₂ in a manner similar to those in leaf segments. On the basis of these experiments, Mott *et al.* (2008) suggested that signals produced in mesophyll controlled stomatal response. Their work was pioneering and highly suggestive in the point that they clearly showed the importance of the mesophyll in stomatal responses by a very straightforward method. However, in the experiment by Mott *et al.* (2008), the stomata in the epidermal strips did not respond to environmental stimuli such as light and CO₂ but kept opening. Since the epidermal cells shrunk due to drying, the guard cells were pulled to the epidermal cells and the stomata might have widely opened in a hydropassive manner. Therefore, it remains unclear whether stomatal responses in epidermal strips are comparable to those in leaves.

Referring to Mott *et al.* (2008), I developed the novel method to microscopically observe stomatal responses under physiologically more natural conditions. By placing epidermal strips on buffer-containing gels, rather than on a solution, I prevented the epidermal strips from being subject to extreme desiccation or hydration for up to 8 h. I aimed to clarify whether the mesophyll plays an important role in stomatal responses to CO₂ by comparing the stomatal

responses of the leaf segments, epidermal strips and epidermal strips placed on mesophyll segments. I used red light, in addition to white light containing a blue light component.

2-2. Materials and Methods

Plant materials

Commelina communis seeds were placed in the dark at 4°C for at least 2 months. This chilling treatment was essential for germination. *C. communis* plants were grown from seeds in a mixture of vermiculite (Nittai, Osaka, Japan) and culture soil (Metro-Mix 350; Sun Gro Horticulture, Bellevue, WA, USA) in pots (SlitPot, 7 cm in diameter and 8 cm in height, one seedling per pot; KANEYA Co., Ltd., Aichi, Japan), and watered every other day with the 10⁻³ (v/v) strength nutrient solution (Hyponex 6-10-5; Hyponex Japan, Tokyo, Japan), in an environmentally controlled room with a 14 h light (10:00–24:00) and 10 h dark (0:00–10:00) cycle, at 23°C and at ca. 60% relative humidity. A bank of fluorescent lamps served as the light source. The photosynthetically active photon flux density (PPFD) at plant height was ca. 350 $\mu\text{mol m}^{-2} \text{s}^{-1}$. Fully expanded mature leaves (showing no signs of senescence) from the plants grown for at least 5 weeks were used for the experiments. Before preparing the samples, light-grown plants with open stomata were kept in the dark for 1 h to close stomata.

Microscopic observation system

I constructed a system to control the environment of the leaf segment or the isolated epidermis, and observe the stomata microscopically (Fig. 2-1). The sample chamber consisted of two brass blocks (45 × 55 × 10 mm). Both half-chambers had glass windows (20 mm square). By circulating water from a temperature-controlled bath, the chamber temperature was maintained at 23°C. I placed the sample on the gel in the lower chamber. The chamber with the sample was mounted on a microscopic stage, and the sample was observed under a microscope (BH2; Olympus, Tokyo, Japan) with a long focal objective lens (SLMPN ×20, working distance 25 mm; Olympus). Digital images were obtained using a digital camera (D5100; Nikon, Tokyo, Japan) and analysed using digital image analysis software (Macromax GOKO Measure; GOKO CAMERA, Kanagawa, Japan).

N₂ and O₂ from cylinders were mixed at a ratio of 80:20 (v/v) using mass flow controllers (Horiba Stec, Kyoto, Japan). The mixture was humidified by bubbling it in water at 23°C. The

dew point of this mixture was controlled using a condenser chilled with a Peltier element. 1% (v/v) CO₂ in N₂ was then mixed using another mass flow controller. The air was divided into two lines, and each of them was introduced to the half-chamber at the flow rate of 50 mL min⁻¹. The sample temperature was measured using a copper-constantan thermocouple. CO₂ and H₂O concentrations were monitored using an infrared gas analyser (LI-840; LI-COR, Lincoln, NE, USA).

The sample was illuminated with a halogen lamp (Projection lamp type 77241; Philips, Eindhoven, Netherlands) attached to the microscope. To illuminate a large area, I removed the condenser unit below the stage, and fully opened the diaphragm of the lighting unit. The light from the lighting unit of the microscope was passed through a reflective filter (03SWP614; Melles Griot, Tokyo, Japan) that removes the infrared component, and used as the white light. Red light was obtained using a red light filter (03LWP610; Melles Griot), in addition to the reflective filter. The spectra of these lights are shown in Fig. 2-2. In the present study, light was illuminated from the adaxial side of the sample. Therefore, the light that reached the abaxial epidermis of the leaf segment was transmitted through the leaf (Fig. 2-3). To examine the stomata in the epidermal strip under similar light conditions, a leaf segment was placed under the gel (Fig. 2-4). I measured apertures of the stomata whose substomatal cavities (Fig. 1-1b) were filled with air. The stomata responded minimally when the substomatal cavities were filled with liquid.

Examination of the effects of KCl concentration in a buffer

Abaxial epidermes were peeled off from the dark-treated leaves of *C. communis* and placed on the filter paper (Whatman No. 5; Whatman international, Maidstone, UK) containing KCl, 1 mM CaCl₂ and 10 mM MES-KOH (pH 6.15). The KCl concentration was 0, 25, 50, 75 or 100 mM. The epidermal strips were placed for 1 h from 14:00 in the dark at room temperature.

Analysis of stomatal responses in epidermal strips

The abaxial epidermis was peeled off from the dark-treated leaf of *C. communis* and placed over a hole (5 mm in diameter) made in the middle of a piece of filter paper (Whatman No. 5; Whatman international, Maidstone, UK) containing a buffer solution (50 mM KCl, 1 mM CaCl₂ and 10 mM MES-KOH adjusted at pH 6.15). The filter paper was sandwiched by

the two brass half-chambers (see ‘Microscopic observation system’) and perfused with the buffer solution outside the chamber. The epidermal strip was illuminated with white light (PPFD $150 \mu\text{mol m}^{-2} \text{s}^{-1}$) for 5 h and then, placed in the dark for 1 h. In this experiment, CO_2 concentration was kept at 120 ppm for 2 h, 540 ppm for 1 h, 780 ppm for 1 h, and at 120 ppm for 2 h. White light was provided by a halogen lamp (Projection lamp type 77241; Philips, Eindhoven, Netherlands) attached to the microscope.

Analysis of stomatal responses in epidermal strips on a buffer-containing gel

The abaxial epidermes were peeled off from the dark-treated leaves of *C. communis* and placed on gels containing 30 mM KCl, 1 mM CaCl_2 and 10 mM MES-KOH (pH 6.15). The epidermal strips were illuminated with white light (PPFD $700 \mu\text{mol m}^{-2} \text{s}^{-1}$) for 4 h from the onset of the experiment. Subsequently, the epidermal strips were in the dark for 1 h. CO_2 concentration was maintained at 120 ppm for 2 h, raised at 540 ppm for 1 h and subsequently lowered at 120 ppm for 1 h. White light was provided by the halogen lamp (Projection lamp type 77241; Philips, Eindhoven, Netherlands) attached to the microscope.

Sample preparations

The presence of the mesophyll signals were analyzed with three types of samples. These samples were placed on the gels containing 30 mM KCl, 1 mM CaCl_2 , 10 mM MES-KOH (pH 6.15), and 1% (w/v) gellanum (Wako, Osaka, Japan). When gellanum solidifies, Ca^{2+} acts as a cross-linker. The concentration of free Ca^{2+} in the gel, measured with a calcium assay kit (Metalloassay Calcium assay kit; AKJ Global Technology, Chiba, Japan), ranged from 0.4 to 0.6 mM.

(1) Leaf segment (Fig. 2-3)

The mesophyll with the adaxial epidermis on the gel was covered with the abaxial epidermis to prevent desiccation from the cut-surface of the mesophyll. Therefore, the area of the abaxial epidermis in the leaf segment was greater than the mesophyll with the adaxial epidermis. The leaf segment (15 mm square) was prepared by cutting a leaf with a razor blade. Mesophyll with the adaxial epidermis was carefully removed from the four edges to obtain the mesophyll with the adaxial epidermis (10 mm square) on the abaxial epidermis (15 mm square).

The leaf segment was placed on a buffer-containing gel with the abaxial side upward, and the free abaxial epidermis was attached to the gel. The air between the abaxial epidermis and the lateral sides of the mesophyll was removed by gently pushing the abaxial epidermis along the lateral edges of the mesophyll.

(2) Epidermal strip (Fig. 2-4)

The abaxial epidermal strip (10 mm square) was prepared using a pair of forceps. The epidermal strip was first floated on a buffer containing 30 mM KCl, 1 mM CaCl₂, and 10 mM MES-KOH (pH 6.15), with the outer part of the epidermis facing upwards. The epidermal strip was gently slid on the gel to remove the buffer occupying the substomatal cavities. When the buffer remained in the substomatal cavities, the guard cells appeared transparent, while the guard cells with air-filled substomatal cavities appeared whitish. After removing the excess buffer, the epidermal strip was placed on a fresh gel.

(3) Epidermal strip placed directly on the mesophyll segment (Fig. 2-5)

The mesophyll with the adaxial epidermis (10 mm square) was prepared by peeling off the abaxial epidermis, and was placed on the buffer-containing gel with the abaxial side upward. I placed the abaxial epidermal strip (15 mm square) on the mesophyll with the adaxial epidermis. The edges of the abaxial epidermis were attached to the gel. The epidermal strip was gently pressed against the mesophyll segment using a pair of forceps to attain close contact.

Analysis of the stomatal responses to Ca²⁺ in the buffer-containing gels

The abaxial epidermes were peeled off from the dark-treated leaf of *C. communis* and placed on a gel containing 30 mM KCl, 10 mM MES-KOH (pH 6.15), 1% (w/v) gellangum (Wako) and CaCl₂. The concentration of CaCl₂ was set at 0, 0.05 and 1 mM. In the Ca²⁺-free gels, 1 mM MgCl₂ was dissolved as a cross-linker for solidification of gellangum instead of CaCl₂. The epidermal strips were illuminated with white light (PPFD 700 μmol m⁻² s⁻¹) for 2 h from the onset of the experiment. CO₂ concentration was kept at 100 ppm.

Analysis of stomatal responses on Ca²⁺-free gel

I analyzed the stomatal responses in the leaf segments, the epidermal strips and the

epidermal strips placed on the mesophyll segments on the Ca^{2+} -free gels. These samples were placed on gels containing 30 mM KCl, 1 mM MgCl_2 , 10 mM MES-KOH (pH 6.15), and 1% (w/v) gellan gum (Wako).

Statistical analysis

Differences between the mean values of data were analysed using analysis of variance (ANOVA) and Tukey's multiple comparison test (Tables 2-1, 2 and 3). The data are shown as means \pm SEM of at least three independent experiments (Figs. 2-9, 10 and 12). The data are shown as means \pm SD (Fig. 2-11). All statistical analyses were conducted using the R statistical software package (ver. 2.15.1.; R development Core Team 2003).

2-3. Results

Effects of KCl concentration on stomatal responses

It is well known that stomatal movements are influenced by the concentration of osmoticum around guard cells. Hence, I examined the suitable KCl concentration in the buffer solution for *C. communis*. Stomata hardly opened when the KCl concentration was < 75 mM in the dark (Fig. 2-6). On the contrary, stomata widely opened when KCl concentration was 100 mM (Fig. 2-6).

Novel method for observing physiological stomatal responses

A previous study (Mott *et al.*, 2008) claimed that stomata in epidermal strips responded minimally to light or CO_2 . However, in their studies, stomata in the epidermal strip were fully open from the onset of the experiment, and that the aperture size did not change throughout the experiment for up to 5 h. To check its reproducibility, I repeated their experiment, using epidermal strips of *C. communis*. The epidermal strip was placed over a hole (5 mm in diameter) made in the filter paper containing the incubation buffer (50 mM KCl, 1 mM CaCl_2 , and 10 mM MES-KOH adjusted at pH 6.15). Because I had treated the epidermal strips in the dark for at least 1 h, stomata were closed at the onset of illumination. Stomata opened in the light and at 120 ppm CO_2 , but gradually became insensitive to high CO_2 or darkness (Fig. 2-7). Even at a very high humidity in the chamber, it was difficult to keep the epidermes on the wet filter paper turgid for a long time. On the other hand, numerous studies have revealed that stomata in

epidermal strips floating on the buffer solution were able to respond to environmental stimuli (e.g. Hsiao & Allaway, 1973; Webb *et al.*, 1996).

I also preliminary examined the stomatal responses in the epidermal strips floated on the buffer solution. The epidermal strips, which had been kept in the dark for 1 h, were illuminated with white light (PPFD 350 $\mu\text{mol m}^{-2} \text{s}^{-1}$) in a growth chamber. I noticed that the stomata with their substomatal cavities filled with the buffer responded to light much less than those with the air-filled cavities and that the proportion of the stomata with buffer-filled cavities increased with time (my personal observation). Because I wanted to examine the roles of mesophyll, it was necessary to keep the substomatal cavities in the air-filled state for a longer time. Therefore, to adequately supply water to the sample, I developed the gel method, with which I was able to easily keep the substomatal cavities filled with air. I used 1% (w/v) the gellangum gel containing 30 mM KCl, 1 mM CaCl_2 and 10 mM MES-KOH (pH 6.15). When the epidermal strips were placed on the gels, stomata filled with air were easily distinguished from those filled with the buffer solution (Fig. 2-8a) and most of the substomatal cavities retained air. Compared with stomata filled with the buffer solution, the stomata filled with air showed sensitive responses to the environmental stimuli (Fig. 2-8b). With this gel system, both stomatal opening and closure in the epidermal strips placed on the gels were observed in white light and in the dark, respectively (Fig. 2-8b). The epidermal strips did not show any symptoms of desiccation for more than 8 h from the onset of the experiments (my personal observation). These indicated that stomata in the epidermal strips placed on the gels were able to both open and close when light and CO_2 conditions were appropriately manipulated (Fig. 2-8b). In other words, placing the samples on the gels allowed us to observe the stomatal responses in the epidermal strips in a more physiological state. Also, using this system, I was able to observe the stomatal responses in the leaf segments for more than 3 h.

CO_2 responses under different light conditions

I checked whether the mesophyll regulates stomatal responses to CO_2 . I compared the stomatal responses in the leaf segments, the epidermal strips and the epidermal strips placed on the mesophyll segments, at low CO_2 (100 ppm) or high CO_2 (700 ppm). I illuminated the sample with red light (PPFD 550 $\mu\text{mol m}^{-2} \text{s}^{-1}$) or white light (PPFD 700 $\mu\text{mol m}^{-2} \text{s}^{-1}$). In the experiments shown in Figs. 2-9 and 10, CO_2 concentration changed from 100 ppm to 700 ppm

at 2 h after the onset of illumination. Before starting the illumination, the samples were kept in the dark at 100 ppm CO₂ for 0.5 h.

Table 2-1 and Fig. 2-9 show the changes in the stomatal aperture in the leaf segments, the epidermal strips, and the epidermal strips placed on the mesophyll segments in red or white light. In red light, stomata in the leaf segments and the epidermal strips placed on the mesophyll segments opened when CO₂ concentration was 100 ppm (Fig. 2-9a and c). The increment of the stomatal aperture in the leaf segments at 2 h after the onset of illumination was 1.8 μm greater in average than that of the epidermal strips placed on the mesophyll segments (Table 2-1). In contrast, stomata in the epidermal strips barely opened (Table 2-1 and Fig. 2-9b). Stomata in the leaf segments and the epidermal strips placed on the mesophyll segments closed rapidly at 700 ppm CO₂ (Fig. 2-9a and c). The rate of stomatal closure was faster in the leaf segments than in the epidermal strips placed on the mesophyll segments (Table 2-1). In the leaf segments, rapid stomatal closure was observed within 0.5 h of the onset of high CO₂ treatment (4.1 μm decrement in 0.5 h). Because the stomata in the epidermal strips only slightly opened at 100 ppm CO₂, I could not evaluate the rate of the stomatal closure in the epidermal strips (Fig. 2-9b).

In white light, stomata in the leaf segments opened widely at 100 ppm CO₂ (Fig. 2-9d). Stomata in the epidermal strips also opened at 100 ppm CO₂ (Fig. 2-9e). However, the increment of the aperture in the epidermal strips at 2 h after the onset of illumination was 2.5 μm smaller in average than that in the leaf segments (Table 2-1). Stomata in the epidermal strips placed on the mesophyll segments opened widely at 100 ppm CO₂ (Fig. 2-9f). The increment of the aperture was 1.2 μm greater than that of the epidermal strips and 1.3 μm less than that of the leaf segments (Table 2-1). Stomata closed rapidly in the leaf segments and the epidermal strips placed on the mesophyll segments at 700 ppm CO₂ (Fig. 2-9d and f). The rate of stomatal closure was faster in the leaf segments than that of the epidermal strips placed on the mesophyll segments (Table 2-1). As observed in red light, the rapid stomatal closure was observed within 0.5 h from the onset of high CO₂ treatment in the leaf segments (Fig. 2-9d). In contrast, stomata in the epidermal strips hardly closed within 1 h at 700 ppm CO₂ (Fig. 2-9e). The rate of stomatal closure was slow, however, stomata continuously closed over 1 h at 700 ppm CO₂ (Fig. 2-10). To check whether stomata in the epidermal strips placed on gels lost the ability to close, I placed the epidermal strips in the dark at 100 ppm CO₂. In this case, stomata closed rapidly within 1 h

(Table 2-1 and Fig. 2-9g).

Stomatal responses in the epidermal strips placed on the Ca²⁺-free gel

In previous studies, Ca²⁺ concentration in the buffer for isolated epidermes were generally set at $\leq 100 \mu\text{M}$ (e.g. Talbott & Zeiger, 1993; Merritt *et al.*, 2001; Hu *et al.*, 2010; Suetsugu *et al.*, 2014). It has been also shown that Ca²⁺ had the potential to induce the stomatal closure at the concentration above $100 \mu\text{M}$ (Schwartz, 1985; De Silva *et al.*, 1985; McAinsh *et al.*, 1995). From these studies, it was probable that the stomatal responses in epidermal strips in Fig. 2-9 were repressed by the high Ca²⁺ concentration in the buffer contained in the gels. I observed that the stomatal opening in white light slowed down with the Ca²⁺ concentration in the gels increased (Table 2-2 and Fig. 2-11). Therefore, I investigated whether the stomatal responses to CO₂ shown in Fig. 2-9 were influenced by the Ca²⁺ concentration in the buffer-containing gels.

Stomatal responses with the Ca²⁺-free gels were generally similar to the stomatal responses with the 1 mM Ca²⁺ gels (compare Fig. 2-9 and Fig. 2-12). With the Ca²⁺-free gels, it was confirmed that both stomatal opening and closure were speeded up when the epidermal strips were touched on the mesophyll segments (Fig. 2-12). Several points, however, differed between the stomatal responses with the Ca²⁺-free gels and those with the 1 mM Ca²⁺ gels. Stomatal opening in white light with the Ca²⁺-free gels was especially faster (compare Fig. 2-9 and Fig. 2-12). In the epidermal strips, stomatal opening in white light was slowed down at 700 ppm CO₂, but, stomata continued to open for 1 h after the onset of high CO₂ treatment with the Ca²⁺-free gels (compare Table 2-1 and Table 2-3; Fig. 2-9e and Fig. 2-12e). In the leaf segments, the rate of stomatal closure at 700 ppm CO₂ was faster with the Ca²⁺-free gels than with the 1 mM Ca²⁺ gels (compare Table 2-1 and Table 2-3; Fig. 2-9d and Fig. 2-12d).

2-4. Discussion

Conditions for the observation of stomatal responses

As described in chapter 1, stomatal responses are divided into two types; hydroactive and hydropassive. In Fig. 2-6, the stomata in the epidermal strips of *C. communis* widely opened in the dark at 100 mM KCl. These results suggested that the epidermal cells osmotically shrunk and the hydropassive stomatal opening was induced. Therefore, in my study, the concentration of KCl in the buffer for epidermal strips should be less than 100 mM. Stomata in the epidermal

strips, placed over the hole in the filter paper containing 50 mM KCl, continued to open in spite of the environmental stimuli (Fig. 2-7). I set the dew point in the sample chamber nearly saturated, however, the water in the epidermal strips would be gradually escaped and the hydropassive opening was also induced due to the drying. For adequate watering to epidermal strips, therefore, the epidermal strips were placed on the buffer-containing gels.

Although substomatal cavities are filled with air in intact leaves (Fig. 1-1b), almost all of the substomatal cavities were filled with the buffer when epidermal strips were floated on a buffer. When epidermal strips were placed on buffer-containing gels, most substomatal cavities were kept to be air-filled (Fig. 2-8a). Stomata with air-filled substomatal cavities were more sensitive to the environmental stimuli than those with the buffer-filled cavities (Fig. 2-8b). It is well known that the ionic concentration such as H^+ , K^+ and Cl^- in the apoplast of guard cells, subsidiary cells and epidermal cells were different from each other (Bowling, 1987; Edwards *et al.*, 1988). When the substomatal cavities were filled with the buffer, the ionic gradient from guard cells to epidermal cells would be disturbed. The ionic movements along the gradients of ions would decline and the stomatal responses become dull. Since I could mimic the intercellular air space in intact leaves by the gel method, the stomata with the air-filled substomatal cavities would show physiologically more natural responses.

Previous studies have reported that 1 mM $CaCl_2$ in the incubation buffer tends to induce stomatal closure (De Silva *et al.*, 1985; Schwartz 1985; McAinsh *et al.*, 1995). When the epidermal strips were placed on the gels, the epidermal cells closely touched with the gels, while the guard cells located above the air-filled substomatal cavities did not directly touch with the gels. In intact leaves, epidermal cells closely touch with the mesophyll. It is probable that the mesophyll apoplastic Ca^{2+} concentrations ranges 0.1–1 mM (Sattelmacher, 2001). The apoplastic Ca^{2+} concentration in epidermal cell walls that are closely associated with the mesophyll are expected to be in the same range as that of the mesophyll apoplast. Therefore, in my system, 0.4–0.6 mM free Ca^{2+} in the gels would not severely inhibit the stomatal opening. Stomatal opening was severely inhibited in white light when the substomatal cavities were filled with the buffer exuding from the gels and the guard cells directly touched with the buffer (Fig. 2-8). With the increase of the Ca^{2+} concentration in the gels, the stomatal opening in white light slowed down (Table 2-2 and Fig. 2-11). To investigate whether the tendencies of stomatal responses were severely influenced by the Ca^{2+} concentration, I also observed the stomatal

responses in the samples placed on the Ca^{2+} -free gels (Table 2-3 and Fig. 2-12). In this gel, Mg^{2+} was used as a cross-linker for solidification of gellan gum. With this gel, the stomatal opening in the epidermal strips moderately speeded up, especially in white light (compare Fig. 2-9 and Fig. 2-12). In the epidermal strips, the induction of stomatal closure at 700 ppm CO_2 was slower on the Ca^{2+} -free gel than on the 1 mM Ca^{2+} gel (compare Fig. 2-9e and Fig. 2-12e). Although the absolute value of the stomatal aperture and the speed of stomatal movements differed depending on the presence of Ca^{2+} in the gels, both stomatal opening and closure were greatly accelerated when the epidermal strips were placed on the mesophyll. Thus, I concluded that the extracellular Ca^{2+} concentration did not markedly influence the tendencies of stomatal responses, and the roles of mesophyll in stomatal responses would be adequately assessed with 1 mM CaCl_2 buffer-containing gels.

Ethylene is expected to arise from the cut surface of the samples (Boller & Kende, 1980). While ethylene is known to affect the regulation of stomatal aperture, the mechanism remains unclear. In some species, ethylene induced stomatal closure (Desikan *et al.*, 2006), whereas in others it mediated the auxin-induced stomatal opening (Merritt *et al.*, 2001). In my system, compared with other environmental variables, the effects of ethylene for the stomatal responses are considered to be small because stomata in each sample responded to light and/or CO_2 as in intact leaves. If the effects of ethylene were stronger than those of other environmental variables, the effects of ethylene would have been superimposed on the physiological responses to light and/or CO_2 .

Stomatal opening

It has been proposed that photosynthesis is involved in the stomatal opening in red light (e.g. Sharkey & Raschke, 1981; Messinger *et al.*, 2006, Wang *et al.*, 2011). However, it remained unclear whether the stomatal opening in red light was dependent on photosynthesis in guard cells or in mesophyll. When a leaf is illuminated with red light, photosynthesis occurs in both the guard cells and the mesophyll. The results of the present study showed that stomata in the epidermal strips of *C. communis* hardly opened in red light at 100 ppm CO_2 (Table 2-1 and Fig. 2-9b). In contrast, stomata in the leaf segments opened widely (Table 2-1 and Fig. 2-9a). When the epidermal strips were placed on the mesophyll segments, stomata widely opened (Fig. 2-9c). These findings indicated that stomatal opening in red light was more strongly

dependent on photosynthesis in the mesophyll than that in the guard cells.

Unlike the stomatal response to red light, stomata in the epidermal strips opened widely when illuminated with white light (compare Fig. 2-9b and e). The blue-light receptors, phototropins, are localized in the guard cells of *A. thaliana*, and it has been established that blue light excites these phototropins, and leads to stomatal opening (Kinoshita *et al.*, 2001; Shimazaki *et al.*, 2007). It is highly likely that the guard cells of *C. communis* also have phototropins (Iino *et al.*, 1985). Hence, when the leaf was illuminated with white light, the blue component in white light (Fig. 2-2d) strongly induced stomatal opening. In white light, it was also shown that stomatal opening was accelerated by transplanting the epidermal strips on the mesophyll segments (Table 2-1 and Fig. 2-9e, f). Therefore, as hypothesized in Mott *et al.* (2008), it was suggested that stomatal opening in both red light and white light should be accelerated by ‘mesophyll signals’.

Stomatal closure

While stomata in the leaf segments closed rapidly in white light at 700 ppm CO₂, stomata in the epidermal strips hardly closed within 1 h under these conditions (Table 2-1 and Fig. 2-9d, e). Previous studies clearly indicated that stomata in the epidermal strips closed at high CO₂ (e.g. Schwartz *et al.*, 1988; Webb *et al.*, 1996; Webb & Hetherington, 1997; Hu *et al.*, 2010). To check whether this phenomenon occurred in my system, the epidermal strips were maintained at 700 ppm CO₂ for more than 1 h. The stomata on the epidermal strips slowly closed from an aperture of 4.6 μm to 2.8 μm over a 3 h period (Fig. 2-10). The degree of stomatal closure was comparable with those in the previous studies. In addition, when the epidermal strips were maintained in the dark, stomata closed rapidly within 1 h (Figs. 2-9g and 10). Therefore, the stomata in the epidermal strips had the potential to close; the closure at 700 ppm CO₂ was not an experimental artifact. In contrast, when the epidermal strips were placed on the mesophyll segments, stomata closed rapidly (Fig. 2-9f). These data indicated that the mesophyll contributed to the rapid induction of stomatal closure at high CO₂. Stomatal closure at high CO₂ were also accelerated by the mesophyll signals.

2-5. Tables

Table 2-1. Extent of stomatal opening and closure on 1 mM Ca²⁺ gels (shown in Fig. 2-9)

	Leaf segment (μm)	Epidermal strip (μm)	Epidermal strip placed on mesophyll (μm)	Epidermal strip Dark treatment (μm)	<i>P</i> -value
RL opening ¹⁾	5.39 ± 0.22 ^a	0.70 ± 0.09 ^b	3.60 ± 0.20 ^c	no data	< 0.001
RL closure ²⁾	- 4.66 ± 0.20 ^a	- 0.28 ± 0.09 ^b	- 2.08 ± 0.17 ^c	no data	< 0.001
WL opening ¹⁾	5.59 ± 0.25 ^a	3.08 ± 0.20 ^b	4.27 ± 0.30 ^c	3.50 ± 0.23 ^{bc}	< 0.001
WL closure ²⁾	- 3.98 ± 0.18 ^a	- 0.35 ± 0.08 ^b	- 2.62 ± 0.25 ^c	- 2.18 ± 0.12 ^c	< 0.001

The leaf segments, the epidermal strips and the epidermal strips placed on the mesophyll segments were prepared. The samples were placed on the 1 mM Ca²⁺ buffer-containing gels.

¹⁾ Difference between the stomatal aperture at 2 h and the stomatal aperture at 0 h.

²⁾ Difference between the stomatal aperture at 3 h and the stomatal aperture at 2 h.

RL, red light (PPFD 550 $\mu\text{mol m}^{-2} \text{s}^{-1}$); WL, white light (PPFD 700 $\mu\text{mol m}^{-2} \text{s}^{-1}$).

Data are shown as the mean ± SEM of at least 50 stomata. *P*-values were calculated using analysis of variance (ANOVA). When ANOVA was significant at $P < 0.05$, Tukey's multiple comparison test among samples was conducted at a significance level of $P < 0.05$. Different lower case letters denote significant differences in Tukey's test for the data shown in each row.

Table 2-2. Extent of stomatal opening in response to Ca²⁺ concentration (shown in Fig. 2-11)

	Ca ²⁺ 0 mM (μm)	Ca ²⁺ 0.05 mM (μm)	Ca ²⁺ 1 mM (μm)	<i>P</i> -value
Opening	7.24 ± 2.00 ^a	5.51 ± 1.68 ^b	4.09 ± 1.34 ^c	< 0.001

The values indicate the difference between the stomatal aperture at 2 h and the stomatal aperture at 0 h. The epidermal strips were placed on the gels containing 0, 0.05 or 1 mM Ca²⁺. The samples were illuminated with white light (PPFD 700 μmol m⁻² s⁻¹). Data are shown as the mean ± SD of at least 17 stomata. *P*-values were calculated using analysis of variance (ANOVA). When ANOVA was significant at *P* < 0.05, Tukey's multiple comparison test among samples was conducted at a significance level of *P* < 0.05. Different lower case letters denote significant differences in Tukey's test.

Table 2-3. Extent of stomatal opening and closure on the Ca²⁺-free gels (shown in Fig. 2-12)

	Leaf segment (μm)	Epidermal strip (μm)	Epidermal strip placed on mesophyll (μm)	<i>P</i> -value
RL opening ¹⁾	5.25 \pm 0.25 ^a	1.54 \pm 0.13 ^b	4.51 \pm 0.32 ^a	< 0.001
RL closure ²⁾	- 4.42 \pm 0.23 ^a	- 0.51 \pm 0.09 ^b	- 2.34 \pm 0.20 ^c	< 0.001
WL opening ¹⁾	9.94 \pm 0.55 ^a	6.95 \pm 0.33 ^b	9.63 \pm 0.34 ^a	< 0.001
WL closure ²⁾	- 9.60 \pm 0.52 ^a	0.67 \pm 0.12 ^b	- 3.50 \pm 0.27 ^c	< 0.001

The leaf segments, the epidermal strips and the epidermal strips placed on the mesophyll segments were prepared. The samples were placed on the Ca²⁺-free gels.

¹⁾ Difference between the stomatal aperture at 2 h and the stomatal aperture at 0 h.

²⁾ Difference between the stomatal aperture at 3 h and the stomatal aperture at 2 h.

RL, red light (PPFD 550 $\mu\text{mol m}^{-2} \text{s}^{-1}$); WL, white light (PPFD 700 $\mu\text{mol m}^{-2} \text{s}^{-1}$).

Data are shown as the mean \pm SEM of at least 25 stomata. *P*-values were calculated using analysis of variance (ANOVA). When ANOVA was significant at $P < 0.05$, Tukey's multiple comparison test among samples was conducted at a significance level of $P < 0.05$. Different lower case letters denote significant differences in Tukey's test for the data shown in each row.

2-6. Figures

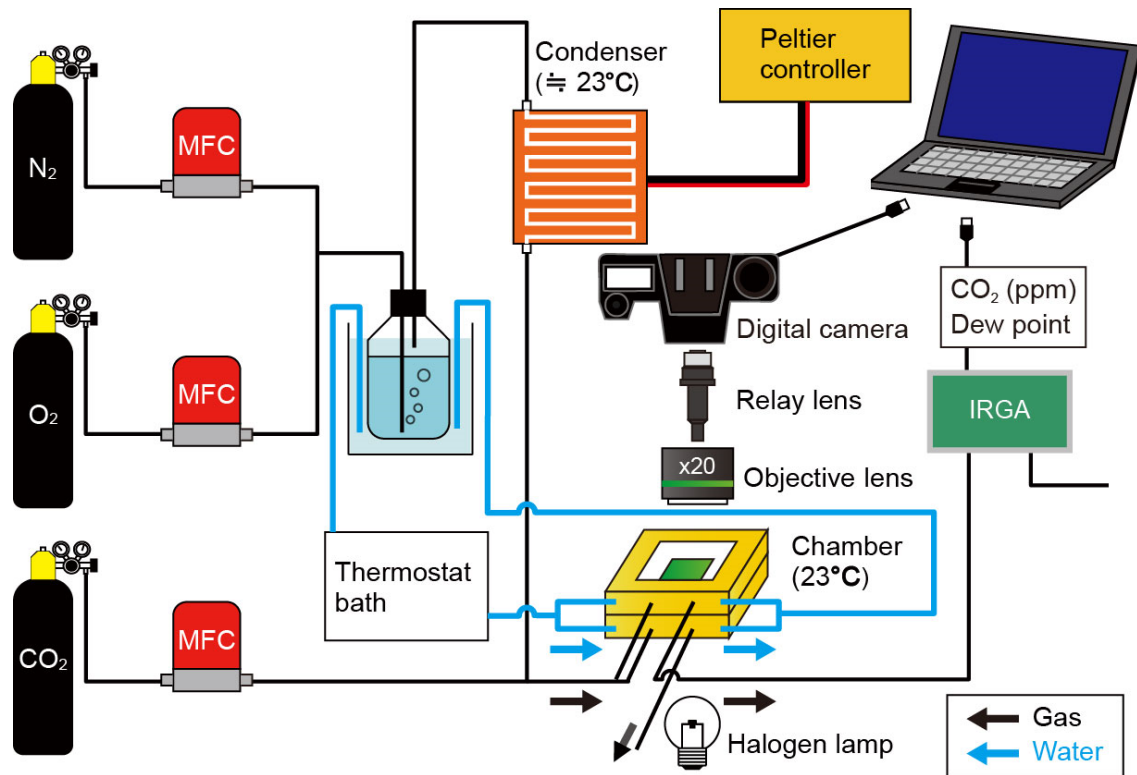


Fig. 2-1. Microscopic observation system. The chamber was mounted on the microscope stage. The sample placed on the gel was set in the chamber. The sample was illuminated with the light source of the microscope. Digital images of stomata were obtained using a digital camera attached to the microscope. Water from a temperature-controlled bath was circulated through the chamber and the reservoir. The mixed gas consisted of humidified N₂ and O₂, and the dew point of this mixture was controlled with a condenser. This mixture was mixed with 1% (v/v) CO₂ before entering the chamber. The mixed gas that passed through the chamber entered infrared gas analyser (IRGA) for measurements of the concentrations of CO₂ and H₂O.

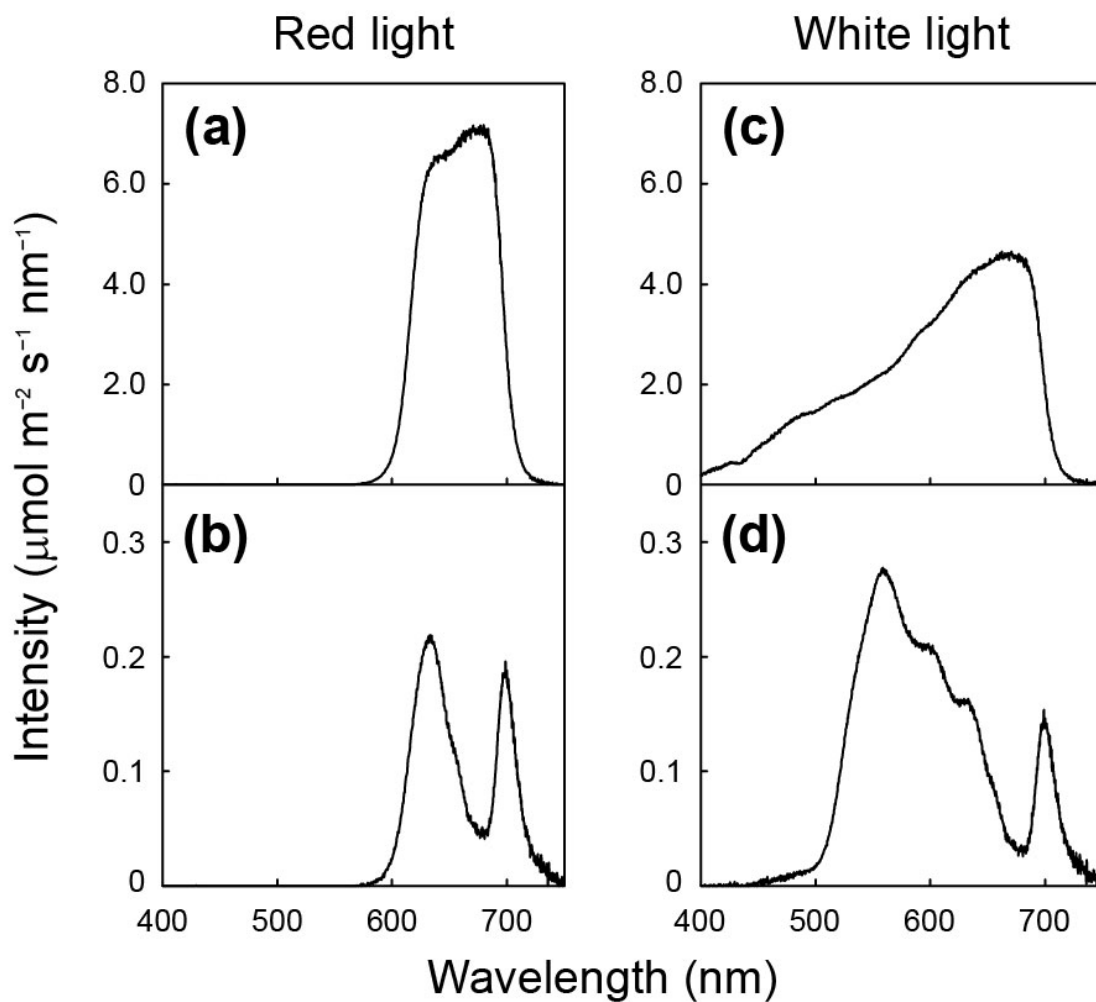


Fig. 2-2. Spectra of the red light (a) and white light (c) that incident on the samples. The spectra in (b) and (d) are the red and white light that transmitted the leaf of *C. communis*, respectively.

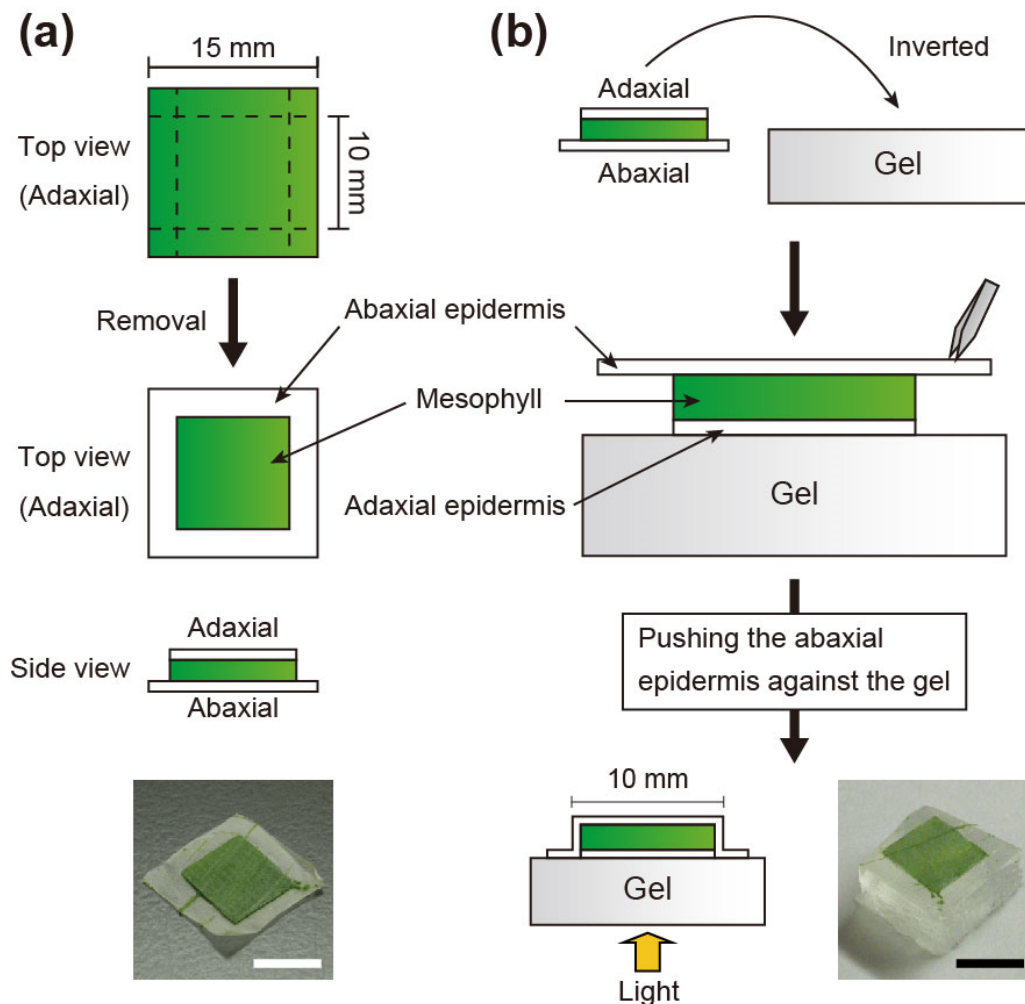


Fig. 2-3. Preparation of the leaf segment sample from *C. communis*. (a) Procedures for the preparation of a leaf segment. From the adaxial side, along the dashed lines, a leaf segment (15 mm square) was shallowly cut with a razor blade. Mesophyll with the adaxial epidermis was carefully removed from the four edges to prepare a square-shaped mesophyll with the adaxial epidermis (10 mm square) on the adaxial epidermis (15 mm square); (b) the leaf segment was placed on a buffer-containing gel with the abaxial side upward. The free abaxial epidermis was attached to the gel with a pair of forceps. The light was illuminated from the adaxial side. Bars = 10 mm.

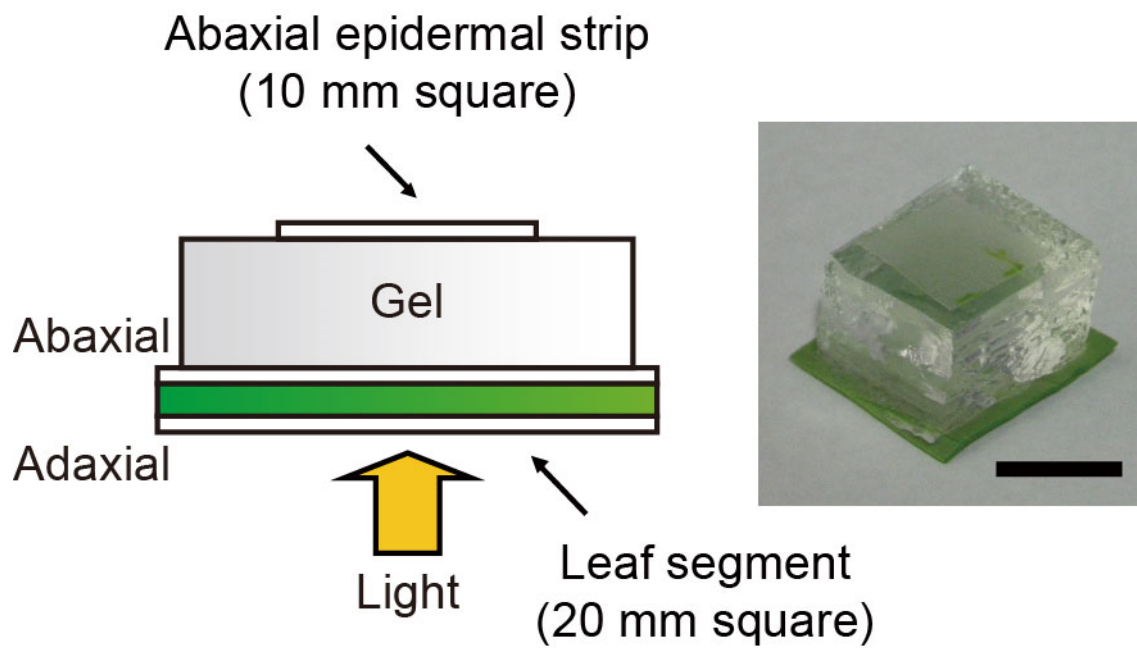


Fig. 2-4. Preparation of the epidermal strip sample from *C. communis*. An abaxial epidermal strip (10 mm square) was placed on a buffer-containing gel. The gel was placed on a leaf segment (20 mm square). Light was illuminated through the leaf segment and the gel. Bar = 10 mm.

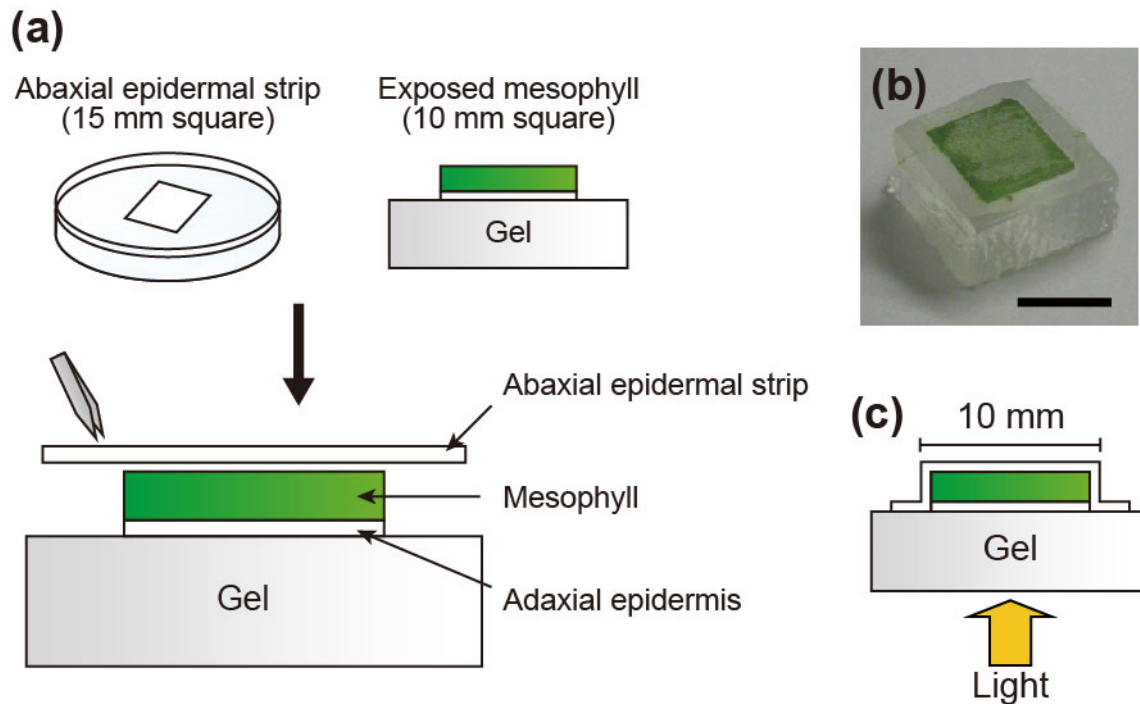


Fig. 2-5. Preparation of the epidermal strip placed on mesophyll sample from *C. communis*. (a) Procedures for preparation of an epidermal strip placed on a mesophyll. The abaxial epidermal strip was first floated on the buffer containing 30 mM KCl, 1 mM CaCl₂, and 10 mM MES-KOH (pH 6.15). After removing the buffer in the substomatal cavities, the epidermal strip was placed on the mesophyll with the adaxial epidermis. The epidermal strip was gently pressed against the mesophyll segment using a pair of forceps; (b) an epidermal strip placed on a mesophyll with the adaxial epidermis. Bar = 10 mm; (c) Light was illuminated from the gel side.

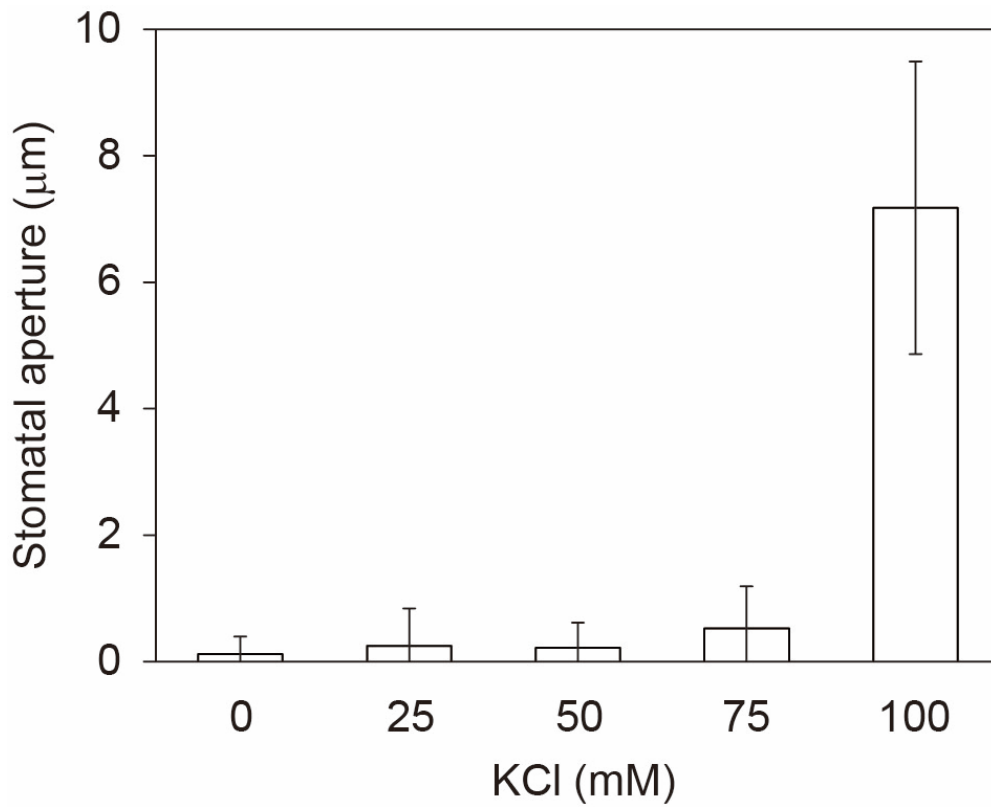


Fig. 2-6. Stomatal responses to KCl concentration in the buffer. Abaxial epidermal strips were placed on the filter paper containing 1 mM CaCl₂, 10 mM MES-KOH (pH 6.15) and KCl. The KCl concentration was 0, 25, 50, 75 or 100 mM. The epidermal strips were placed in the dark for 1 h from 14:00 at room temperature. Data are the mean \pm SD of 21 stomata.

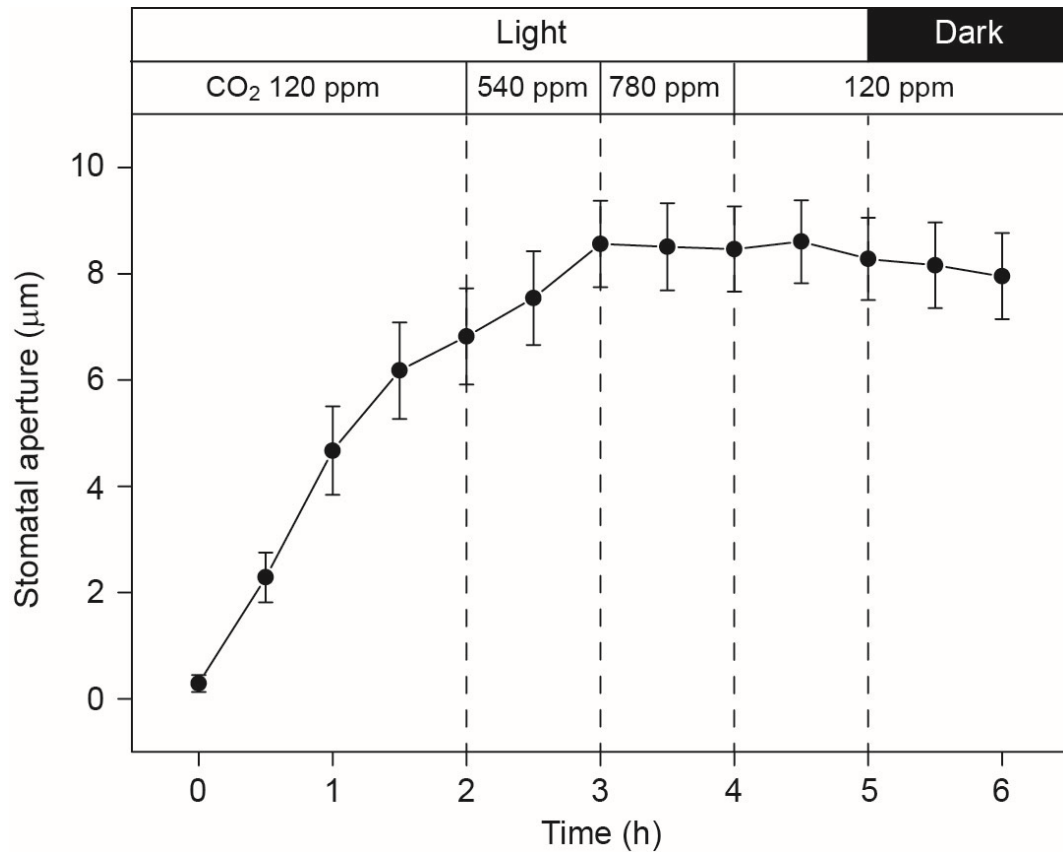


Fig. 2-7. Hydropassive stomatal opening in an epidermal strip placed over a hole (5 mm in diameter) made in the middle of a piece of filter paper containing a 50 mM KCl buffer solution. The epidermal strip was placed in the dark for at least 1 h before the onset of illumination. The epidermal strip was illuminated with white light (PPFD $150 \mu\text{mol m}^{-2} \text{s}^{-1}$) for 5 h and then, placed in the dark for 1 h. CO₂ concentration was maintained at 120 ppm for 2 h, at 540 ppm for 1 h, at 780 ppm for 1 h and subsequently at 120 ppm for 2 h. Data are the mean \pm SD of 15 stomata.

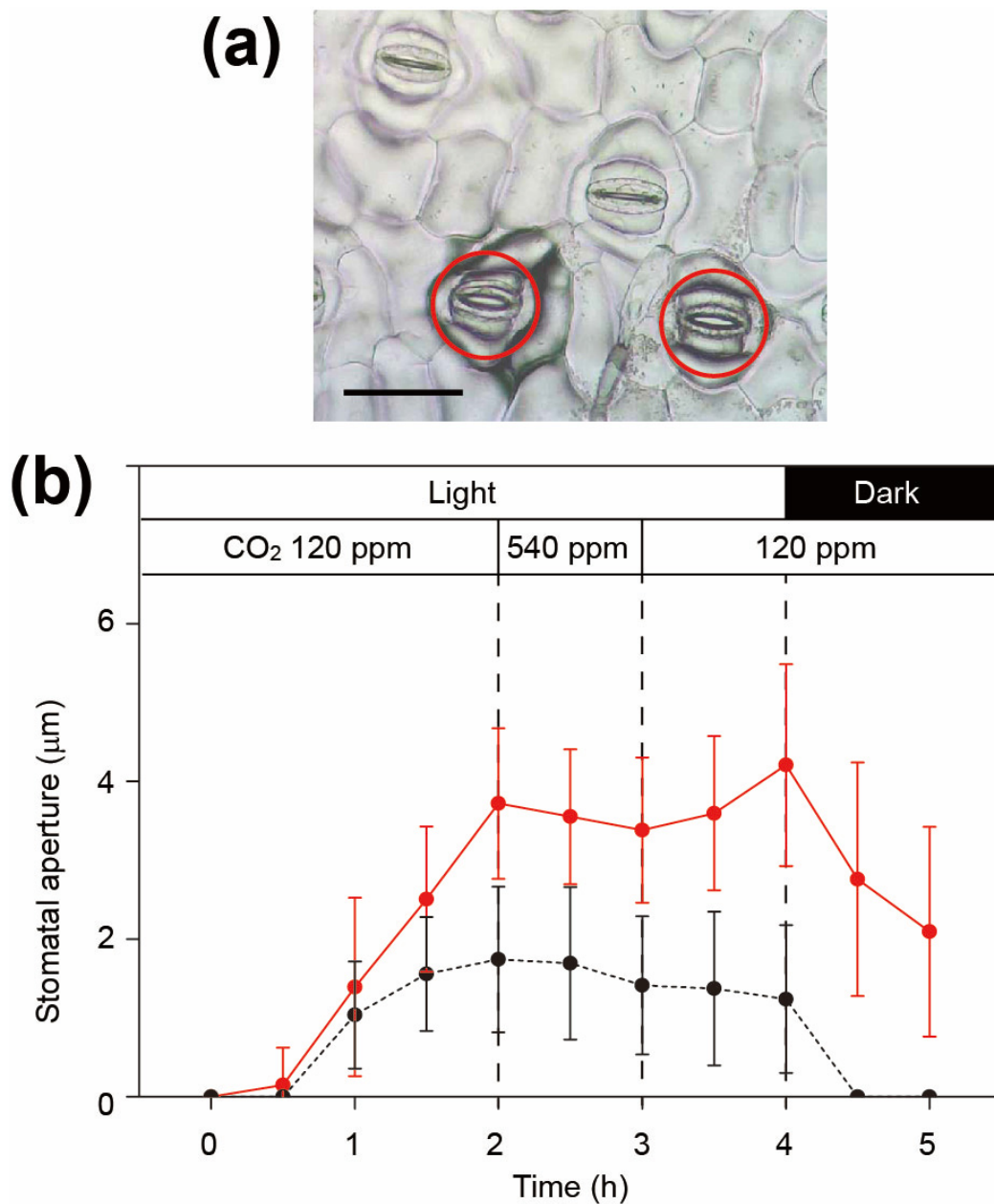


Fig. 2-8. (a) Photograph taken at 4 h from the onset of the experiment. Red circles represent the stomata with the air-filled substomatal cavities. Bar = 100 μm ; (b) Responses of stomata with air-filled or buffer-filled substomatal cavities in the epidermal strips placed on the buffer-containing gels. Red line represents the responses of the stomata with the air-filled substomatal cavities. Black broken line represents the responses of stomata with the buffer-filled substomatal cavities. The epidermal strips were illuminated with white light (PPFD 700 $\mu\text{mol m}^{-2} \text{s}^{-1}$) for 4 h from the onset of the experiment. Subsequently, the epidermal strips were kept in the dark for 1 h. CO₂ concentration was maintained at 120 ppm for 2 h and subsequently at 540 ppm for 1 h. Then, CO₂ concentration was lowered to 120 ppm for 1 h. Data are the mean \pm SD of at least 10 stomata.

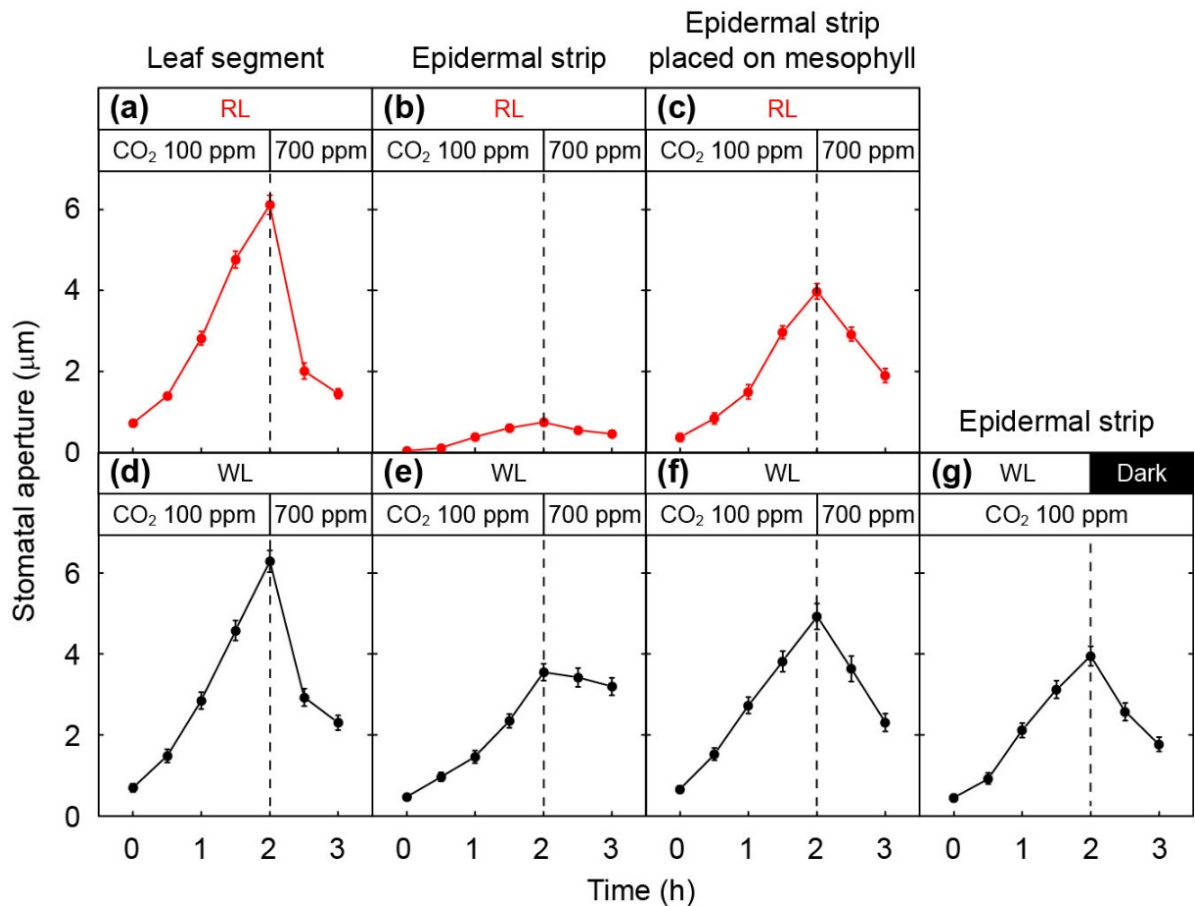


Fig. 2-9. Changes in stomatal aperture in the leaf segments (a and d), the epidermal strips (b, e, and g), and the epidermal strips placed on a mesophyll segments (c and f) in *C. communis*. The samples were illuminated from the adaxial side with red light (RL; PPFD $550 \mu\text{mol m}^{-2} \text{s}^{-1}$) or white light (WL; PPFD $700 \mu\text{mol m}^{-2} \text{s}^{-1}$). Data are the mean \pm SEM of at least 51 stomata obtained from three independent measurements. Before measurements, the samples maintained in the dark for 0.5 h to close the stomata. In (a)–(f), the CO₂ concentration was changed from 100 ppm to 700 ppm at 2 h after the onset of illumination (dashed lines). In (g), the epidermal strip was placed in the dark at 2 h after the onset of illumination (dashed line).

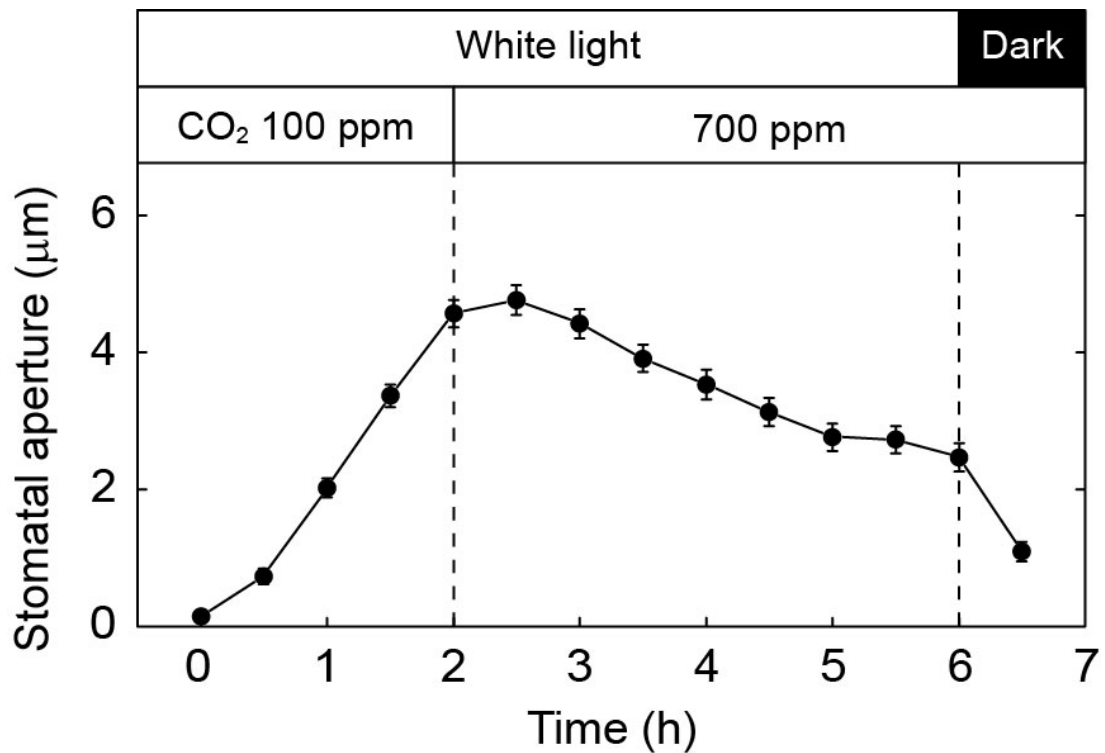


Fig. 2-10. Stomatal responses in the epidermal strips of *C. communis*. The abaxial epidermal strips were illuminated with white light (PPFD 700 $\mu\text{mol m}^{-2} \text{s}^{-1}$). Data are the mean \pm SEM of 56 stomata. Before measurements, the samples were maintained in the dark for 0.5 h to close stomata. The CO₂ concentration was changed from 100 ppm to 700 ppm at 2 h after the onset of illumination. The epidermal strips were again placed in the dark at 6 h after the onset of illumination.

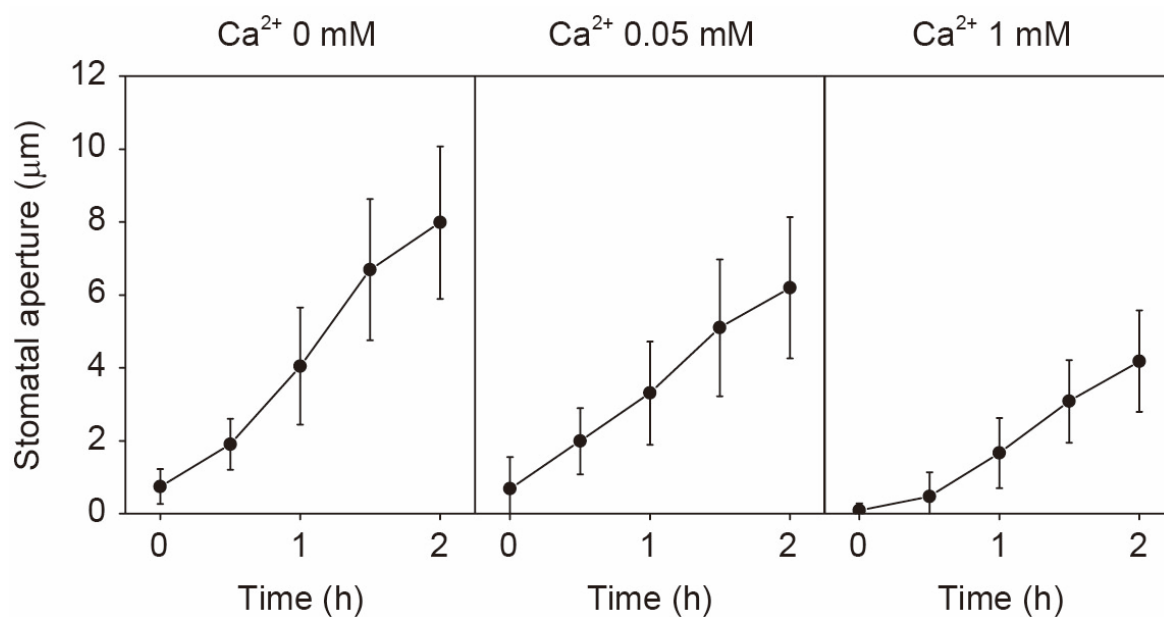


Fig. 2-11. Stomatal responses to Ca^{2+} in the buffer-containing gels. The gels contained 30 mM KCl, 10 mM MES-KOH (pH 6.15), 1% (w/v) gellangum and CaCl_2 . The concentration of CaCl_2 was set at 0, 0.05 and 1 mM. In the Ca^{2+} 0 mM gel, 1 mM MgCl_2 was dissolved instead of CaCl_2 . The epidermal strips were illuminated with white light (PPFD $700 \mu\text{mol m}^{-2} \text{s}^{-1}$) for 2 h from the onset of the experiment. CO_2 concentration was kept at 100 ppm. Data are the mean \pm SD of at least 17 stomata.

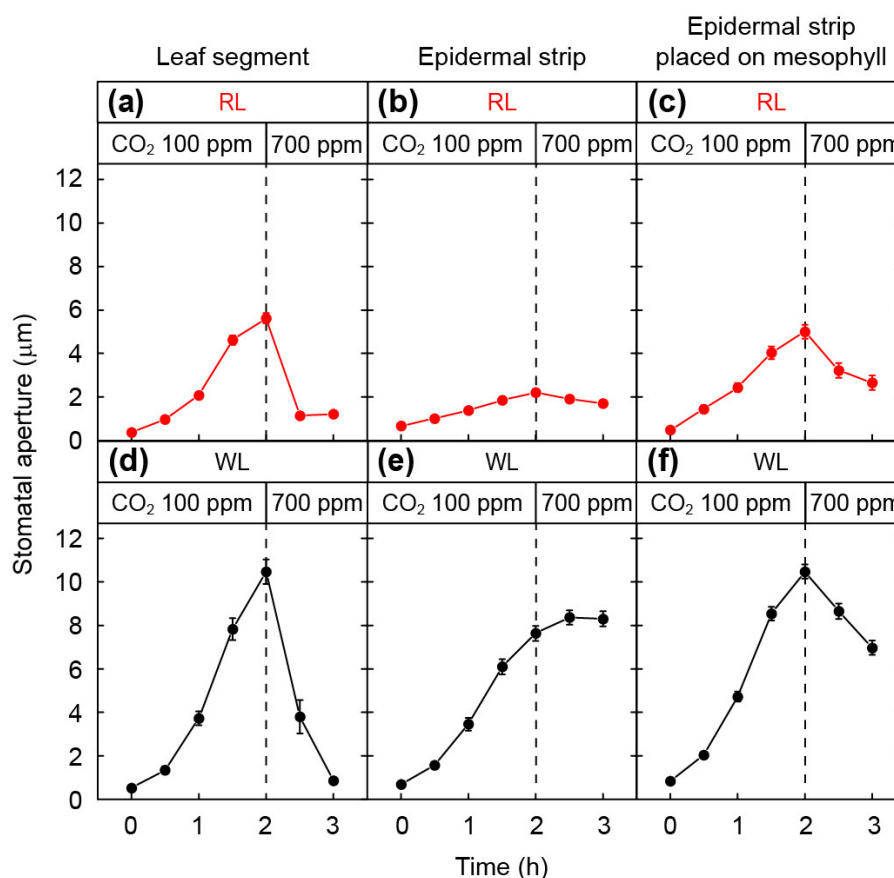


Fig. 2-12. Stomatal responses with the Ca^{2+} -free gels. Changes in the stomatal aperture of the leaf segments (a and d), the epidermal strips (b and e), and the epidermal strips placed on mesophyll segments (c and f) in *C. communis* are shown. The samples were placed on 1% (w/v) gellan gum gels containing 30 mM KCl, 1 mM MgCl_2 and 10 mM MES-KOH (pH 6.15). In this gel, Mg^{2+} was used as a cross-linker for solidification of gellan gum. The epidermal strips were floated on the Ca^{2+} -free buffer containing 30 mM KCl, 10 mM MES-KOH (pH 6.15), before they were placed on the Ca^{2+} -free gels or the mesophyll segments. The samples were illuminated from the adaxial side with red light (RL; PPFD $550 \mu\text{mol m}^{-2} \text{s}^{-1}$) or white light (WL; PPFD $700 \mu\text{mol m}^{-2} \text{s}^{-1}$). Data are the mean \pm SEM of at least 26 stomata. Before measurements, the samples were kept in the dark for 0.5 h to close the stomata. In (a)–(f), the CO_2 concentration was changed from 100 ppm to 700 ppm at 2 h after the onset of illumination (dashed lines).

Chapter 3

Analysis on the characteristics of the mesophyll signals

3-1. Introduction

In chapter 2, it has been shown that the stomatal responses to light and CO₂ were controlled by mesophyll. Stomatal opening in red light was especially dependent on mesophyll. It has been revealed that stomatal responses in red light is highly dependent on photosynthesis (e.g. Sharkey & Raschke; 1981; Messinger *et al.*, 2006; Wang *et al.*, 2011). Therefore, it was probable that the stomatal opening in red light was induced or accelerated by photosynthesis in mesophyll. However, it has not been investigated whether the stomatal closure is dependent on photosynthesis.

As mentioned in Mott *et al.* (2008), I also claimed that mesophyll released ‘mesophyll signals’ that controlled stomatal responses. It was unclear whether the mesophyll signals were aqueous or gaseous. Sibbernsen & Mott (2010) found that stomatal opening declined when various liquids were injected into the intercellular spaces of leaves, and suggested that mesophyll signals were gaseous. In contrast, Lee & Bowling (1993, 1995) showed that stomata responded to light when epidermal strips were floated on the solution that had been illuminated with mesophyll cells or chloroplasts. When the epidermal strips were floated on the same buffer without mesophyll or chloroplasts, the stomata did not respond to light (Lee & Bowling, 1992, 1995). Stomatal opening was also observed when epidermal strips were floated on the supernatant of the solution that had been illuminated with mesophyll cells (Lee & Bowling, 1992). The authors also observed that the guard cell protoplasts swelled in the supernatant (Lee & Bowling, 1993). These studies indicated that mesophyll signals were aqueous.

In this chapter, I investigated whether stomatal responses, accelerated by mesophyll, were dependent on photosynthesis, using the inhibitor of photosynthetic electron transport. I examined whether mesophyll signals moved to the epidermis via the aqueous phase, by inserting various films between the epidermal strips and the mesophyll segments. Metabolites in the epidermal strips were analyzed with CE-MS. I also analyzed the stomatal responses to the organic acids detected as candidates of the mesophyll signals.

3-2. Materials and Methods

Plant materials

Commelina communis plants were grown as described in chapter 2. *Commelina benghalensis* plants were multiplied by a cutting. The growth condition for *C. benghalensis* was same as that for *C. communis* described in chapter 2.

DCMU treatment

The distal half of the leaf lamina was cut off and the resultant half leaf with the petiole was immersed in a solution containing 0.2 mM 3-(3,4-dichlorophenyl)-1,1-dimethylurea (DCMU; Sigma-Aldrich Japan, Tokyo, Japan) and 0.1% (v/v) dimethyl sulfoxide (DMSO; Wako, Osaka, Japan). The pressure was reduced to 0.08 MPa for 5 min, to infiltrate the solution into the leaf. 0.1% (v/v) DMSO was used as the control. The infiltrated leaf was maintained in the dark for approximately 1.5 h to allow the solution in the intercellular spaces to evaporate. The leaf segment was then prepared as described in Fig. 2-3. The leaf segment was placed in the chamber and maintained in the dark for more than 0.5 h before measurements were taken.

Measurement of chlorophyll fluorescence

Chlorophyll fluorescence was measured using a pulse amplitude-modulated fluorometer (PAM-2500; Waltz, Effeltrich, Germany). The measuring light (PPFD $0.03 \mu\text{mol m}^{-2} \text{s}^{-1}$) was switched on and minimum fluorescence (F_0) was measured. Next, a saturation pulse (PPFD $4,000 \mu\text{mol m}^{-2} \text{s}^{-1}$) was provided for 0.8 s to obtain maximum fluorescence (F_m). Actinic light (PPFD $200 \mu\text{mol m}^{-2} \text{s}^{-1}$) was then provided for 2 min to observe the Kautsky transient.

Sample preparations

(1) Epidermal strip and the mesophyll segment sandwiching a film (Fig. 3-1)

The mesophyll segment (10 mm square) was prepared by peeling off the abaxial epidermis and was placed on the buffer-containing gel. A polyethylene (L-LDPE; Okura, Kagawa, Japan) or cellophane (PT#300; Heiko, Tochigi, Japan) film (20 mm square, thickness 50 μm) with a square hole (4 mm square) in the center of the film was placed on the mesophyll segment. The epidermal strip was placed on the film. A piece of filter paper (Whatman No. 5; Whatman international, Maidstone, UK) with a circular hole (5 mm in diameter), that had been

dipped in a buffer containing 30 mM KCl, 1 mM CaCl₂, and 10 mM MES-KOH (pH 6.15), was placed on the sample to prevent desiccation. A plastic sheet with a hole (5 mm in diameter) was placed on the filter paper to prevent excess evaporation from the filter paper.

(2) Epidermal strip and the mesophyll segment sandwiching a dialysis membrane

The mesophyll segment (10 mm square) was prepared by peeling off the abaxial epidermis and was placed on the buffer-containing gel. A dialysis membrane (Biotech cellulose ester membrane; Spectrum Laboratories, Inc., Rancho Dominguez, CA, USA) with a square hole (4 mm square) in the center of the membrane was placed on the mesophyll segment. The epidermal strip was placed on the dialysis membrane to cover the mesophyll segments and the dialysis membrane. A plastic sheet with a hole (5 mm in diameter) was placed on the filter paper to prevent excess evaporation from the sample.

Quantitative metabolome analysis by CE-MS

I quantified the metabolites in the epidermal strips placed directly on the buffer-containing gels and in the epidermal strips peeled off from the leaf segments of *C. communis*. The epidermal strips were sampled at 0.5 h after the onset of the treatment in the dark at 100 ppm CO₂, or at 2 h after the onset of the treatment in red light (PPFD 550 $\mu\text{mol m}^{-2} \text{s}^{-1}$) at 100 ppm CO₂. According to the method of Sato *et al.* (2004) and Sato & Yanagisawa (2010), metabolites were extracted and determined with slight modifications. Frozen epidermal strips were ground in liquid N₂ with a mortar and pestle. After adding 200 μL of ice-cold 80% (v/v) methanol, 200 μL of an internal standard solution containing 200 μM 1,4-piperazine diethane sulfonic acid (PIPES) and L-methionine sulfone (MeS) were added to the extract. The mixture was centrifuged at $1,900 \times g$ for 1 min at 4°C. The supernatant was filtered through a 3 kD cut-off membrane (PALL Corporation, Port Washington, NY, USA) by the centrifugation at $15,000 \times g$ for 15 min at 4°C. The filtered samples were freeze-dried using a freeze dryer (Alpha 2-4 LDplus Freeze Dryer; Martin Christ, Osterode am Harz, Germany) and stored at -80°C. The samples were dissolved in 20 μL of Milli-Q water and mixed well with a mixer (MT-360; TOMY Seiko Co., Ltd., Tokyo, Japan). The samples were analyzed using a capillary electrophoresis system with a built-in diode-array detector, a 1100 series MSD mass spectrometer, a 1100 series isocratic HPLC pump, a G1603A CE-MS adapter kit and a G1607A

CEESI-MS sprayer kit (all from Agilent Technologies, Santa Clara, CA, USA). The amounts of metabolites were calculated using the values of internal standards.

Analysis of stomatal responses to organic acids

When I launched the analysis of the stomatal responses to organic acids, *C. communis* plants were not available. Instead of *C. communis* plants, I used *C. benghalensis* plants for this analysis. The epidermes of *C. benghalensis* were also easily peeled from the abaxial side of leaves.

Abaxial epidermes were peeled off from dark-treated leaves of *C. benghalensis*. Citrate, fumarate or malate was dissolved in the buffer containing 30 mM KCl, 100 μ M CaCl₂, and 10 mM MES-KOH (pH 6.15). The epidermal strips were floated on the buffer and illuminated with red light (PPFD 550 μ mol m⁻² s⁻¹) for 2 h at 23°C. During the experiment, CO₂ concentration was maintained at 390 ppm.

Statistical analysis

In Tables 3-1 and 3-3, the differences between the mean values of data were analysed using Student's *t*-test or Welch's *t*-test. In Table 3-2, the differences between the mean values of data were analysed using ANOVA and Tukey's multiple comparison test. In Figs. 3-3, 4 and 5, the data are shown as means \pm SEM of at least three independent experiments. In Figs. 3-6 and 7, the data are shown as means \pm SD. In Fig. 3-6, the differences between the mean values of data were analysed using Student's *t*-test or Welch's *t*-test. In Fig. 3-7, differences between the mean values of data were analysed using ANOVA and Tukey's multiple comparison test. All statistical analyses were conducted using the R statistical software package (ver. 2.15.1.; R Development Core Team 2003).

3-3. Results

Effects of photosynthesis on stomatal responses

To investigate the role of photosynthesis on the stomatal responses, I used the leaves treated with 0.2 mM DCMU in a solution of 0.1% (v/v) DMSO. The control leaves were treated with 0.1% (v/v) DMSO.

Chlorophyll fluorescence transients in these leaves are shown in Fig. 3-2. Chlorophyll

fluorescence in the control leaf sharply increased in the actinic light and then gradually decreased, exhibiting the typical Kautzky transient (Fig. 3-2a). Chlorophyll fluorescence in the DCMU-treated leaf increased to the level attained by the saturating flash, and remained at that level for 2 min, indicating the complete inhibition of photosynthetic electron transport (Fig. 3-2b).

Changes in the stomatal aperture in the control leaf segments and the DCMU-treated leaf segments in red and white light are shown in Table 3-1 and Fig. 3-3. In red light, stomata in the control leaf segments opened rapidly at 100 ppm CO₂ and closed rapidly at 700 ppm CO₂ (Fig. 3-3a). In contrast, stomata in the DCMU-treated leaf segments hardly opened at 100 ppm CO₂ (Table 3-1 and Fig. 3-3b). Since the stomata hardly opened in the DCMU-treated leaf segments at the onset of 700 ppm CO₂ (shown in Fig. 3-3b), it was difficult to determine whether the stomata in the DCMU-treated leaf segments close.

In white light, stomata in the control leaf segments opened and closed rapidly (Fig. 3-3c). Stomata in the DCMU-treated leaf segments opened at 100 ppm CO₂ (Fig. 3-3d and e), however, the aperture was smaller compared to that in the control leaf segments (Table 3-1). Stomata in the DCMU-treated leaf segments closed rapidly at 700 ppm CO₂ (Fig. 3-3d).

Effects of the apoplastic continuum between the epidermis and the mesophyll

I investigated the importance of physical contact between the epidermis and mesophyll in the stomatal responses. Small molecules in the liquid may diffuse through a cellophane film, but not through polyethylene. I inserted polyethylene or cellophane films (50 µm thick) between the epidermal strips and the mesophyll segments. Aqueous substances released from the mesophyll segments would reach the epidermal strips in the cellophane-inserted samples, and would not in the polyethylene-inserted samples. In these film-inserted samples, the stomata positioned in the hole were observed.

The data in Table 3-2 and Fig. 3-4 show the changes in the stomatal aperture in the epidermal strips placed directly on the mesophyll segments, the epidermal strips placed on the mesophyll segments with polyethylene films inserted between them (the polyethylene film-inserted sample) and the epidermal strips placed on the mesophyll segments with cellophane films inserted between them (the cellophane film-inserted sample) in red or white light. In red light, stomata opened widely in the epidermal strips placed directly on the mesophyll segments,

and in the cellophane film-inserted samples at 100 ppm CO₂ (Fig. 3-4a and c). The increment of the stomatal aperture in the cellophane film-inserted samples at 2 h after the onset of illumination was 1.5 μm greater in average than that of the epidermal strips placed directly on the mesophyll segments (Table 3-2). In contrast, stomata opened only slightly in the polyethylene film-inserted sample at 100 ppm CO₂ (Table 3-2 and Fig. 3-4b). Stomata closed rapidly in the epidermal strips placed directly on the mesophyll segments and in the cellophane film-inserted samples at 700 ppm CO₂ (Fig. 3-4a and c). Stomata hardly closed within 1 h in the polyethylene film-inserted samples at 700 ppm CO₂ (Table 3-2 and Fig. 3-4b).

In white light, the stomata opened widely in all samples (Fig. 3-4d, e and f). The increment of the stomatal aperture in the cellophane film-inserted samples was highest (5.61 μm at 2 h after the onset of illumination; see Table 3-2). Stomata closed rapidly in the epidermal strips placed directly onto the mesophyll segments and in the cellophane film-inserted samples at 700 ppm CO₂ (Fig. 3-4d and f). Stomata hardly closed within 1 h in the polyethylene film-inserted sample at 700 ppm CO₂ (Table 3-2 and Fig. 3-4e).

Stomata in the polyethylene film-inserted samples responded to CO₂ in a manner similar to the stomata in the epidermal strips, regardless of light color (Fig. 2-9b versus Fig. 3-4b, Fig. 2-9e versus Fig. 3-4e).

Effects of the dialysis membranes inserted between the epidermal strips and the mesophyll segments

The molecular size of mesophyll signals were estimated by inserting the dialysis membranes having the 4 mm square hole between the epidermal strips and the mesophyll segments. Two types of dialysis membranes were used; one with the molecular weight cut off (MWCO) 500–1,000 D and the other with MWCO 100–500 D. The mesophyll signals smaller than the pore of the dialysis membranes would reach the guard cells. The stomata positioned in the 4 mm square hole of the dialysis membrane were observed.

The data in Table 3-3 and Fig. 3-5 show the changes in the stomatal aperture in the epidermal strips placed on the mesophyll segments with the dialysis membranes inserted between them. In red light, stomata opened widely in the samples inserted with either the MWCO 500–1,000 D or the MWCO 100–500 D dialysis membranes (Fig. 3-5a and b). The increment of the stomatal aperture in the samples inserted with the MWCO 100–500 D dialysis

membranes was greater than that in the samples inserted with the MWCO 500–1,000 D dialysis membranes by 0.69 μm at 2 h after the onset of illumination (Table 3-3). Stomata in the samples inserted with either MWCO 500–1,000 D or MWCO 100–500 D dialysis membranes closed rapidly at 700 ppm CO_2 (Table 3-3 and Fig. 3-5a, b).

In white light, stomata opened widely in the samples inserted with either MWCO 500–1,000 D or MWCO 100–500 D dialysis membranes (Fig. 3-5c and d). The increment of the stomatal aperture in the samples inserted with the MWCO 100–500 D dialysis membranes was greater than that in the samples inserted with the MWCO 500–1,000 D dialysis membranes by 0.76 μm at 2 h after the onset of illumination (Table 3-3). On the other hand, stomatal closure in white light was somewhat delayed in the samples inserted with MWCO 100–500 D dialysis membranes, compared with the samples inserted with MWCO 500–1,000 D dialysis membranes (Fig. 3-5c and d).

Metabolites in the leaf epidermes of *C. communis*

I quantified the metabolites in the epidermal strips placed directly on the buffer-containing gels and in the epidermal strips peeled off from the leaf segments, in order to narrow down the candidates of mesophyll signals. The data in Fig. 3-6 show the concentrations of several metabolites in the epidermal strips. The epidermal strips were sampled at 0.5 h after the onset of the treatment in the dark at 100 ppm CO_2 , or at 2 h after the onset of the treatment in red light (PPFD 550 $\mu\text{mol m}^{-2} \text{s}^{-1}$) at 100 ppm CO_2 .

After the treatment in the dark at 100 ppm CO_2 for 0.5 h, the concentrations of pyruvate, PGA, ATP and nicotinamide adenine dinucleotide phosphate (NADP) in the epidermal strips peeled off from the leaf segments were significantly higher than those in the epidermal strips placed directly on the buffer-containing gels. After the treatment in red light at 100 ppm CO_2 , the concentrations of malate, citrate, fumarate and *cis*-aconitate in the epidermal strips peeled off from the leaf segments were significantly higher than those in the epidermal strips placed directly on the buffer-containing gels (Fig. 3-6).

Stomatal responses to organic acids

As shown in Fig. 3-6, after the treatment in red light at 100 ppm CO_2 , the concentrations of malate, citrate, and fumarate in the epidermal strips peeled off from the leaf segments of *C.*

communis were significantly higher than those in the epidermal strips placed directly on the buffer-containing gels. In addition, the concentrations of malate, citrate and fumarate were relatively high compared with other metabolites. Thus, I analyzed the stomatal responses to those organic acids in *C. benghalensis*.

Citrate promoted stomatal opening in the range from 0.01 to 10 mM in *C. benghalensis* (Fig. 3-7). 100 mM citrate, however, did not promote stomatal opening. Fumarate and malate had no effect of stomatal opening (Fig. 3-7). Unlike citrate, stomatal closure was significantly induced by the addition of 10 mM fumarate or malate.

3-4. Discussion

Relationship between stomatal responses and photosynthesis

Stomatal opening

Previous studies supported the contention that photosynthesis in both guard cells and mesophyll was involved in the regulation of stomatal responses (e.g. Sharkey & Raschke, 1981; Messinger *et al.*, 2006; Wang *et al.* 2011). It was also known that the chloroplasts in guard cells exhibited high photosynthetic electron transport activities (Lawson *et al.*, 2002, 2003; Lawson, 2009). In chapter 2, it was suggested that the mesophyll was required for the rapid stomatal opening in both red light and white light. Moreover, stomata in the leaf segments that had been treated with DCMU, which is a potent inhibitor of photosynthetic electron transport, hardly opened in red light at 100 ppm CO₂ (Table 3-1 and Fig. 3-3b). In white light, stomata in the leaf segments treated with DCMU opened slowly than those in the control leaf segments (Table 3-1 and Fig. 3-3c, d). Therefore, it was concluded that stomatal opening in the leaf segments was dependent on the photosynthesis in mesophyll cells and, in other words, hardly dependent on the photosynthesis in guard cells.

Stomata in the leaf segments treated with DCMU opened in white light (Fig. 3-3d and e). When stomata open, H⁺-ATPase in guard cell plasma membranes consumes cytosolic ATP (Shimazaki *et al.*, 2007). Since photosynthesis was inhibited in the DCMU-treated leaf segments, the ATP for H⁺-ATPases would be produced by respiration, with carbohydrates stored in the guard cell being consumed (Mawson, 1993). However, stomata in the leaf segments treated with DCMU did not open in red light (Fig. 3-3b), even though carbohydrates would be available. Although blue light activated H⁺-ATPases in guard cell protoplasts (without

mesophyll cells), red light had no such function in guard cell protoplasts (Taylor & Assmann, 2001). Hence, it is probable that mesophyll signals induce stomatal opening via the activation of H⁺-ATPase in guard cells (see Chapter 5).

In addition to the regulation of H⁺-ATPases, the regulation of S-type anion channels in guard cells would be also important for the fast stomatal opening. In the intact plants, the inhibition of S-type anion channels in guard cells occurred in red light or at low CO₂ (Roelfsema *et al.*, 2002; Marten *et al.*, 2008). Loss of SLAC1, a major S-type anion channel in guard cells, leads to the slow stomatal closure in the dark (Negi *et al.*, 2008; Vahisalu *et al.*, 2008). In other words, the deactivation of S-type anion channels would lead to fast stomatal opening in the light. Mesophyll signals at low CO₂ in the light may deactivate S-type anion channels, and accelerate the stomatal opening.

Stomatal closure

Stomata in the leaf segments treated with DCMU closed rapidly in white light at 700 ppm CO₂ in a manner similar to that of the control (Fig. 3-3c and d). Hence, I asked what would be responsible for the rapid stomatal closure in the DCMU-treated leaf segment. Since photophosphorylation was inhibited in the DCMU-treated leaf segments, the ATP required for stomatal opening would decline. However, stomata in the DCMU-treated leaf segments continued to gradually open for at least 3 h when CO₂ concentration was maintained at 100 ppm (Fig. 3-3e). On the basis of this information, it is unlikely that the stomatal closure in the DCMU-treated leaf segments at 700 ppm CO₂ was caused by a shortage of ATP. It is also unlikely that stomatal closure at 700 ppm CO₂ is dependent on mesophyll photosynthesis. In contrast to the effects of low CO₂, S-type anion channels were activated at high CO₂ (Roelfsema *et al.*, 2002). Mesophyll signals at 700 ppm CO₂ may cause the activation of the S-type anion channels for the fast stomatal closure.

Mesophyll signals move from the mesophyll to the epidermis via the apoplast

My data demonstrated that the mesophyll played a critical role in controlling stomatal aperture. Like previous studies, I also support the existence of ‘mesophyll signals’ (substances controlling stomatal aperture), which are released from mesophyll and move toward the epidermis (Lee & Bowling, 1992, 1993, 1995; Mott *et al.*, 2008). Sibbersen & Mott (2010)

found that stomata close rapidly when liquids are microinjected into the intercellular spaces of leaves. Since the transfer of gaseous substances from the mesophyll to the epidermis was blocked by microinjection, the authors suggested that mesophyll signals should be gaseous. However, the results of Sibbersen & Mott (2010) would not rule out the involvement of aqueous mesophyll signals. My study showed that mesophyll signals inducing stomatal opening are probably produced in the course of photosynthesis and released from mesophyll. For photosynthesis, a CO₂ supply to the mesophyll is required. When the intercellular space is immersed, the CO₂ supply to the mesophyll is blocked, which would consequently suppress the production of both gaseous and aqueous mesophyll signals. It is also possible that the liquid occupying the substomatal cavities suppresses the respiration in guard cells, inhibiting the O₂ supply from intercellular space to the guard cells.

I examined whether the mesophyll signals were aqueous. Small molecules in the liquid may diffuse across the cellophane film, but not across the polyethylene one. I inserted these films between the epidermal strips and the mesophyll, and investigated whether the mesophyll signals controlling the stomatal responses were aqueous. In my system, the mesophyll segments were sandwiched by the gels and the films having the square holes (Fig. 3-1). As described in the ‘stomatal opening’ section in this chapter, stomatal opening was strongly dependent on the photosynthesis. With the film having no holes, CO₂ for photosynthesis cannot be supplied to the mesophyll and thereby the release of the mesophyll signals would be inhibited. Therefore, I used the films having the square holes to deliver the CO₂ through the stomata in the epidermis to the mesophyll (Fig. 3-1).

When the polyethylene films having the square holes (50 μm thick) was inserted between the epidermal strips and the mesophyll, the stomata could not respond to CO₂ (Fig. 3-4b and e). However, when the cellophane film having the square holes (50 μm thick) was inserted between the epidermal strips and the mesophyll segments, the stomata opened at 100 ppm CO₂ (Fig. 3-4c and f) and closed at 700 ppm CO₂ (Fig. 3-4c and f). It was indicated that the stomata in the cellophane film-inserted samples rapidly responded to CO₂ in a manner similar to that the stomata in the leaf segments responded to CO₂ (Fig. 2-9a and d). The movements of the aqueous substances from the mesophyll should change dependently on the materials of the films. On the basis of these results, the mesophyll signals inducing both stomatal opening and closure appear to move from the mesophyll to the epidermis via the aqueous phase in the apoplast. Gaseous

substances could move from the mesophyll to the epidermis through the square hole in the polyethylene or cellophane film. If gaseous mesophyll signals were present, the effects on the regulation of stomatal apertures would be less important compared to those of the aqueous mesophyll signals.

Stomata in the cellophane film-inserted samples opened wider than those in the epidermal strips placed directly on the mesophyll (Table 3-2 and Fig. 3-4). The cellophane film might block the movements of the substances inducing the stomatal closure such as ABA and jasmonate from the mesophyll segments.

Estimation of the molecular size of mesophyll signals

Instead of the polyethylene or the cellophane films, the dialysis membranes were inserted between the epidermal strips and the mesophyll segments. Two types of the dialysis membranes were prepared; MWCO 500–1,000 D and MWCO of 100–500 D. In the samples that epidermal strips were placed directly on mesophyll segments, the substances released from mesophyll could move to the epidermal strips without any barrier. On the other hand, in the samples that polyethylene films were inserted between the epidermal strips and the mesophyll segments, movement of the aqueous substances from mesophyll would be completely blocked by the polyethylene films (Fig. 3-4b and e). When the mesophyll signals were smaller than the pores of the dialysis membranes, the mesophyll signals could move from the mesophyll segments to the epidermal strips, and therefore stomatal movements would be accelerated. In both red light and white light, stomatal opening was not repressed when the MWCO 100–500 D dialysis membranes were inserted (Figs. 3-5b and d). Therefore, the mesophyll signals inducing stomatal opening was estimated to be less than 500 D. Average molecular size of amino acid is 110 D. If the mesophyll signals are consisted from amino acids, the signals would be the peptides including less than 4 amino acids. Stomatal opening was faster with the MWCO 100–500 D dialysis membranes than with the MWCO 500–1,000 D dialysis membranes (Table 3-3). Substances that have the potential to induce stomatal closure such as ABA (M.W. 264) or sucrose (M.W. 342) might be trapped in the MWCO 100–500 D dialysis membranes, and consequently stomatal opening would be further enhanced.

Stomatal closure was slowed down with the MWCO 100–500 D dialysis membranes, especially in white light (Table 3-3). This suggested that the mesophyll signals inducing

stomatal closure at 700 ppm CO₂ would be partly trapped in the MWCO 100–500 D dialysis membrane. Thus, the molecular size of mesophyll signals inducing stomatal closure was estimated to be 100–1,000 D.

The molecular size of the mesophyll signals was estimated from Table 3-3 and Fig. 3-5. However, the results in Table 3-3 and Fig. 3-5 might be interpreted in another way. When the dialysis membranes were inserted between the epidermal strips and the mesophyll segments, the liquid junction between the epidermal strips and the mesophyll segments was possibly formed at the edge of the square hole in the dialysis membrane. The water contents in the dialysis membranes would decrease with the pore size of the dialysis membranes becomes smaller. The formation of the liquid junction would be easier with MWCO 500–1,000 D dialysis membranes than with MWCO 100–500 D dialysis membranes. From this point of view, the mesophyll signals might move from the mesophyll segments to the epidermal strips through the liquid junction at the edge of the square hole in MWCO 500–1,000 D dialysis membranes.

Stomatal responses to the candidates of mesophyll signals

I compared the concentrations of metabolites between the epidermal strips placed on the buffer-containing gels and the epidermal strips peeled off from the leaf segments (Fig. 3-6). The difference in the metabolite concentrations between them was due to the presence of the mesophyll. After the treatment in red light at 100 ppm CO₂, the amount of malate, citrate, fumarate and *cis*-aconitate in the epidermal strips peeled off from the leaf segments were significantly higher than those in the epidermal strips placed directly on the gels (Fig. 3-6). It was probable that those metabolites released from the mesophyll and moved to the epidermal strips. Namely, these metabolites would be the candidates of mesophyll signals related to the stomatal opening in red light. It is also possible that the mesophyll signals activated the respiration in the epidermal cells and thereby these metabolites increased.

I analyzed stomatal responses to malate, citrate and fumarate to investigate whether these organic acids to induce stomatal opening. As shown in Fig. 3-7, only citrate have the potential to induce stomatal opening. Citrate might be mesophyll signals related to stomatal opening. Fumarate and malate were proposed to be the signals that are derived from mesophyll and induce stomatal closure (Araújo *et al.*, 2011). The result in Fig. 3-7 was consistent with this proposal.

3-5. Tables

Table 3-1. Extents of stomatal opening and closure in the control leaf segments and the DCMU-treated leaf segments in *C. communis* (shown in Fig. 3-3)

	Control leaf segment (μm)	DCMU-treated leaf segment (μm)	<i>P</i> -value
RL opening¹⁾	3.03 \pm 0.13	0.18 \pm 0.06	< 0.001
RL closure²⁾	- 2.32 \pm 0.13	- 0.22 \pm 0.06	< 0.001
WL opening¹⁾	4.69 \pm 0.21	2.61 \pm 0.17	< 0.001
WL closure²⁾	- 3.04 \pm 0.16	- 2.33 \pm 0.20	0.00638

¹⁾ Difference between the stomatal aperture at 2 h and the stomatal aperture at 0 h.

²⁾ Difference between the stomatal aperture at 3 h and the stomatal aperture at 2 h.

RL, red light (PPFD 550 $\mu\text{mol m}^{-2} \text{s}^{-1}$); WL, white light (PPFD 700 $\mu\text{mol m}^{-2} \text{s}^{-1}$).

Data are shown as the mean \pm SEM of at least 54 stomata. *P*-values were calculated using Welch's *t*-test (RL and WL open) and Student's *t*-test (WL close).

Table 3-2. Extents of stomatal opening and closure in the epidermal strips placed directly on the mesophyll segments, the polyethylene film-inserted samples, and the cellophane film-inserted samples in *C. communis* (shown in Fig. 3-4)

	Epidermal strip placed on mesophyll (μm)	Polyethylene film (μm)	Cellophane film (μm)	<i>P</i> -value
RL opening¹⁾	3.18 \pm 0.14 ^a	0.73 \pm 0.11 ^b	4.72 \pm 0.34 ^c	< 0.001
RL closure²⁾	- 1.55 \pm 0.11 ^a	- 0.03 \pm 0.08 ^b	- 2.28 \pm 0.19 ^c	< 0.001
WL opening¹⁾	3.61 \pm 0.26 ^a	3.56 \pm 0.17 ^a	5.61 \pm 0.23 ^b	< 0.001
WL closure²⁾	- 2.29 \pm 0.19 ^a	- 0.13 \pm 0.09 ^b	- 2.70 \pm 0.12 ^a	< 0.001

¹⁾ Difference between the stomatal aperture at 2 h and the stomatal aperture at 0 h.

²⁾ Difference between the stomatal aperture at 3 h and the stomatal aperture at 2 h.

RL, red light (PPFD 550 $\mu\text{mol m}^{-2} \text{s}^{-1}$); WL, white light (PPFD 700 $\mu\text{mol m}^{-2} \text{s}^{-1}$).

Data are shown as the mean \pm SEM of at least 40 stomata. *P*-values were calculated using ANOVA. When ANOVA was significant at $P < 0.05$, Tukey's multiple comparison test among samples was conducted at the significance level of $P < 0.05$. Different lower case letters denote significant differences in Tukey's test for the data shown in each row.

Table 3-3. Extents of stomatal opening and closure in the epidermal strips placed on the mesophyll segments with dialysis membranes inserted between them in *C. communis* (shown in Fig. 3-5)

	MWCO 500–1,000 D (μm)	MWCO 100–500 D (μm)	<i>P</i> -value
RL opening¹⁾	3.57 \pm 0.18	4.26 \pm 0.24	< 0.05
RL closure²⁾	– 1.78 \pm 0.13	– 1.45 \pm 0.18	0.127
WL opening¹⁾	5.12 \pm 0.20	5.88 \pm 0.22	< 0.05
WL closure²⁾	– 1.64 \pm 0.13	– 1.11 \pm 0.17	< 0.05

¹⁾ Difference between the stomatal aperture at 2 h and the stomatal aperture at 0 h.

²⁾ Difference between the stomatal aperture at 3 h and the stomatal aperture at 2 h.

MVCO ranges of the dialysis membranes were 500–1000 D, and 100–500 D.

RL, red light (PPFD 550 $\mu\text{mol m}^{-2} \text{s}^{-1}$); WL, white light (PPFD 700 $\mu\text{mol m}^{-2} \text{s}^{-1}$).

Data are shown as the mean \pm SEM of at least 58 stomata. *P*-values were calculated using Welch's *t*-test (RL and WL close) and Student's *t*-test (WL open).

3-6. Figures

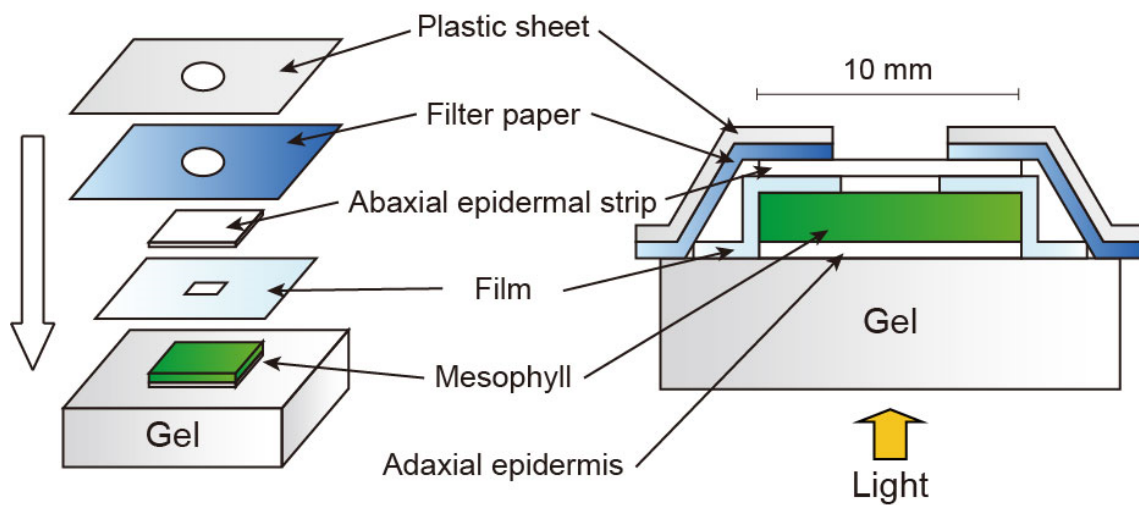


Fig. 3-1. Preparation of a film-inserted sample from *C. communis*. Components of the film-inserted sample are shown. The components were placed on the gel (Left). Side view of a film-inserted sample (Right). Light was illuminated from the gel side. A film having a square hole was inserted between an abaxial epidermal strip and a mesophyll segment. A piece of buffer-containing filter paper and a plastic sheet were placed on this sample to prevent desiccation. The filter paper and the plastic sheet had a common hole (5 mm in diameter). The holes were arranged to form one common hole.

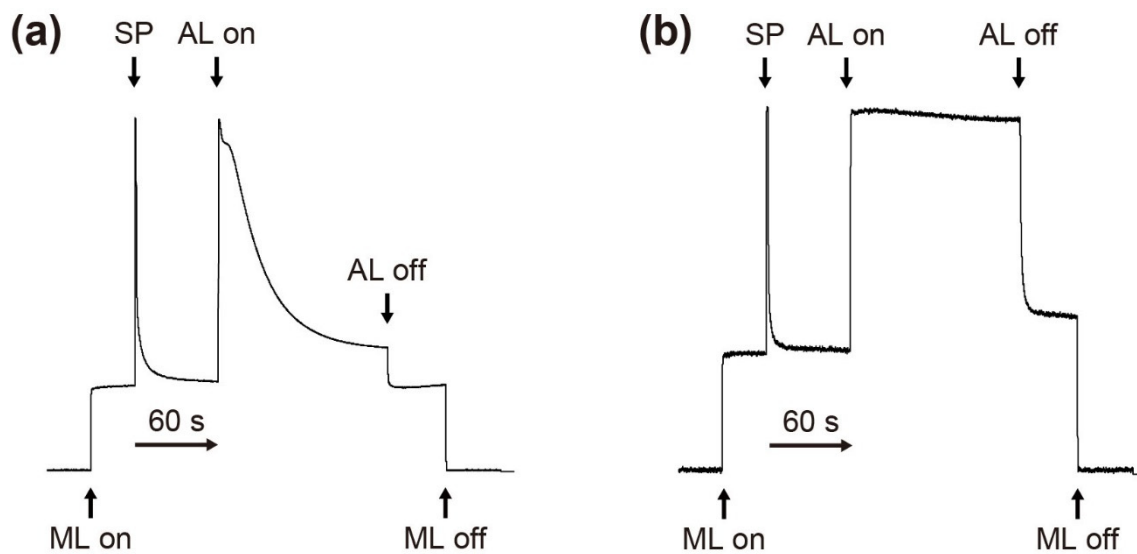


Fig. 3-2. Changes in chlorophyll fluorescence in a control leaf (a) and a DCMU-treated leaf of *C. communis* (b). The measuring beam, actinic light, and saturating flash were given from the adaxial side and the fluorescence from the adaxial side was recorded. Measuring light (ML; PPFD $0.03 \mu\text{mol m}^{-2} \text{s}^{-1}$) was switched on and minimum fluorescence (F_0) was measured. Next, the sample was illuminated with the saturation pulse (SP; PPFD $4,000 \mu\text{mol m}^{-2} \text{s}^{-1}$) for 0.8 s and maximum fluorescence (F_m) was measured. Finally, the sample was illuminated with actinic light (AL; PPFD $200 \mu\text{mol m}^{-2} \text{s}^{-1}$) for 2 min to observe the Kautsky transient.

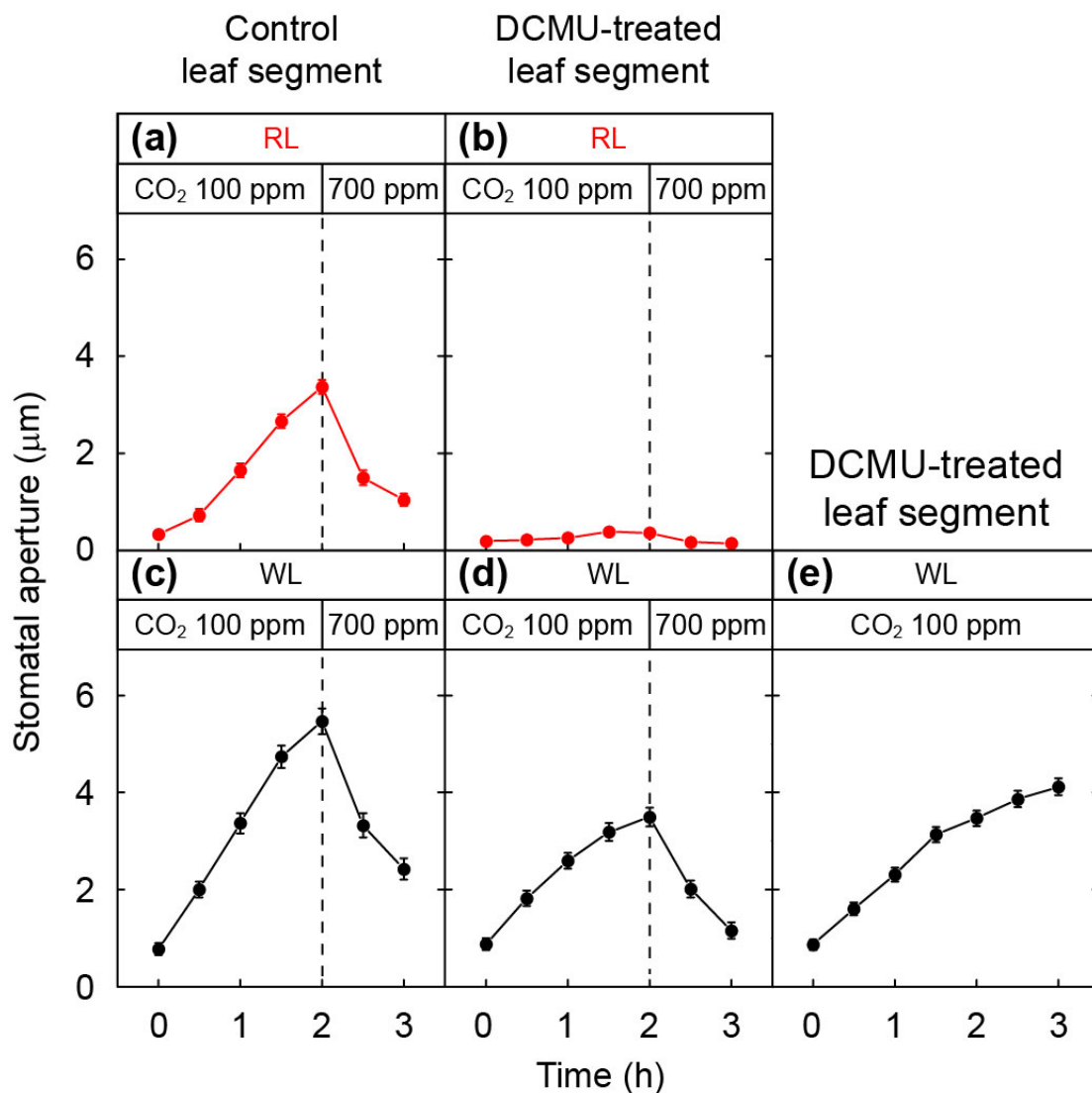


Fig. 3-3. Changes in the stomatal aperture in the control leaf segments (a and c) and the DCMU-treated leaf segments (b, d, and e) in *C. communis*. The samples were illuminated from the adaxial side with red light (RL; PPFD 550 $\mu\text{mol m}^{-2} \text{s}^{-1}$) or white light (WL; PPFD 700 $\mu\text{mol m}^{-2} \text{s}^{-1}$). Data are the mean \pm SEM of at least 55 stomata obtained from three independent measurements. Before measurements, the samples were maintained in the dark for 0.5 h to close the stomata. In (a)–(d), the CO₂ concentration was changed from 100 ppm to 700 ppm at 2 h after the onset of illumination (dashed lines). In (e), the CO₂ concentration was maintained at 100 ppm throughout the measurements.

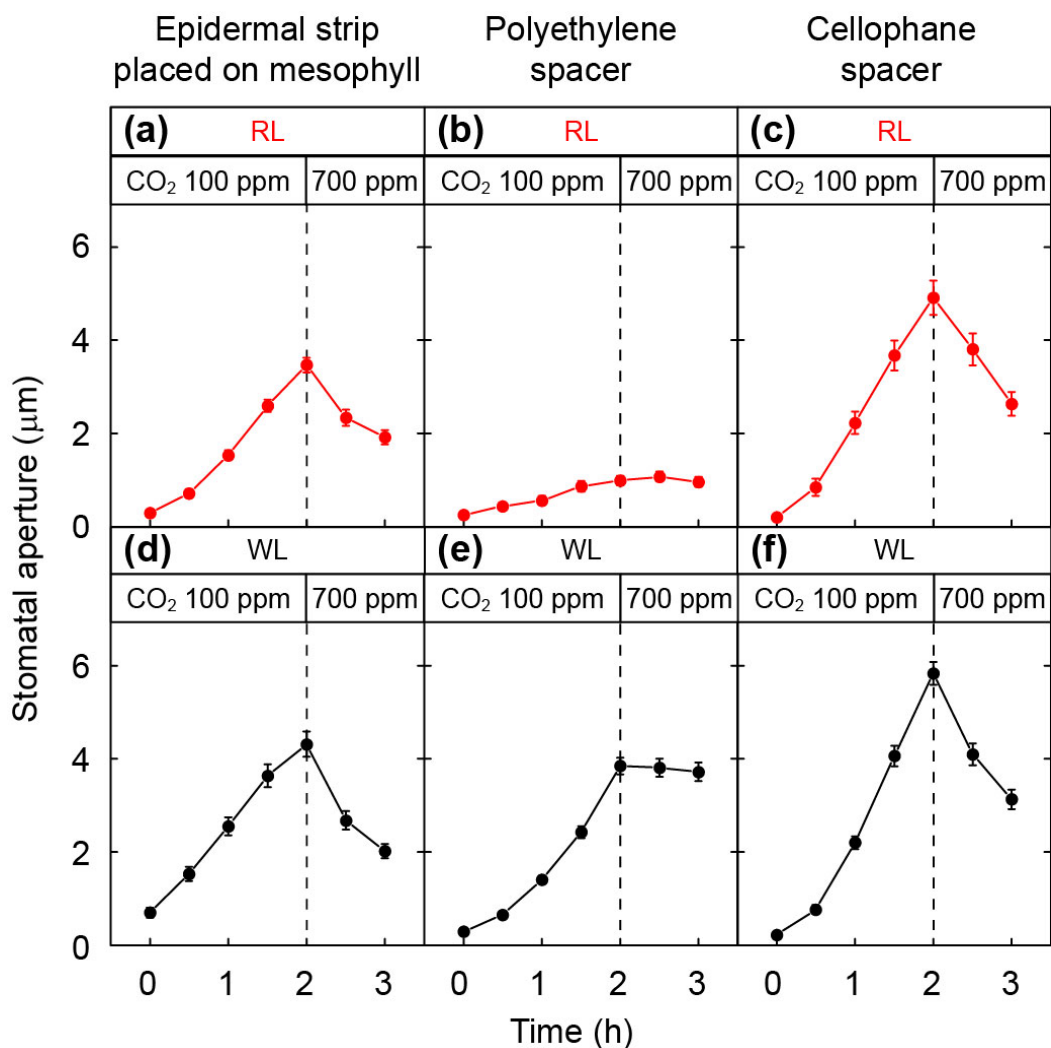


Fig. 3-4. Changes in the stomatal aperture in the epidermal strips placed directly on the mesophyll segments (a and d), the epidermal strips placed on the mesophyll segments with the polyethylene films inserted between them (b and e) and the epidermal strips placed on the mesophyll segments with the cellophane films inserted between them (c and f) in *C. communis*. The samples were illuminated from the adaxial side with red light (RL; PPFD $550 \mu\text{mol m}^{-2} \text{s}^{-1}$) or white light (WL; PPFD $700 \mu\text{mol m}^{-2} \text{s}^{-1}$). Data are the mean \pm SEM of at least 41 stomata obtained from three independent measurements. Before measurements, the samples were maintained in the dark for 0.5 h to close the stomata. The CO₂ concentration was changed from 100 ppm to 700 ppm at 2 h after the onset of illumination (dashed lines).

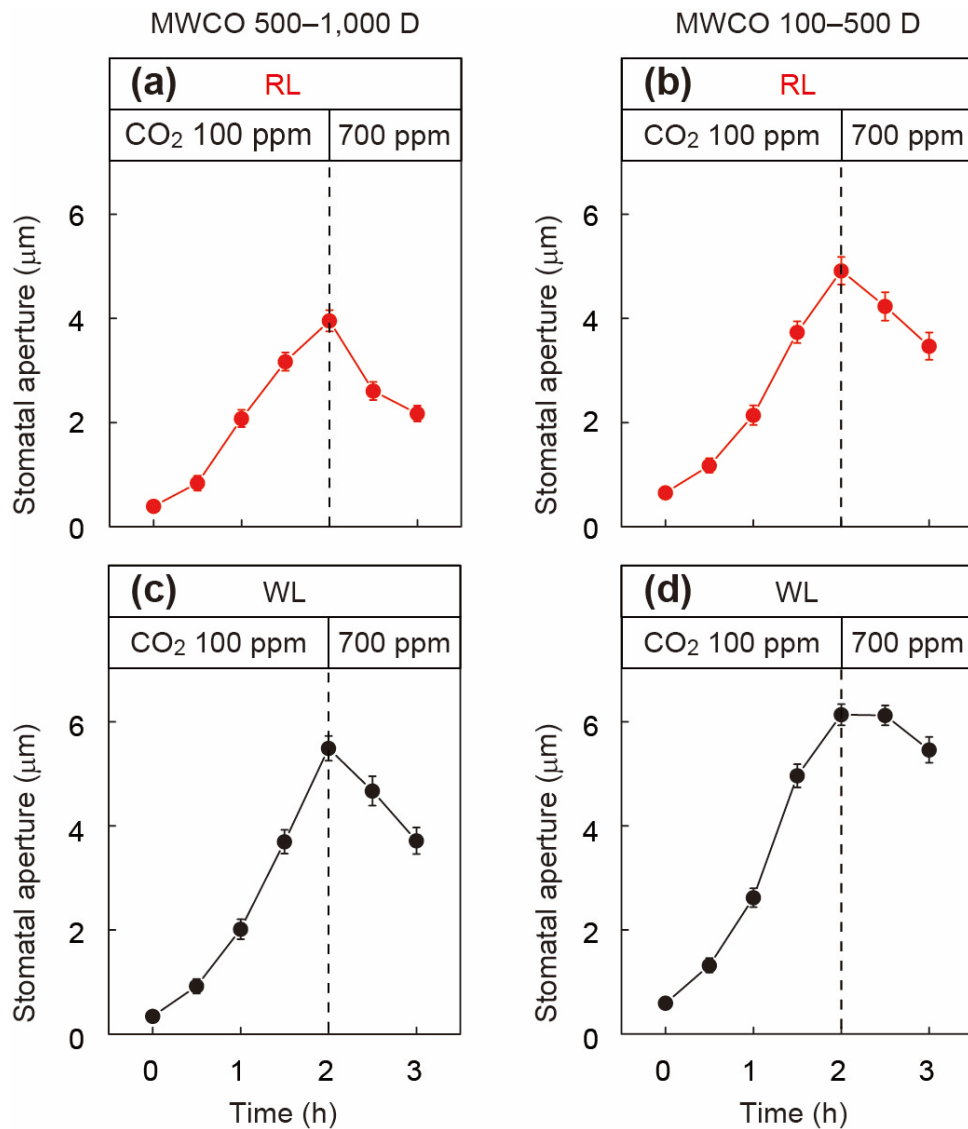


Fig. 3-5. Changes in the stomatal aperture in the epidermal strips placed on the mesophyll segments with dialysis membranes inserted between them in *C. communis*. MWCO ranges of the dialysis membranes were 500–1000 D (a and c) and 100–500 D (b and d). The sample was illuminated from the adaxial side with red light (RL; PPFD $550 \mu\text{mol m}^{-2} \text{s}^{-1}$) or white light (WL; PPFD $700 \mu\text{mol m}^{-2} \text{s}^{-1}$). Data are the mean \pm SEM of at least 58 stomata obtained from three independent measurements. Before measurements, the samples were kept in the dark for 0.5 h to close the stomata. The CO₂ concentration was changed from 100 ppm to 700 ppm at 2 h after the onset of illumination (dashed lines)

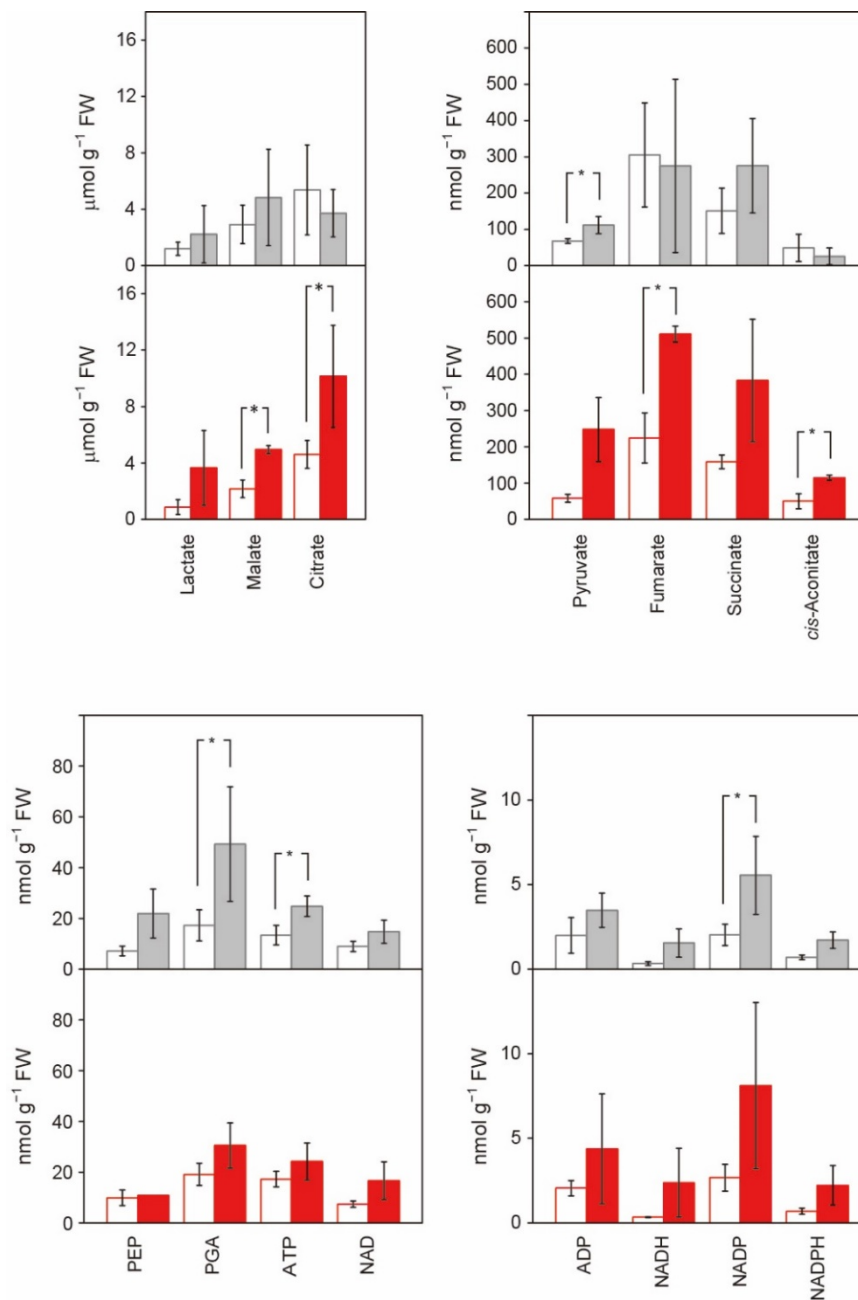


Fig. 3-6. Metabolite concentrations in epidermal strips of *C. communis*. The epidermal strips on the buffer-containing gel (open bars) and the epidermal strips peeled off from leaf segments (solid bars) were used for the quantitative analysis of metabolites. The epidermal strips were sampled at 0.5 h after the onset of dark/100 ppm CO₂ treatment (upper) or at 2 h after the onset of red light (PPFD 550 μmol m⁻² s⁻¹)/100 ppm CO₂ treatment (lower). Data are shown as the mean ± SD of at least 3 epidermal strips. *P*-values were calculated using Welch's *t*-test. Asterisks denote significant differences between the epidermes from the epidermal-strip samples and those from the leaf-segment samples in Welch's *t*-test (*P* < 0.05).

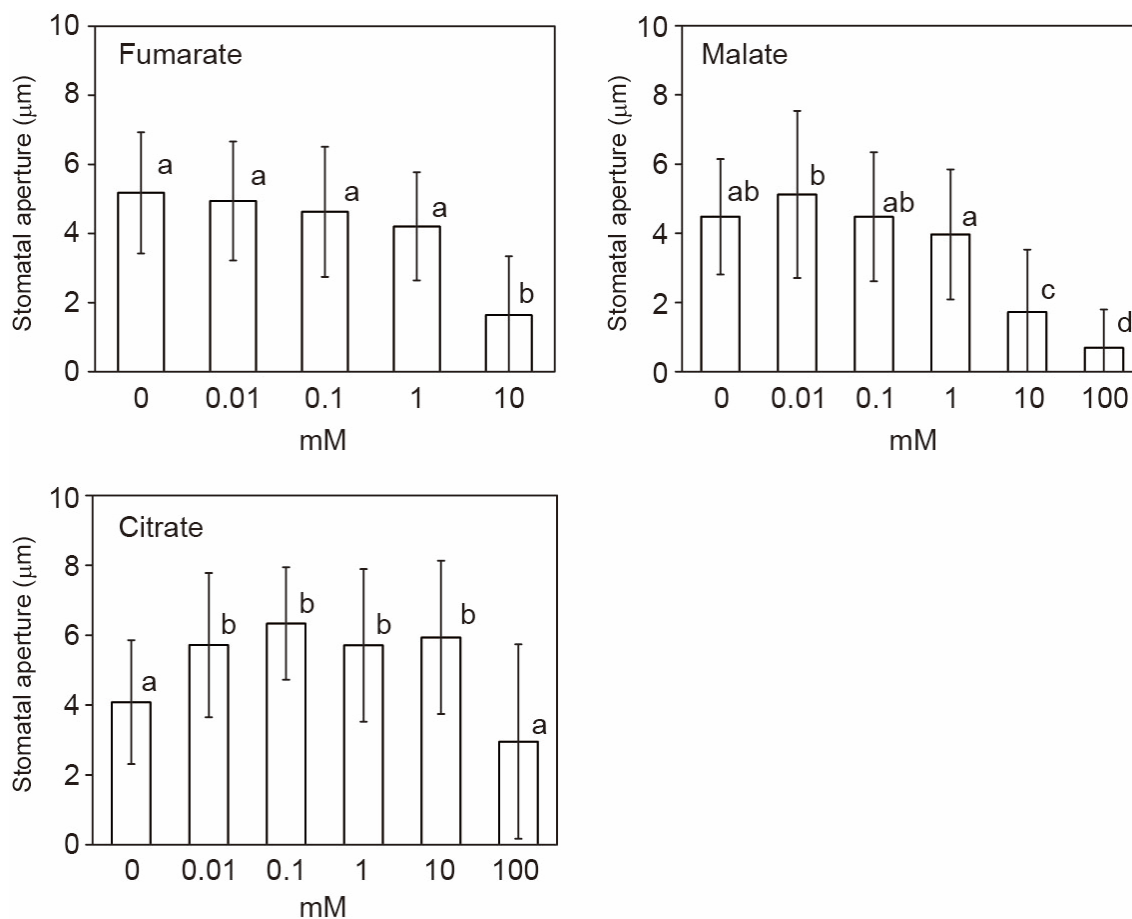


Fig. 3-7. Responses of stomata in the epidermal strips of *C. benghalensis* to organic acids. Each of the organic acids was dissolved in the buffer containing 30 mM KCl, 100 µM CaCl₂, and 10 mM MES-KOH (pH 6.15). The epidermal strips were illuminated with red light (PPFD 550 µmol m⁻² s⁻¹) for 2 h at 23°C. During the experiment, CO₂ concentration was maintained at 390 ppm. Data are shown as the mean ± SD of at least 45 stomata obtained from two epidermal strips. When ANOVA was significant at $P < 0.05$, Tukey's multiple comparison test among samples was conducted at the significance level of $P < 0.05$. Different lower case letters denote significant differences in Tukey's test conducted at the significance level of $P < 0.01$.

Chapter 4

Re-examination for the presence of the mesophyll signals

4-1. Introduction

As described in chapter 2, I revealed the presence of mesophyll signals by comparing the stomatal responses among leaf segments, epidermal strips and epidermal strips placed on the mesophyll segments. In the meantime, I noticed the problem of this method. In this method, the epidermal strips were directly placed on the buffer-containing gels and thereby the apoplastic solution in the epidermal strips would be replaced with the buffer solution. On the other hand, the epidermes in the leaf segments touched with the mesophyll, and not directly contacted with the buffer-containing gel. Therefore, apoplastic environment in the epidermal strips directly placed on the buffer-containing gels would be significantly different from that in the leaves.

Stomatal responses are significantly influenced by the apoplastic environment around the guard cells. For example, the electrochemical proton gradient across the plasma membrane, generated by the plasma membrane H^+ -ATPase, triggers stomatal movements (e.g. Shimazaki *et al.*, 2007). In numerous studies of stomatal physiology, the buffer solution for isolated leaf epidermes generally contains 5–10 mM MES (e.g. Travis & Mansfield, 1979; Kinoshita *et al.*, 2001; Hu *et al.*, 2010). Similarly, the buffer in my study contained 10 mM MES. On the other hand, for the analysis of H^+ extrusion from guard cell protoplasts (GCPs), the incubation buffer for GCPs contained 125–500 μ M MES (e.g. Shimazaki *et al.*, 1986; Mawson, 1993; Ueno *et al.*, 2005). Thus, I concerned about that 10 mM MES in the buffer solution was too strong, counteracted to the effect of H^+ extrusion from guard cells and repressed stomatal movements.

In the method described in chapter 2, stomatal responses in the epidermal strips might be repressed by the buffer-containing gels. If so, the presence of mesophyll signals might not be elucidated. Signals should be confirmed with the method that avoids the direct contact of the epidermes to the buffer. Therefore, I further developed a novel method to confirm the presence of mesophyll signals. It is widely known that stomatal responses are strongly influenced by the

circadian clock (e.g. Martin & Meidner, 1971; Hennessey *et al.*, 1993; Wang *et al.*, 2014). To diminish the variations in the stomatal aperture, the experiments were always started at the same time of the day.

4-2. Materials and Methods

Plant materials

Commelina communis plants were grown as described in chapter 2. The light and dark periods were 14 h (10:00–24:00) and 10 h (0:00–10:00).

Analysis of the stomatal responses in the epidermal strip overlaid on the other epidermal strip

Abaxial epidermes were peeled off from the dark-treated leaves of *C. communis*. I prepared two types of the epidermal strips (15 mm square and 10 mm square). After peeling off the two abaxial epidermes from the leaves, the epidermal strip (15 mm square) were immediately overlaid on the other epidermal strip (10 mm square) with their inner sides facing each other. I observed the stomatal responses in the area where the two epidermal strips were overlaid. The samples were treated in the dark for 0.5 h and subsequently in red light (RL; PPFD 550 $\mu\text{mol m}^{-2} \text{s}^{-1}$) or white light (WL; PPFD 700 $\mu\text{mol m}^{-2} \text{s}^{-1}$) for 3 h. CO₂ concentration was maintained at 100 ppm for 2.5 h and at 700 ppm for 1 h.

Analysis of the relationship between the stomatal responses and the circadian clock

Abaxial epidermes were peeled off from the dark-treated leaves of *C. communis* and placed on the gels containing 30 mM KCl, 100 μM CaCl₂ and 0.1 mM MES-KOH (pH 6.15). The epidermal strips were illuminated with blue light (BL; PPFD 50 $\mu\text{mol m}^{-2} \text{s}^{-1}$) supplemented with RL (PPFD 500 $\mu\text{mol m}^{-2} \text{s}^{-1}$) at 23°C for 2 h from 13:00, 16:00 or 19:00. Both red and blue monochromatic lights were provided by light-emitting photodiodes (red-LED, maximum intensity at 660 nm; blue-LED, maximum intensity at 450 nm; Valore, Kyoto, Japan). During the experiment, the CO₂ concentration was maintained at 390 ppm.

Analysis of stomatal responses to MES concentration in the gel

Abaxial epidermes were peeled off from the dark-treated leaves of *C. communis* and

placed on the gels containing 30 mM KCl, 100 μ M CaCl₂ and MES-KOH (pH 6.15). The MES concentration was 0.1, 1 or 10 mM. The epidermal strips were illuminated with BL (PPFD 50 μ mol m⁻² s⁻¹) supplemented with RL (PPFD 500 μ mol m⁻² s⁻¹) at 23°C for 2 h from 13:00. Both red and blue monochromatic lights were provided by light-emitting photodiodes (red-LED, maximum intensity at 660 nm; blue-LED, maximum intensity at 450 nm; Valore, Kyoto, Japan). During the experiment, the CO₂ concentration was maintained at 390 ppm.

Comparison of the roles in the stomatal responses between the light-treated and the dark-treated mesophyll

Plants were kept in the dark from 10:30. The leaf segments were prepared as illustrated in Fig. 2-3 from 11:30. The leaf segments on the buffer-containing gels were placed in the sample chamber. The sample chamber (190 × 120 × 10 mm) consisted of two aluminum blocks (a lid and a lower chamber). The lid had glass windows (150 × 100 mm). By circulating water from a temperature-controlled bath, the chamber temperature was maintained at 23°C. The gas flowing into the chamber was the mixture of N₂, O₂ and CO₂, and the CO₂ concentration and the dew point of the gas were controlled. The leaf segments in the chamber were illuminated from 12:00. The mesophyll segments with the adaxial epidermes were prepared by peeling off the abaxial epidermes from the leaf segment at 13:00. Also, the abaxial epidermes were peeled off from the dark-treated plants and immediately placed on the mesophyll segments without floating on the buffer solution. I illuminated the epidermal strips placed directly on the mesophyll segments from 13:30 for 1 h or 2 h.

Statistical analysis

In Table 4-1, the differences between the mean values of data were analysed using Student's *t*-test or Welch's *t*-test. In Fig. 4-1, the data are shown as means ± SD. In Figs. 4-2 and 3, the data of stomatal apertures in the epidermal strips placed on the buffer-containing gels are shown in the statistical box-chart plot. Kruskal-Wallis test and Steel-Dwass test for multiple comparison were conducted at a significance level of $P < 0.01$. In Fig. 4-4–Fig. 4-7, the data are shown as means ± SD. Differences between the mean values of the data were analysed using Student's *t*-test or Welch's *t*-test. All statistical analyses were conducted using the R statistical software package (ver. 2.15.1.; R Development Core Team 2003).

4-3. Results

Stomatal responses in the epidermal strips overlaid on the other epidermal strip

I observed the stomatal responses in the epidermal strip overlaid on the other epidermal strip with their inner sides facing each other (Table 4-1 and Fig. 4-1). In both RL and WL, stomata opened widely at 100 ppm CO₂ and closed rapidly at 700 ppm CO₂. The increment of the stomatal aperture in WL was greater than that in RL by 4.2 μm at 2 h after the onset of illumination (Table 4-1). At 700 ppm CO₂, the decrement of the stomatal aperture in WL was less than that in RL by 1.1 μm (Table 4-1).

Relationship between the stomatal responses and the circadian clock

I investigated whether the stomatal responses in the epidermal strips were influenced by the circadian clock. I analyzed the stomatal responses in the epidermal strips illuminated from 13:00, 16:00 or 19:00. Fig. 4-2 shows the stomatal aperture after the illumination of BL supplemented with RL at 390 ppm CO₂ for 2 h from 13:00, 16:00 or 19:00. The stomatal aperture in the epidermal strips illuminated from 13:00 was significantly highest (Fig. 4-2).

Effects of MES concentration in the buffer-containing gels on stomatal responses

To examine whether the MES concentration in the buffer-containing gel was too strong to induce stomatal opening, I placed the epidermal strips on the gels containing 0.1, 1 or 10 mM MES. Fig. 4-3 shows the data of the stomatal aperture after the illumination of BL supplemented with RL at 390 ppm CO₂ for 2 h. With the decrease of MES concentration, the stomatal aperture increased. The stomatal aperture with the gels containing 0.1 mM MES was significantly highest (Fig. 4-3).

Effects of pretreatment for the mesophyll segments on stomatal responses

To confirm that the hydropassive stomatal opening hardly occur with the newly developed method in this chapter, the epidermal strips from the dark-treated plants were placed on the mesophyll segments pretreated in the dark or in the red light, and kept in the dark at 390 ppm CO₂ for 1 h. Irrespective of the pretreatment, the stomata in the epidermal strips on the mesophyll segments hardly opened (Fig. 4-4).

I investigated whether the mesophyll segments pretreated in the light could open stomata

widely in the light. In the experiments shown in Fig. 4-5a, the mesophyll segments were pretreated in the dark or in BL (PPFD $50 \mu\text{mol m}^{-2} \text{s}^{-1}$) supplemented with RL (PPFD $500 \mu\text{mol m}^{-2} \text{s}^{-1}$). In every experiment, stomata in the epidermal strips placed on the mesophyll segments pretreated in BL supplemented with RL opened more widely than those in the epidermal strips placed on the mesophyll segments pretreated in the dark. In Fig. 4-5b, the mesophyll segments were pretreated in the dark or in RL (PPFD $500 \mu\text{mol m}^{-2} \text{s}^{-1}$). The pretreatment in RL also induced the wider stomatal opening than that in the dark (Fig. 4-5b).

Secondly, I kept the leaf segments at 100 ppm CO_2 for the pretreatment of mesophyll. I prepared the mesophyll segments pretreated in BL (PPFD $50 \mu\text{mol m}^{-2} \text{s}^{-1}$) supplemented with RL (PPFD $500 \mu\text{mol m}^{-2} \text{s}^{-1}$) or in RL (PPFD $500 \mu\text{mol m}^{-2} \text{s}^{-1}$) only. As shown in Fig. 4-6a, stomata with the mesophyll segments pretreated in BL supplemented with RL opened more widely. Unlike BL supplemented with RL illumination, the mesophyll segments from the leaf segments pretreated in RL only at 100 ppm CO_2 , did not enhance the stomatal opening, compared with the mesophyll segments from the leaf segments pretreated in the dark (Fig. 4-6b).

Effects of pretreatment at high CO_2

I investigated whether the mesophyll, pretreated at high CO_2 , had the effect of the acceleration of stomatal closure. For the pretreatment of mesophyll, I kept the leaf segments at 700 ppm CO_2 in the dark or in BL (PPFD $50 \mu\text{mol m}^{-2} \text{s}^{-1}$) supplemented with RL (PPFD $500 \mu\text{mol m}^{-2} \text{s}^{-1}$). Stomatal apertures with the mesophyll segments from the leaf segments pretreated in BL supplemented with RL were greater than those on the mesophyll segments in the dark (Fig. 4-7). Stomata opening was slightly inhibited by the pretreatment at 700 ppm CO_2 (compare Fig.4-5a and Fig. 4-7)

4-4. Discussion

Stomatal responsiveness in the epidermal strips

In both RL and WL, stomata in the epidermal strip overlaid on the other epidermal strip rapidly opened at 100 ppm CO_2 and closed at 700 ppm CO_2 (Fig. 4-1). The inner sides of the two epidermal strips faced each other. Therefore, the apoplast in the epidermal strips would not change from that in the leaves. In chapter 2, I placed the epidermal strips directly on the buffer-

containing gels and the apoplast in the epidermal strips would be replaced with the buffer. Contrary to Fig. 4-1, the stomatal in the epidermal strips directly placed on the gels hardly opened in RL and closed at 700 ppm CO₂ (Fig. 2-9b and e). Stomatal responses in the epidermal strips might be repressed by the buffer in the gels. Thus, there remained the possibility that the stomata in the epidermal strips were sensitive to environmental stimuli.

Stomatal responses dependent on the circadian clock

As shown in Fig. 4-2, the stomatal responsiveness changed dependently on the start time of the experiment, even in the same experimental condition. In my experiments, the stomata illuminated during 13:00–15:00 opened wider compared with those illuminated during 16:00–18:00 and during 19:00–21:00. In the light period, carbohydrates such as sucrose would be produced in photosynthesis, transported from the mesophyll to the guard cell apoplast and accumulated in the guard cells (Lu *et al.*, 1995, 1997; Outlaw & De Vlieghere-He, 2001). It has been suggested that the glucose derived from the sucrose in the guard cells evoked the signaling for the stomatal closure via hexokinase (Kelly *et al.*, 2012, 2013). The stomatal opening would be gradually inhibited over the light period by the sucrose accumulated in the guard cells. Therefore, I decided to analyze the stomatal responses induced by 16:00 in the further studies.

Effects of MES concentration around guard cells

Stomatal movements are greatly influenced by the apoplast of guard cells. For example, in guard cells, the electrochemical proton gradient across the plasma membrane is the key to control the voltage-gated channels (e.g. Shimazaki *et al.*, 2007). Isolated epidermes were generally floated on the buffer containing 5–10 mM MES (e.g. Travis & Mansfield, 1979; Kinoshita *et al.*, 2001; Hu *et al.*, 2010). I followed the method of previous studies and observed that the stomatal responses in the epidermal strips were less sensitive than those in the leaves (see chapter 2). However, I considered that the buffer would exert some inhibitory effects on the stomatal responses. MES concentration in the buffer solution was one of the possible factors to influence the stomatal responsiveness. For the analysis of the proton extrusion from guard cell protoplasts (GCPs), the incubation buffer for GCPs contained 125–500 μM MES (e.g. Shimazaki *et al.*, 1986; Mawson, 1993; Ueno *et al.*, 2005). Hence, it was hypothesized that MES at high concentrations diminished the effect of proton extrusion from guard cells and

inhibited the hyperpolarization in guard cells.

As shown in Fig. 4-3, stomatal aperture increased with the decrease of the MES concentration in the buffer. In stomatal opening in blue light, it has been revealed that the hyperpolarization around guard cells are important to induce the stomatal opening (e.g. Shimazaki *et al.*, 2007). It was suggested that the buffering effect of MES at high concentrations counteracted the effect of proton extrusion from guard cells and stomatal responses became dull. When the apoplast in the epidermal strips did not changed from that in the leaves, stomata in the epidermal strips showed the sensitive responses to the environmental stimuli (Fig. 4-1). In chapter 2, the apoplast in the epidermal strips placed directly on the gels changed and there is the possibility that the stomatal responses in the epidermal strips were inhibited by the buffer in the gels. Therefore, the method in chapter 2 would be insufficient to confirm the presence of mesophyll signals, even though the suggestive results were obtained.

Novel method for the confirmation of the presence of mesophyll signals

I decided to re-examine the presence of mesophyll signals with the novel method. I prepared the mesophyll segments from the leaf segments pretreated in the light or in the dark, and placed the dark-treated epidermal strips on them. Therefore, the apoplast of the epidermal strips on the light-treated mesophyll segments and on the dark-treated mesophyll segments would be the same except for the conditions of the pretreatment. The different stomatal responses between the samples with the light-treated mesophyll and with the dark-treated mesophyll should be derived from the different pretreatments.

I immediately placed the epidermal strips on the mesophyll segments after I peeled off the epidermes without floating the epidermal strips on the buffer. Since I excluded the step of the additional watering to the epidermal strips described in chapters 2 and 3, I concerned about the hydropassive stomatal opening due to the drying during the experiment. To confirm that the hydropassive stomatal opening were not induced during the experiment, I analyzed the stomatal response of the sample placed in the dark. Stomatal opening was not observed irrespective of the pretreatments in the dark or in the light (Fig. 4-4). I concluded that the hydropassive stomatal opening due to the drying did not occur with the present procedure in this chapter.

The presence of mesophyll signals

The samples were illuminated with BL supplemented with RL for 1 h and with RL only for 2 h. The maximum stomatal aperture was expected to be the same in the epidermal strips placed on the dark-treated and the light-treated mesophyll segments. To analyze the rate of the stomatal opening between the epidermal strips placed on the dark-treated and the light-treated mesophyll segments, I observed the stomata before the stomatal aperture reached to the maximum value. In BL supplemented with RL, the stomatal opening was fast, and the difference of the stomatal aperture between in the epidermal strips placed on the dark-treated and the light-treated mesophyll segments could be observed at 1 h after the onset of the illumination. In RL only, the stomatal opening was slow, and it took for 2 h after the onset of the illumination to observe the difference of the stomatal aperture between in the epidermal strips placed on the dark-treated and the light-treated mesophyll segments.

At 390 ppm CO₂, stomatal opening was enhanced with the mesophyll pretreatment in the light, regardless of the presence or absence of the supplementary BL (Fig. 4-5a and b). The difference of the stomatal aperture between the samples should be derived from mesophyll signals accumulated in the mesophyll segments. Stomatal aperture in Fig. 4-5a was greater than that in Fig. 4-5b. It has been shown that stomata open more widely when the supplementary BL is present and phototropins are involved in this blue light responses (e.g. Hsiao & Allaway, 1973; Iino *et al.*, 1985; Kinoshita *et al.*, 2001). Therefore, stomatal opening in Fig. 4-5a would be induced by phototropins.

At 100 ppm CO₂, the stomatal opening was enhanced with the mesophyll pretreatment in BL supplemented with RL (Fig. 4-6a). However, there was not a significant difference in the stomatal aperture between the epidermal strips with the mesophyll pretreated in red light only and those on the mesophyll pretreated in the dark (Fig. 4-6b). In CO₂-free air, stomata in the leaves were able to open, even in the dark (Doi & Shimazaki, 2008). It would be possible that mesophyll signals accumulated in the mesophyll cells when the leaf segments were treated at 100 ppm CO₂ regardless of the light conditions. Mesophyll signals derived from low CO₂ treatment might be different from those derived from mesophyll photosynthesis. Therefore, when the mesophyll segments were treated at low CO₂ in RL, both the mesophyll signals derived from the mesophyll photosynthesis and those derived from low CO₂ treatment would accumulate in the mesophyll segments and induce the stomatal opening. As shown in Fig. 4-5,

the effect of the mesophyll signals in RL was weaker than that in BL supplemented with RL. The effect of the mesophyll signals produced in RL would be relatively weak and masked by the effect of the mesophyll signals derived from the treatment at 100 ppm CO₂ (Fig. 4-6b).

I planned to show the presence of mesophyll signals that induce stomatal closure at 700 ppm CO₂. However, it was difficult to directly evaluate the effect of stomatal closure. Thus, I analyzed the inhibition of stomatal opening to detect the presence of mesophyll signals inducing stomatal closure. I pretreated the leaves in the dark or in BL supplemented with RL at 700 ppm CO₂. It was expected that the mesophyll signals inducing stomatal closure accumulated in mesophyll cells. Stomatal opening was significantly inhibited with the mesophyll pretreated at 700 ppm CO₂, compared with the stomatal responses with the mesophyll pretreated at 390 ppm CO₂ (Welch's *t*-test, $P < 0.01$; compare Fig. 4-5a and Fig. 4-7). This result suggested that mesophyll signals inhibiting stomatal opening would accumulate at 700 ppm CO₂.

In each experiment for Fig. 4-4–Fig. 4-7, I prepared six transplanted samples. During the transplanting, the transplanted samples were kept in the dark. It took about 0.5 h to place the epidermal strips on the mesophyll segments for six samples. Therefore, it was suggested that the effects of mesophyll signals lasted for at least 0.5 h. It might be possible that the apoplastic mesophyll signals produced in the pre-treatment return to the mesophyll during the transplanting and are released again to the apoplast in the treatment after the transplanting. In the electrophysiological studies, the membrane potential of guard cells changes within several minutes after the input of the environmental stimuli (Hanstein & Felle, 2002). Mesophyll signals would not be electrical signals but some substances more stable. In conclusion, I confirmed the presence of mesophyll signals inducing the stomatal opening and closure with the newly developed, more straightforward method.

4-5. Table

Table 4-1. Extents of stomatal opening and closure in the epidermal strips overlaid on the other epidermal strip in *C. communis* (shown in Fig. 4-1)

RL opening¹⁾ (μm)	WL opening¹⁾ (μm)	<i>P</i>-value
5.47 ± 2.56	9.67 ± 2.56	< 0.01

RL closure²⁾ (μm)	WL closure²⁾ (μm)	<i>P</i>-value
$- 5.21 \pm 1.94$	$- 4.07 \pm 3.61$	< 0.01

¹⁾ Difference between the stomatal aperture at 2.5 h and the stomatal aperture at 0.5 h.

²⁾ Difference between the stomatal aperture at 3.5 h and the stomatal aperture at 2.5 h.

RL, red light (PPFD $550 \mu\text{mol m}^{-2} \text{s}^{-1}$); WL, white light (PPFD $700 \mu\text{mol m}^{-2} \text{s}^{-1}$).

Data are shown as the mean \pm SD of at least 59 stomata. *P*-values were calculated using Student's *t*-test (opening) and Welch's *t*-test (closure).

4-6. Figures

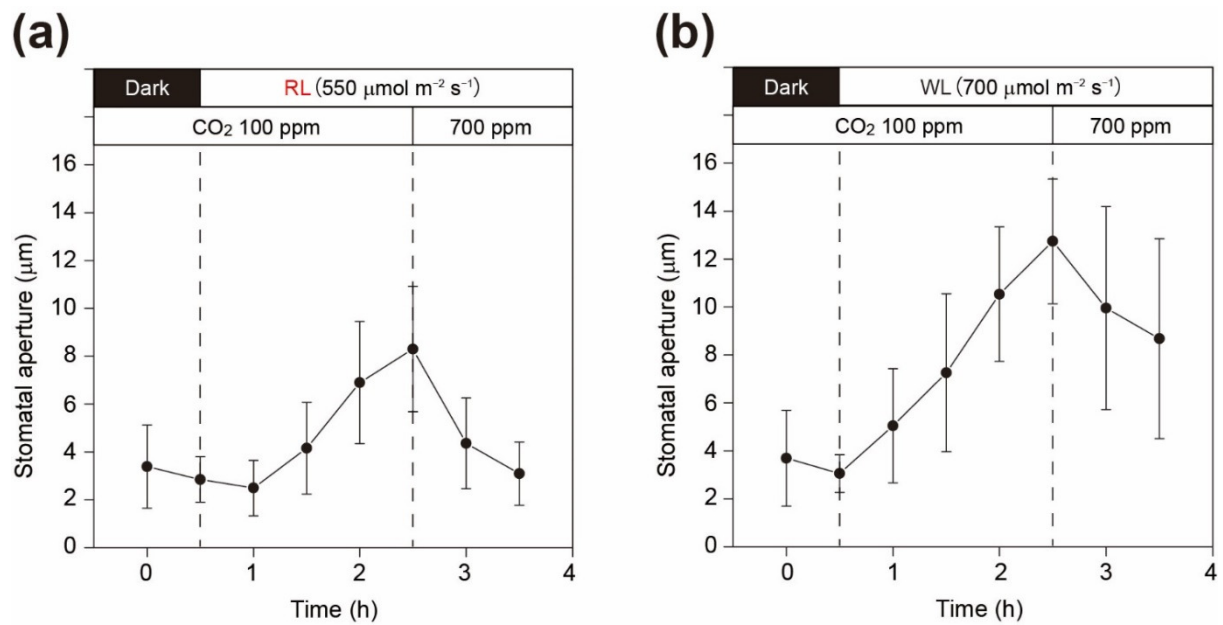


Fig. 4-1. Stomatal responses in the epidermal strip overlaid on the other epidermal strip. After peeling off two abaxial epidermes from the leaves, the epidermal strips were immediately overlaid with their inner sides facing each other and observed the stomatal responses in the epidermal strip on the upper side. CO₂ concentration was maintained at 100 ppm for 2.5 h and at 700 ppm for 1 h. The samples were treated in the dark for 0.5 h and subsequently in the light for 3 h. (a) The samples were illuminated with RL (PPFD 550 μmol m⁻² s⁻¹). (b) The samples were illuminated with WL (PPFD 700 μmol m⁻² s⁻¹).

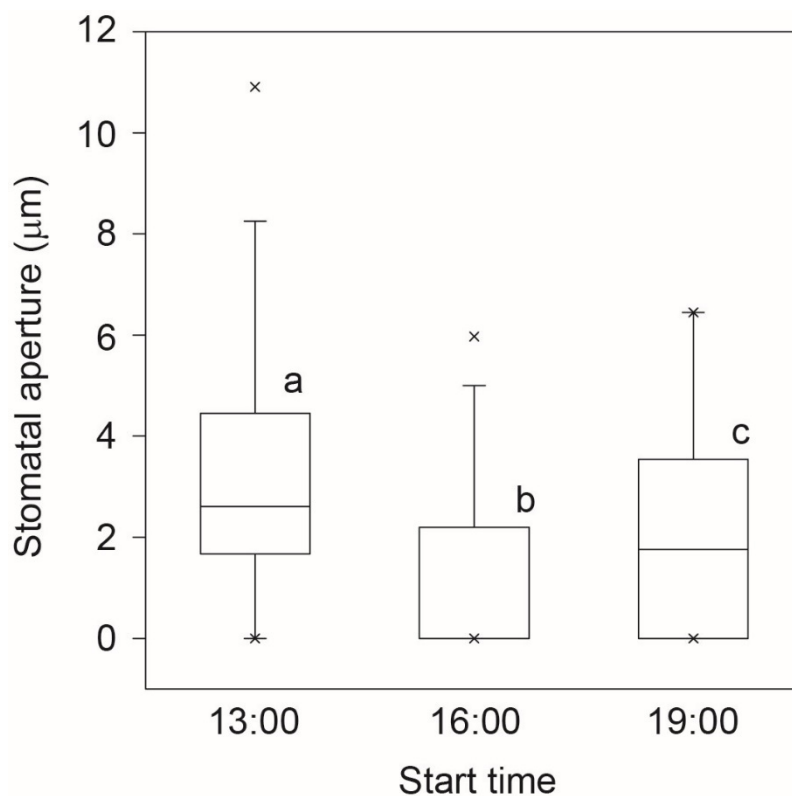


Fig. 4-2. Statistical box-chart plot of stomatal apertures in the epidermal strips of *C. communis* placed on the gels containing 0.1 mM MES. The horizontal lines in the box denote the 25th, 50th, and 75th percentile values. Maximum and minimum stomatal apertures are expressed as x-marks. Stomatal aperture of at least 160 stomata was measured. The epidermal strips were illuminated with BL (PPFD $50 \mu\text{mol m}^{-2} \text{s}^{-1}$) supplemented with RL (PPFD $500 \mu\text{mol m}^{-2} \text{s}^{-1}$) at 23°C for 2 h from 13:00, 15:00 or 19:00. CO_2 concentration was maintained at 390 ppm. Kruskal-Wallis test was conducted at a significance level of $P < 0.01$. There were significant differences in the stomatal aperture among the groups. Different lower case letters denote significant differences in Steel-Dwass test for multiple comparison conducted at a significance level of $P < 0.01$.

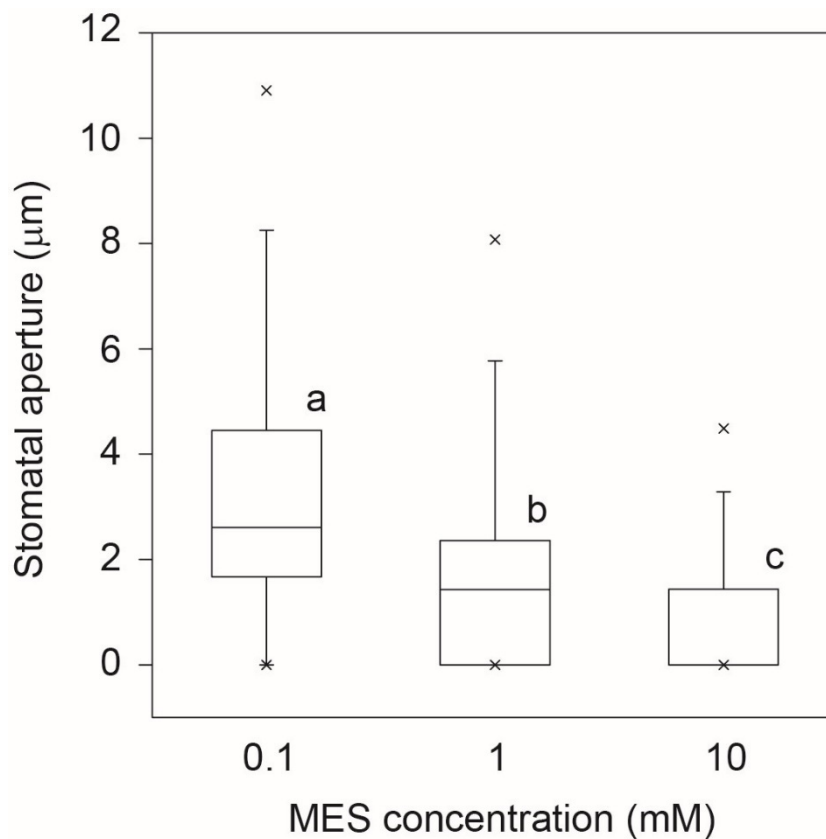


Fig. 4-3. Statistical box-chart plot of stomatal apertures in the epidermal strips of *C. communis* placed on the gels containing 0.1, 1 or 10 mM MES. The horizontal lines in the box denote the 25th, 50th, and 75th percentile values. Maximum and minimum stomatal apertures are expressed as x-marks. Stomatal aperture of at least 150 stomata was measured. The epidermal strips were illuminated with BL (PPFD $50 \mu\text{mol m}^{-2} \text{s}^{-1}$) supplemented with RL (PPFD $500 \mu\text{mol m}^{-2} \text{s}^{-1}$) at 23°C for 2 h from 13:00. CO_2 concentration was maintained at 390 ppm. Kruskal-Wallis test was conducted at a significance level of $P < 0.01$. There were significant differences in the stomatal aperture among the groups. Different lower case letters denote significant differences in Steel-Dwass test for multiple comparison conducted at a significance level of $P < 0.01$.

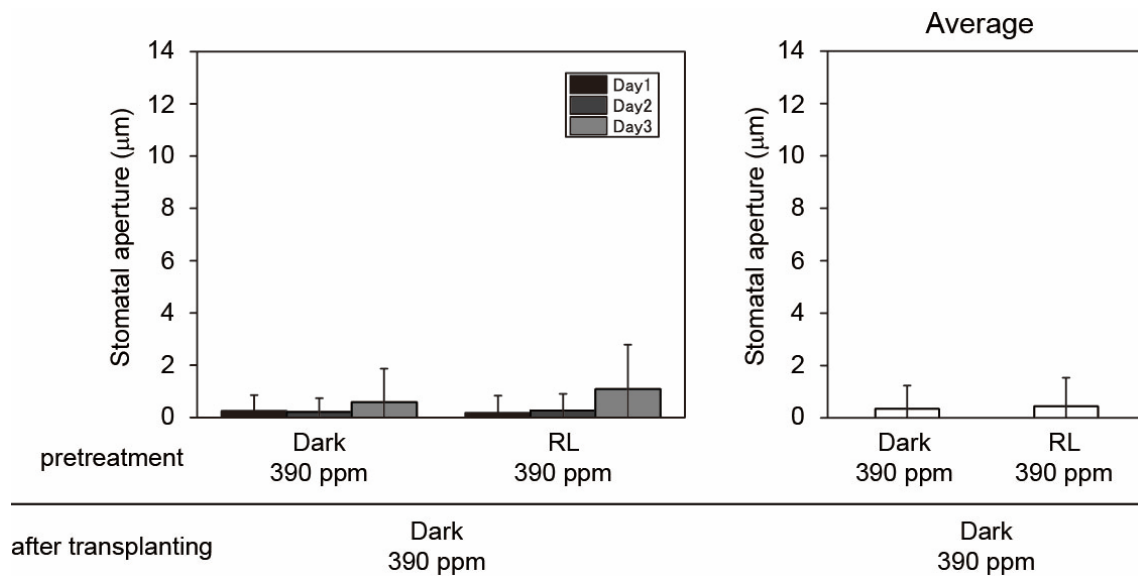


Fig. 4-4. Effects of the mesophyll pretreatment in the dark and in the red light on the stomatal aperture on the epidermal strips placed on the mesophyll segments in *C. communis*. Leaf segments were pretreated at 390 ppm CO₂, in the dark or illuminated with RL (PPFD 500 µmol m⁻² s⁻¹) for 1 h from 12:00. The mesophyll segments for the transplanting were prepared from the leaf segments. I placed the epidermal strips from dark-treated leaves on the mesophyll segments (transplanting). After transplanting, the samples were placed in the dark at 390 ppm CO₂ for 1 h from 13:30. (Left) Results obtained from three trials are shown separately. Data are the mean ± SD of 30 stomata; (Right) Average values of the results obtained from three trials. Data are the mean ± SD of 90 stomata. *P*-value was calculated using Welch's *t*-test.

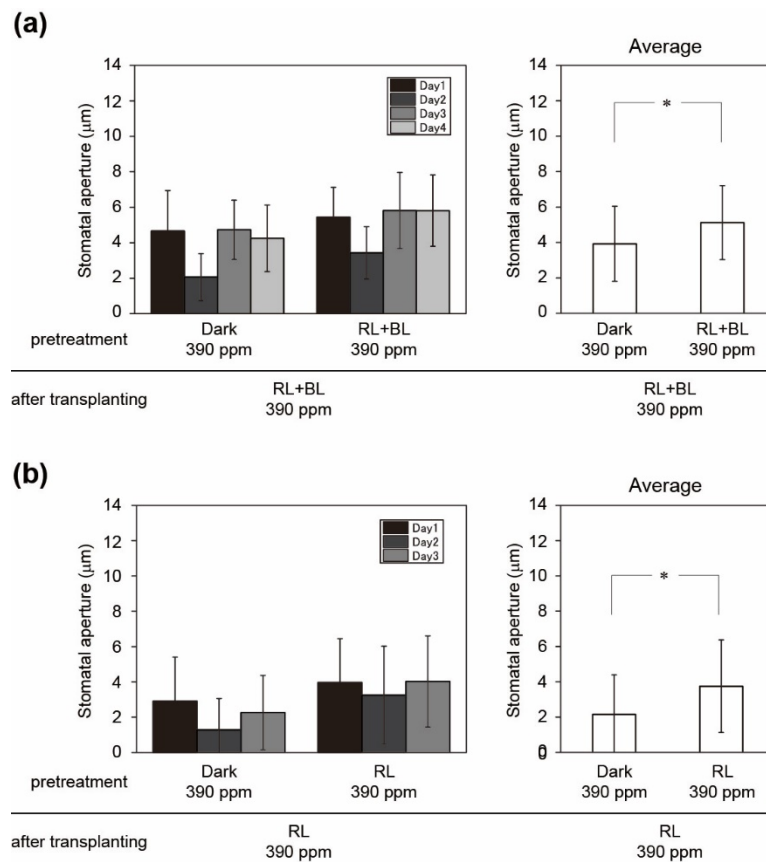


Fig. 4-5. Stomatal responses in the epidermal strips from the dark-treated plants placed on the mesophyll segments pretreated in the dark or in the light at 390 ppm CO₂ in *C. communis*. (a) Leaf segments were pretreated at 390 ppm CO₂, in the dark or illuminated with BL (PPFD 50 μmol m⁻² s⁻¹) supplemented with RL (PPFD 500 μmol m⁻² s⁻¹) for 1 h from 12:00. Mesophyll segments for the transplanting were prepared from the leaf segments. I placed epidermal strips of dark-treated plants on the mesophyll segments (transplanting). After the transplanting, the samples were illuminated with BL (PPFD 50 μmol m⁻² s⁻¹) supplemented with RL (PPFD 500 μmol m⁻² s⁻¹) at 390 ppm CO₂ for 1 h from 13:30. (Left) Results obtained from four trials are shown separately. Data are the mean ± SD of 30 stomata; (Right) Average values of the results obtained from four trials. Data are the mean ± SD of 120 stomata. Asterisk denotes significant difference in Student's *t*-test ($P < 0.01$). (b) Leaf segments were pretreated at 390 ppm CO₂, in the dark or illuminated with RL (PPFD 500 μmol m⁻² s⁻¹) for 1 h from 12:00. After the transplanting, the samples were illuminated with RL (PPFD 500 μmol m⁻² s⁻¹) only at 390 ppm CO₂ for 2 h from 13:30. (Left) Results obtained from four trials are shown separately. Data are the mean ± SD of 30 stomata; (Right) Average values of the results obtained from three trials. Data are the mean ± SD of 90 stomata. Asterisk denotes significant difference in Welch's *t*-test ($P < 0.01$).

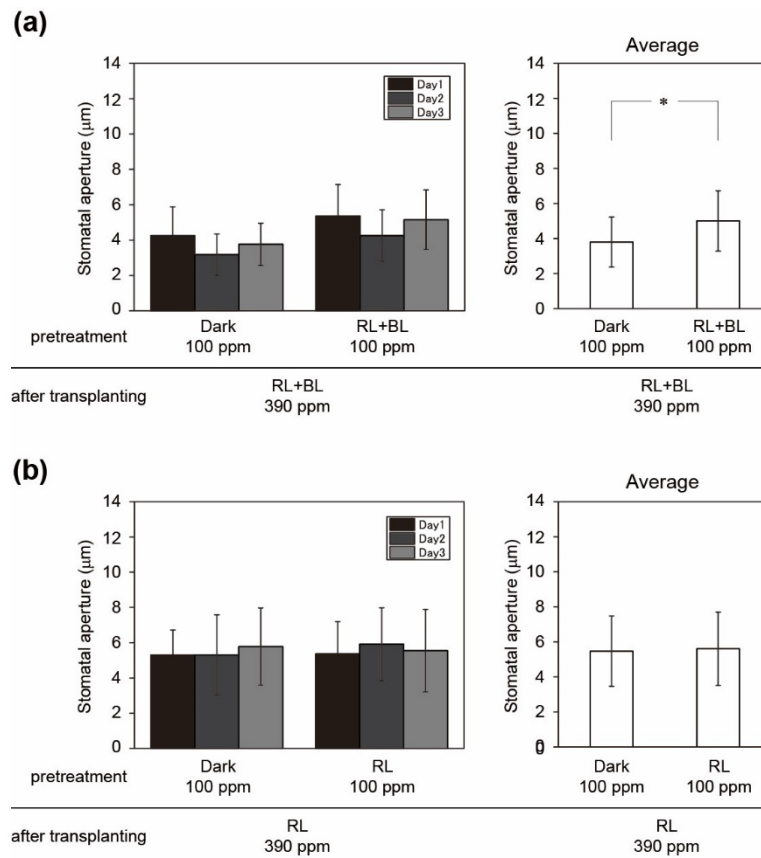


Fig. 4-6. Stomatal responses in the epidermal strips from the dark-treated plants placed on the mesophyll segments pretreated in the dark or in the light at 100 ppm CO₂ in *C. communis*. (a) Leaf segments were pretreated at 100 ppm CO₂, in the dark or illuminated with BL (PPFD 50 µmol m⁻² s⁻¹) supplemented with RL (PPFD 500 µmol m⁻² s⁻¹) for 1 h from 12:00. Mesophyll segments for the transplanting were prepared from the leaf segments. I placed epidermal strips of dark-treated plants on the mesophyll segments (transplanting). After the transplanting, the samples were illuminated with BL (PPFD 50 µmol m⁻² s⁻¹) supplemented with RL (PPFD 500 µmol m⁻² s⁻¹) at 390 ppm CO₂ for 1 h from 13:30. (Left) Results obtained from three trials were shown separately. Data are the mean ± SD of 30 stomata; (Right) Average values of the results obtained from three trials. Data are the mean ± SD of 90 stomata. Asterisk denotes significant difference in Welch's *t*-test (*P* < 0.01). (b) Leaf segments were pretreated at 100 ppm CO₂, in the dark or illuminated with RL (PPFD 500 µmol m⁻² s⁻¹) for 1 h from 12:00. After the transplanting, the samples were illuminated with RL (PPFD 500 µmol m⁻² s⁻¹) at 390 ppm CO₂ for 2 h from 13:30. (Left) Results obtained from three trials were shown separately. Data are the mean ± SD of 30 stomata; (Right) Average values of the results obtained from three trials. Data are the mean ± SD of 90 stomata. *P*-value was calculated using Student's *t*-test.

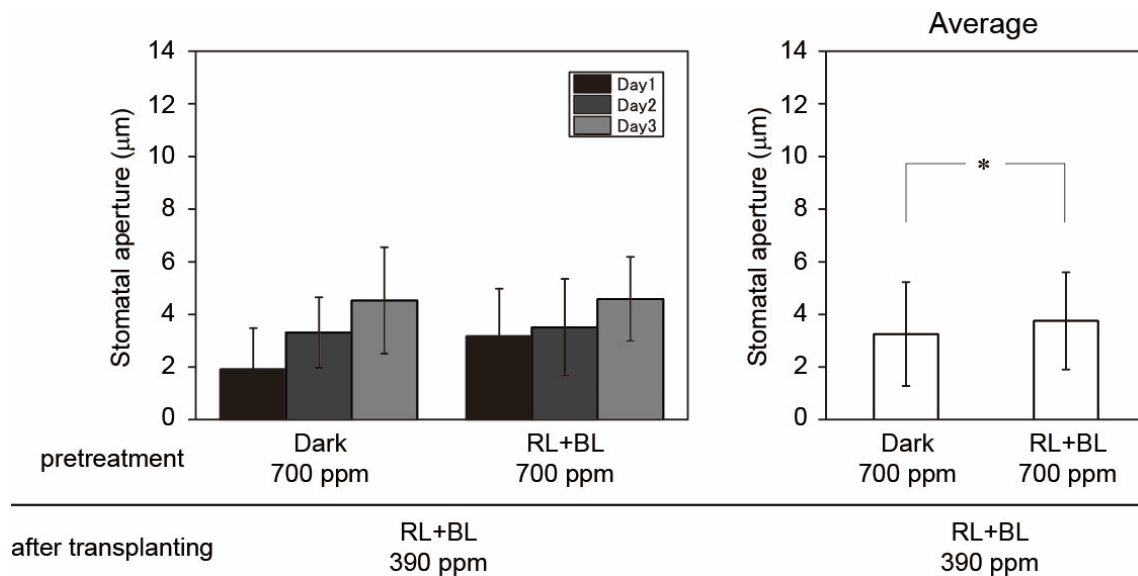


Fig. 4-7. Stomatal responses in the epidermal strips from the dark-treated plants placed on the mesophyll segments pretreated in the dark or in BL supplemented with RL at 700 ppm CO₂ in *C. communis*. Leaf segments were pretreated at 700 ppm CO₂, in the dark or illuminated with BL (PPFD 50 µmol m⁻² s⁻¹) supplemented with RL (PPFD 500 µmol m⁻² s⁻¹) for 1 h from 12:00. Mesophyll segments for the transplanting were prepared from the leaf segments. I placed the epidermal strips of dark-treated plants on the mesophyll segments (transplanting). After the transplanting, the samples were illuminated with BL (PPFD 50 µmol m⁻² s⁻¹) supplemented with RL (PPFD 500 µmol m⁻² s⁻¹) at 390 ppm CO₂ for 1 h from 13:30. (Left) Results obtained from three trials were shown separately. Data are the mean ± SD of 30 stomata; (Right) Average values of the results obtained from three trials. Data are the mean ± SD of 90 stomata. Asterisk denotes significant difference in Student's *t*-test ($P < 0.01$).

Chapter 5

Methodology: Detection of the phosphorylation of the plasma membrane H⁺-ATPase in *Commelina communis*

5-1. Introduction

Stomata open widely in response to blue light (e.g. Hsiao & Allaway, 1973; Iino *et al.*, 1985; Kinoshita *et al.*, 2001). It is well established that phototropins are the blue-light receptors and induce stomatal opening (Kinoshita *et al.*, 2001; Shimazaki *et al.*, 2007). Blue light activates the plasma membrane H⁺-ATPase of guard cells and causes the hyperpolarization by the extrusion of H⁺ (Assmann *et al.*, 1985; Shimazaki *et al.*, 1986; Kinoshita & Shimazaki, 1999; Ueno *et al.*, 2005). The voltage-gated K⁺ channels opened by the hyperpolarization and the K⁺ uptake into a guard cell is induced (Shimazaki *et al.*, 2007; Kollist *et al.*, 2014). Subsequently, water moves into guard cells in accordance with the water potential gradient and guard cells swell out.

In *Arabidopsis thaliana*, blue light activates the plasma membrane H⁺-ATPase in guard cells through the phosphorylation of a penultimate threonine in the C-terminus and 14-3-3 protein binds to the site of phosphorylation (Kinoshita & Shimazaki, 1999; Kinoshita & Shimazaki, 2002). The phosphorylation of the H⁺-ATPase was biochemically detected using the guard cell protoplasts (GCPs). However, for the preparation of GCPs, a large number of leaves were necessary and it took over 8 h to prepare GCPs. Recently, the method of immunocytochemical detection of H⁺-ATPase has been developed for *A. thaliana* (Hayashi *et al.*, 2011). This technique greatly facilitated the detection of phosphorylation state of H⁺-ATPase.

For the narrowing down the candidates of mesophyll signals, it was necessary to devise the bio-assay technique for the detection of mesophyll signals. Firstly, I planned the detection of mesophyll signals by observing the stomatal movements. However, because stomatal responses are generally slow and required several hours, it took many hours to collect reliable data. In addition, stomatal aperture varies greatly even in the same epidermal strip. In contrast to the observation of stomatal movements, when blue light was applied to the GCPs, H⁺-ATPase

was activated and H⁺ extrusion from the GCPs occurred within several minutes (Kinoshita & Shimazaki, 1999). When *Vicia faba* leaves were treated at high CO₂ for 2 min, the membrane potential of guard cells changed, whereas the stomatal aperture was not affected (Hanstein & Felle, 2002). These studies indicated that the membrane potential of guard cells showed more sensitive and rapid responses to environmental stimuli than stomatal movements.

As shown in Fig. 2-9 in chapter 2, I proposed that mesophyll signals should induce rapid stomatal movements. I considered the possibility that, in the presence of mesophyll signals, the membrane potential of a guard cell was drastically changed. In particular, it was hypothesized that mesophyll signals for stomatal opening activated the plasma membrane H⁺-ATPase and induced the hyperpolarization. For the sensitive detection of mesophyll signals, referring to Hayashi *et al.* (2011), I modified the immunocytochemical detection of phosphorylation of plasma membrane H⁺-ATPase for *C. communis*.

5-2. Materials and Methods

Plant materials

C. communis plants were grown as described in chapter 2.

Antibodies

Antibodies were kind gifts from Prof. Toshinori Kinoshita, Nagoya University. For the detailed information about polyclonal anti-H⁺-ATPase and anti-pThr antibodies, see Hayashi *et al.* (2010). The antibodies were raised in rabbits. The anti-H⁺-ATPase antibody recognizes the conserved catalytic domain of the plasma membrane Arabidopsis H⁺-ATPase 2 (AHA2). The anti-pThr antibody recognizes the penultimate phosphorylated Thr947 of AHA2. For the detection of the nonspecific signals, anti-LacZ antibody raised in rabbits (ICN/CAPPEL, OH, USA) was added to the sample instead of the primary antibodies.

Western blotting of the plasma membrane H⁺-ATPase

The abaxial epidermal strips were peeled off from the leaves of *C. communis*. I ground 30 mg of the epidermal strips in 120 µL of a grinding buffer containing 50 mM 3-morpholinopropanesulfonic acid-KOH (MOPS-KOH adjusted at pH 7.5), 100 mM NaCl, 2.5 mM 2,2',2'',2'''-(ethane-1,2-diyl dinitrilo)tetraacetic acid (EDTA adjusted at pH 8.0), 10 mM NaF,

1 mM dithiothreitol (DTT), 1 mM phenylmethanesulfonyl fluoride (PMSF) and 20 μ M leupeptine at room temperature. PMSF and leupeptine were added into the grinding buffer just before use, as they were unstable. I mixed 40 μ L of the extracted sample with 40 μ L of the sodium dodecyl sulfate (SDS) buffer containing 3% (w/v) SDS, 30 mM tris(hydroxymethyl)aminomethane-HCl (Tris-HCl adjusted at pH 8.0), 3 mM EDTA (pH 8.0), 30% (w/v) sucrose, 0.012% (w/v) Coomassie Brilliant Blue G-250 (Nacalai Tesque, Inc., Tokyo, Japan) and 15% (v/v) 2-mercaptoethanol at room temperature. The samples mixed with the SDS buffer were centrifuged with a tabletop centrifuge at room temperature and the supernatants were kept at room temperature before loading onto a polyacrylamide gel (Bio-Rad, Hercules, CA, USA). For the western blotting of the plasma membrane H⁺-ATPase, it was the important point that the temperature of polyacrylamide gels and the electrophoresis buffer, containing 25 mM Tris, 192 mM glycine and 0.1% (w/v) SDS, were kept at around room temperature. I loaded 20 μ L of the supernatant onto each lane of a 10% (w/v) polyacrylamide gel. SDS-polyacrylamide gel electrophoresis (SDS-PAGE) was conducted at a constant current of 20 mA per gel.

After the separation of proteins by SDS-PAGE in a 10% (w/v) polyacrylamide gel, individual proteins were transferred to nitrocellulose membranes at a constant current of 2 mA cm⁻² in a transfer buffer containing 25 mM Tris, 192 mM glycine and 20% (v/v) methanol by an electroblotter (AE-6677; ATTO, Tokyo, Japan). The membranes were incubated in a blocking buffer, Blocking One (Nacalai Tesque, INC.) for 0.5 h at room temperature and reacted with the anti-H⁺-ATPase or the anti-pThr antibody at the 1:5,000 strength Can get signal solution 1 (Toyobo Co., Ltd., Osaka, Japan) overnight at 4°C. The membrane was rinsed three times for 5 min each in the TTBS buffer containing 0.05% (v/v) Tween-20 (Sigma-Aldrich, St. Louis, MO, USA), 137 mM NaCl, 2.7 mM KCl and 25 mM Tris-HCl (pH 7.4) and then reacted with a donkey anti-rabbit IgG secondary antibody conjugated to horseradish peroxidase (HRP) (GE healthcare, Buckinghamshire, UK) at the 1:10,000 strength Can get signal solution 2 (Toyobo Co., Ltd.) for 2 h at room temperature. Amersham ECL Prime Western Blotting Detection Reagent (GE healthcare, Buckinghamshire, UK) was used as a chemiluminescence substrate. Chemiluminescence with the HRP reaction was detected with a LAS-4000 (Fujifilm Corporation, Tokyo, Japan).

Preparation of the cover glass coated with poly-L-lysine

I dropped 20 μL of 80% (v/v) acetone in distilled water on a 22 mm square cover glass (Matsunami Glass Ind., Ltd., Osaka, Japan) and the surface of the glass was wiped with a thin paper wiper (Prowipe; Daio Paper Corporation, Tokyo, Japan). Also, the bottom of plastic plate was cleaned with 80% (v/v) acetone and 80 μL of 0.01% (w/v) poly-L-lysine (Sigma-Aldrich) dropped on it. The cover glass was placed onto the droplet of poly-L-lysine and kept for 30–50 min. The cover glass was turned upside down. The excess droplets on the cover glass were blotted with a thin paper wiper and the cover glass was fully dried in the room. The cover glass was dipped into Milli-Q water for 1 s. Again, the excess droplets on the surface coated with poly-L-lysine were blotted. The hydrophobic barrier was lined roundly on the glass surface, using a fast-drying liquid wax pen (Super PAP Pen; Funakoshi Co., Ltd., Tokyo, Japan). The cover glass coated with poly-L-lysine can be used for 1 week.

Preparation of fixation solution

I added 3 g of paraformaldehyde (PFA) and 330 μL of 1N NaOH to 30 mL distilled water. The mixture was heated at around 65°C in a draft chamber and gently shaken to solve paraformaldehyde. Ten milliliters of the fixation solution consisted of 1 mL of reverse osmosis (RO) water, 4 mL of 10% (w/v) PFA, 5 mL of a microtubule stabilizing buffer containing 10 mM MgSO_4 , 10 mM EGTA and 100 mM PIPES (pH 7.0). pH of the fixation solution was near-neutral.

Immunocytochemical detection of the plasma membrane H^+ -ATPase in guard cells

The abaxial epidermes were peeled off with a pair of forceps and cut into small segments (3 \times 3 mm) using a razor blade. The segments were floated on the fixation solution for 2 h at room temperature and washed sufficiently with RO water. In order to remove chlorophyll, the segments were dipped in methanol for 10 min at 37°C, and repeated two more times. I added 10 mL of chloroform in 50 mL polypropylene tube (Iwaki & Co., Ltd., Tokyo, Japan). For removal of cuticular wax, the segments were added to the tube and vigorously shaken for 10 s. When the chloroform treatment was finished, the segments were immediately washed with RO water. The segments were placed inside the hydrophobic barrier of the cover glass coated with poly-L-lysine, with their inner side facing the glass. Small bubbles between the segments and

the glass were gently removed using the tip of a pair of forceps. The sample plates were air-dried for 1 h and the epidermal segments adhered to the cover glass. The plates were placed in dishes of 3.5 cm in diameter (Nunc cell culture dish; Thermo Fisher Scientific, Inc., Waltham, MA, USA).

An enzyme solution containing 5% (w/v) Cellulase R-10 (Yakult Pharmaceutical Industry Co., Ltd., Tokyo, Japan), 1% (w/v) Macerozyme R-10 (Yakult Pharmaceutical Industry Co., Ltd.) and 10 mM MES-KOH (pH 5.5), was dropped inside the hydrophobic barrier and treated for 1 h at 37 °C to digest cell walls. A piece of wet tissue paper was placed around the dishes to prevent desiccation. After the enzyme digestion, the enzyme solution was washed away twice with a phosphate buffered saline (PBS) containing 137 mM NaCl, 2.7 mM KCl, 10 mM Na₂HPO₄ and 1.8 mM KH₂PO₄ (pH 7.4). I dropped 1 mL of 0.5% (v/v) Tween-20 in the dish and the samples were treated for 0.5 h at room temperature to make the plasma membrane permeable. After the permeabilization of the plasma membrane, the detergent was washed away twice with PBS. I dropped 1.5 mL of 3% (w/v) BSA (Thermo Fisher Scientific, Inc.) in PBS inside the dish and the samples were treated for 1 h at room temperature (Blocking). After the blocking, BSA solution was removed, and the remaining solution, especially on the hydrophobic barrier, was blotted with a thin paper wiper.

Anti-H⁺-ATPase, anti-pThr and anti-LacZ antibodies were diluted 1,000 fold with 3% (w/v) BSA in PBS. The samples were incubated with anti-H⁺-ATPase and anti-pThr antibody at 4°C overnight. The primary antibodies were washed away six times at five-minute intervals with PBS. Alexa Fluor 488 goat anti-rabbit IgG (Thermo Fisher Scientific, Inc.) was diluted 500 fold with 3% (w/v) BSA in PBS. The samples were incubated with Alexa Fluor 488 goat anti-rabbit IgG at 37°C for 3 h in the dark. After washing away the secondary antibody six times at five-minute intervals with PBS, the samples were mounted on a microscope slide with 50% (v/v) glycerol. The samples were observed using a fluorescence microscope (BX50; Olympus, Tokyo, Japan) with a combination of a narrow excitation band-pass filter set: BP460–490 BA510IF (U-MWIB/GFP; Olympus, Tokyo, Japan) for Alexa Fluor 488 using an Hg arc lamp as a source of excitation light. Fluorescent images were collected using a CCD camera system (DP71; Olympus). For the estimation of fluorescence intensities, the pictures in the same experiment were taken at identical exposure time.

Estimation of fluorescence intensity

The pictures of stomata were split into three separate color images (Red, Blue and Green), using ImageJ software. The images of the green channel were used for the estimation of fluorescence intensity. The intensity of the area, where no fluorescence from guard cells was observed, was measured as the background intensity. The fluorescence values for the estimation were calculated by subtracting the background values from the fluorescence intensities from guard cells.

Statistical analysis

The data are shown as means \pm SD (Fig. 5-4). Differences between the mean values of data were analysed using ANOVA and Tukey's multiple comparison test (Fig. 5-4). All statistical analyses were conducted using the R statistical software package (ver. 2.15.1.; R Development Core Team 2003).

5-3. Results

Detection of the H⁺-ATPase by western blotting

The antibodies were designed to recognize the plasma membrane H⁺-ATPase of *A. thaliana*. Thus, it was necessary to check whether the antibodies could specifically bind to the plasma membrane H⁺-ATPase of *C. communis*. Using the anti-H⁺-ATPase antibody of *A. thaliana* as the primary antibody of western blotting, one major band was detected around 100 kD and several indistinct non-specific bands were detected around 37 kD and 50 kD (Fig. 5-1, Left). With the anti-pThr antibody of *A. thaliana* binding to the phosphorylated H⁺-ATPase, one major band was detected around 100 kD and non-specific bands were not detected (Fig. 5-1, Right).

Relationship between the signals from the guard cells and the time for the digestion of cell walls

In my previous method, 5% (w/v) Cellulase R-10 and 1% (w/v) Macerozyme R-10 were dissolved in a PBS containing 137 mM NaCl, 2.7 mM KCl, 10 mM Na₂HPO₄ and 1.8 mM KH₂PO₄ (pH 7.4). The cell walls were digested for 1, 9 or 18 h (Fig. 5-2). For the permeabilization of the plasma membrane, 1 mL of 3.8% (v/v) Triton X-100 (Sigma-Aldrich)

was treated for 1 h at room temperature. As the time for the digestion became longer, the outline of cells, especially in epidermal cells, became indistinct (Fig. 5-2a, c and e). The signals from guard cells were obtained in the samples digested for more than 18 h (Fig. 5-2f).

Immunocytochemical detection of plasma membrane H⁺-ATPase in *C. communis*

Referring to Hayashi *et al.* (2011), I performed the immunocytochemical detection of the plasma membrane H⁺-ATPase in epidermal strips of *C. communis* with the anti-H⁺-ATPase antibody. As shown in Fig. 5-3a and b, the H⁺-ATPase was detected mainly in guard cells and subsidiary cells. Fluorescence from nuclei of guard cells, subsidiary cells and epidermal cells was also clearly detected. In the bright field image, outlines of epidermal cells were not clear (Fig. 5-3a).

With the anti-pThr antibody, I performed the detection of phosphorylation of H⁺-ATPase. The epidermal strips were treated with fusicoccin. The fluorescence was detected mainly in guard cells and subsidiary cells (Fig. 5-3c and d). In addition, fluorescence from nuclei of guard cells, subsidiary cells and epidermal cells was detected (Fig. 5-3d). In the bright field image, outline of epidermal cells were not clear (Fig. 5-3c).

Comparison of the phosphorylation levels among the epidermal strips placed in several conditions

I checked whether the immunocytochemical detection for the phosphorylation of H⁺-ATPase works properly in *C. communis*. Stomatal opening were tested in the epidermal strips floated on a buffer solution (Fig. 5-4a). Stomatal opening was strongly induced by the treatment with 10 μM fusicoccin (FC). In this experiment, stomatal opening in red light (RL) and stomatal opening in blue light (BL) supplemented with RL was not statistically different (Fig. 5-4a).

I estimated the amount of H⁺-ATPase with anti H⁺-ATPase antibody (Fig. 5-4b). The fluorescence signal intensity in Fig. 5-4b represents the amount of H⁺-ATPase. As a background control, I added the anti-LacZ antibody instead of anti-H⁺-ATPase antibody and detected the non-specific background signals. In this case, the signal intensity of the LacZ samples was significantly weakest. The signals of RL and BL supplemented with RL samples were slightly weaker than those of dark (DK) and FC samples (Fig. 5-4b).

I also estimated the level of phosphorylation of H⁺-ATPase with anti-pThr antibody (Fig.

5-4c). The fluorescence signal intensity in Fig. 5-4c represents the level of phosphorylation of H⁺-ATPase. As a background control, I added the anti-LacZ antibody instead of anti-pThr antibody and detected the non-specific background signals. The fluorescence intensity of fusicoccin-treated sample was highest. The fluorescence intensity of BL supplemented with RL sample was somewhat higher than that of DK sample. The differences in the fluorescence level between RL sample and BL supplemented with RL sample was not statistically significant.

5-4. Discussion

Western blotting of plasma membrane H⁺-ATPase in *C. communis*

The antibodies, used in the present study, were designed to recognize the plasma membrane AHA2. Since I aimed to develop the method for the immunocytochemical detection of H⁺-ATPase in *C. communis*, I checked whether the anti-AHA2 antibody also recognizes the plasma membrane H⁺-ATPase of *C. communis*, using western blotting. The plasma membrane H⁺-ATPase is known to be expressed not only in epidermal cells but also in mesophyll cells (Ueno *et al.*, 2005). In *A. thaliana*, it is difficult to prepare the isolated epidermis without the contamination of mesophyll cells. Therefore, the preparation of GCPs was necessary for the analysis of the H⁺-ATPase in guard cells (e.g. Kinoshita & Shimazaki, 1999; Ueno *et al.*, 2005; Hayashi *et al.*, 2010). In *C. communis*, epidermes can be easily peeled off without the contamination of mesophyll cells. Thus, I expected to detect the signal of epidermal H⁺-ATPase using epidermal strips of *C. communis*. It has been reported that AHA2 is detected around 97 kD (Regenberg *et al.*, 1995; Hayashi *et al.*, 2011). With the epidermal strips of *C. communis*, the strong signal was detected around 100 kD. This would be the signal of H⁺-ATPase of *C. communis* (Fig. 5-1).

In *C. communis*, several indistinct non-specific bands were detected with the anti-H⁺-ATPase antibody (Fig. 5-1a). It would be caused by the difference of species (compare with Hayashi *et al.*, 2011). The non-specific bands are relatively weak compared with the signal from H⁺-ATPase, and therefore I concluded that anti-AHA2 antibody could be used for the detection of plasma membrane H⁺-ATPase in *C. communis*.

Immunocytochemical detection of H⁺-ATPase in *C. communis*

Referring to Hayashi *et al.* (2011), I modified the method for immunocytochemical

detection of plasma membrane H⁺-ATPase for *C. communis*. Two points are especially important to gain the signals from H⁺-ATPase, (i) Removal of cuticular wax with chloroform and (ii) pH of the enzyme solution.

(i) Removal of cuticular wax with chloroform

Unlike *A. thaliana*, epidermal strips of *C. communis*, adhered onto a cover glass, were easily peeled off. The loss of specimen was an annoying problem. To avoid this problem, I added the process for the removal of cuticular wax with chloroform.

(ii) pH of the enzyme solution

For *A. thaliana*, cellulase and macerozyme were dissolved in PBS and therefore the pH was set at around 7 (Hayashi *et al.*, 2011). In *A. thaliana*, the signal from guard cell was detected when the specimen were treated with the enzyme solution for only 15 min at 37°C. Under the same conditions, it took more than 18 h to obtain the signal from guard cell in *C. communis* (Fig. 5-2). I adjusted the pH of the enzyme solution at 5.5, treated specimen in the enzyme solution for only 1 h and could obtain the signal from guard cells (Fig. 5-3). I succeeded the substantial shortening for the digestion step of cell wall.

The signal of H⁺-ATPase were detected not only from guard cells, but also from subsidiary cells (Fig. 5-3b). Similarly, H⁺-ATPase phosphorylated by fusicoccin were detected from both guard cells and subsidiary cells (Fig. 5-3d). This suggested that the plasma membrane H⁺-ATPase of subsidiary cells were also activated by environmental stimuli. The regulation of the activity of plasma membrane H⁺-ATPase in both guard cells and subsidiary cells would contribute to the active water transport between them. In the bright field, the outline of epidermal cells were indistinct (Fig. 5-3a and c). However, the fluorescent signals from guard cells and subsidiary cells could be the clearly recognized (Fig. 5-3b and d). These pictures indicated that the drastic digestion of cell walls was necessary for antibodies to permeate into guard cells and subsidiary cells. In my method, the signals in subsidiary cells were frequently not observed. The enzyme digestion of cell walls might be drastic to preserve the signal in subsidiary cell. For the observation of the signals in subsidiary cells, it would be better to shorten the digestion time and/or reduce the enzyme concentration in the digestion solution. As shown in Fig. 5-3b and d, the signal intensities detected from guard cells and subsidiary cells

were significantly higher than those from other epidermal cells. Therefore, I concluded that the signal detected around 100 kD represented the H⁺-ATPase from guard cells and subsidiary cells (Fig. 5-1).

In addition to the signals from plasma membrane, strong signals were observed in nuclei (Fig. 5-3b and d). I considered that the signals from nuclei were non-specific, since the antibody recognized several proteins except H⁺-ATPase (Fig. 5-1). I tried to several fixation methods to quench the non-specific signals, however, I could not find the way for the quenching of these non-specific signals. Thus, for the quantification and the analysis of the phosphorylation level of H⁺-ATPase, the fluorescence intensity of guard cells was measured excluding the fluorescence from nuclei. There remained another possibility that the signals from nuclei were derived from H⁺-ATPase. For removal of cuticular wax, the epidermal strips were treated in chloroform. This process might damage the plasma membrane and the fractions of the plasma membrane adhere with the nuclear membranes.

Estimation of the phosphorylation level in the plasma membrane H⁺-ATPase

As described above, I confirmed to obtain the signals of H⁺-ATPase in guard cells and subsidiary cells (Fig. 5-3). I also ensured whether the immunocytochemical detection of H⁺-ATPase was acceptable for the estimation of the phosphorylation level in *C. communis*.

The epidermal strips treated in the light or with FC were used for this analysis. FC strongly stabilize the binding between phosphorylated H⁺-ATPase and 14-3-3 protein and induce stomatal opening (e.g. Pemadasa, 1981; Jahn *et al.*, 1997; Oecking *et al.*, 1997). Thus, the treatment with FC was used as the positive control of phosphorylation. As shown in numerous studies, stomata widely opened with FC (Fig. 5-4a). Although there is the tendency that stomata in BL supplemented with RL opened wider than that in RL, the difference between them was not statistically significant (Fig. 5-4a). This experiment was preliminary and the number of biological replicates should be increased.

Immunocytochemical detection of anti-H⁺-ATPase antibody enabled to estimate the amount of H⁺-ATPase in the guard cells (Fig. 5-4b). I expected that there was no significant differences in signals with anti-H⁺-ATPase antibody among different conditions. However, there were the significant differences in the signals (Fig. 5-4b). From Fig. 5-4b, the amount of H⁺-ATPase might be controlled dependently on the conditions. Also, the differences in signals

from H⁺-ATPase might become smaller with the increase of the trial number.

On the other hand, the immunocytochemical detection of anti-pThr antibody enabled to estimate the phosphorylation level of H⁺-ATPase (Fig. 5-4c). It has been revealed that BL strongly phosphorylate the plasma membrane H⁺-ATPase, compared with RL (e.g. Ueno *et al.*, 2005; Hayashi *et al.*, 2010). I expected that the significant difference was observed between RL and BL supplemented with RL. Similar to the stomatal aperture, however, the phosphorylation level was significantly high in FC treatment, while, the effect of light condition was not clear. The tendency of these preliminary results were generally consistent with previous studies (Hayashi *et al.*, 2011).

5-5. Figures

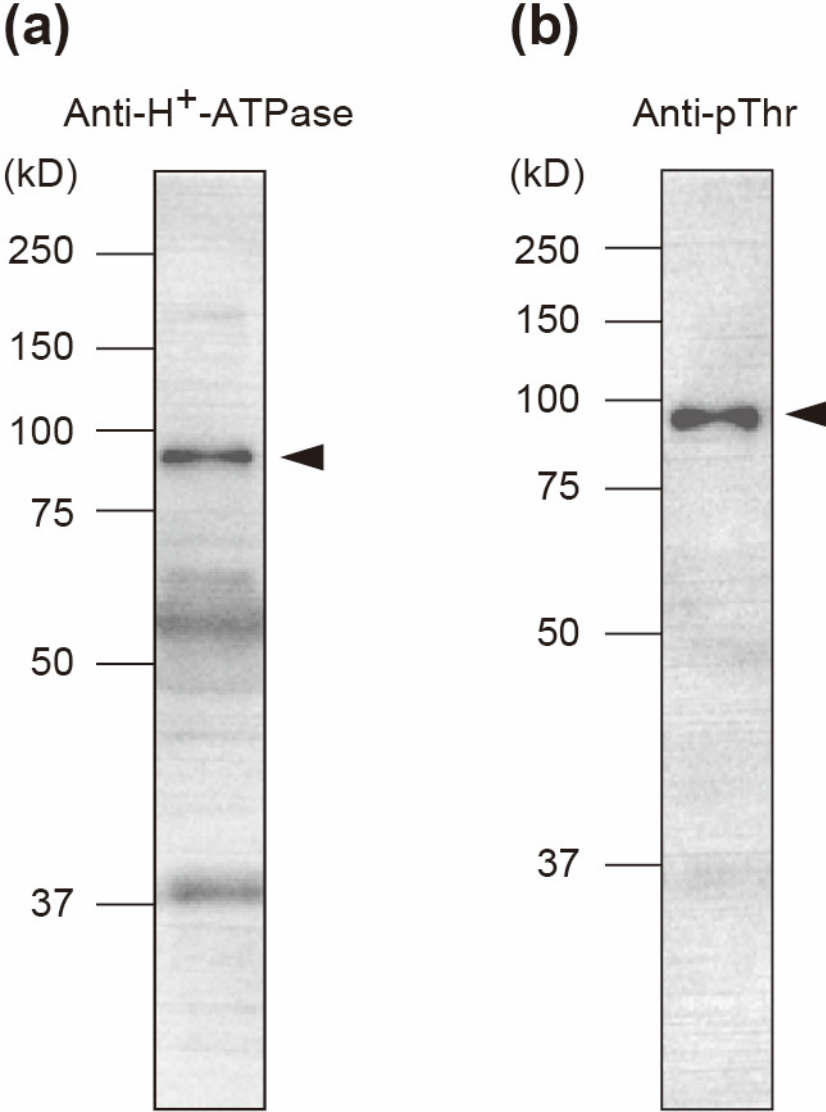


Fig. 5-1. Detection of the plasma membrane H⁺-ATPase by western blotting. The primary antibody was anti-H⁺-ATPase (a) or anti-pThr (b). Arrowheads represent the bands of H⁺-ATPase in *C. communis*.

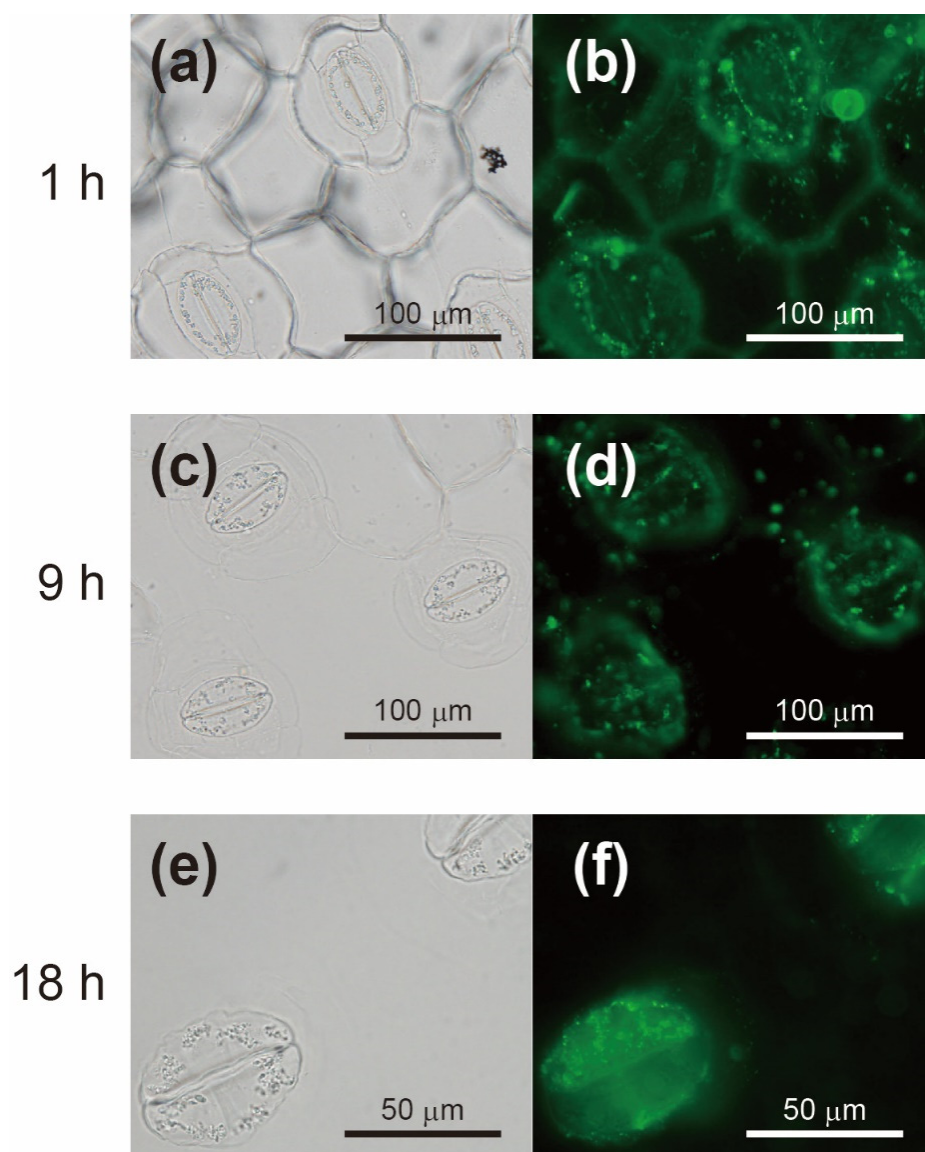


Fig. 5-2. Relationship between the signal from the guard cells and the time for the digestion of cell walls. (a, c and e) Bright field images; (b, d and f) Fluorescence images of Alexa Fluor 488. The primary antibodies were anti-H⁺-ATPase. I dissolved 5% (w/v) Cellulase R-10 and 1% (w/v) Macerozyme R-10 in a PBS containing 137 mM NaCl, 2.7 mM KCl, 10 mM Na₂HPO₄ and 1.8 mM KH₂PO₄ (pH 7.4). The cell walls were digested for 1 (a and b), 9 (c and d) or 18 h (e and f). For the permeabilization of the plasma membrane, 1 mL of 3.8% (v/v) Triton X-100 was treated for 1 h at room temperature.

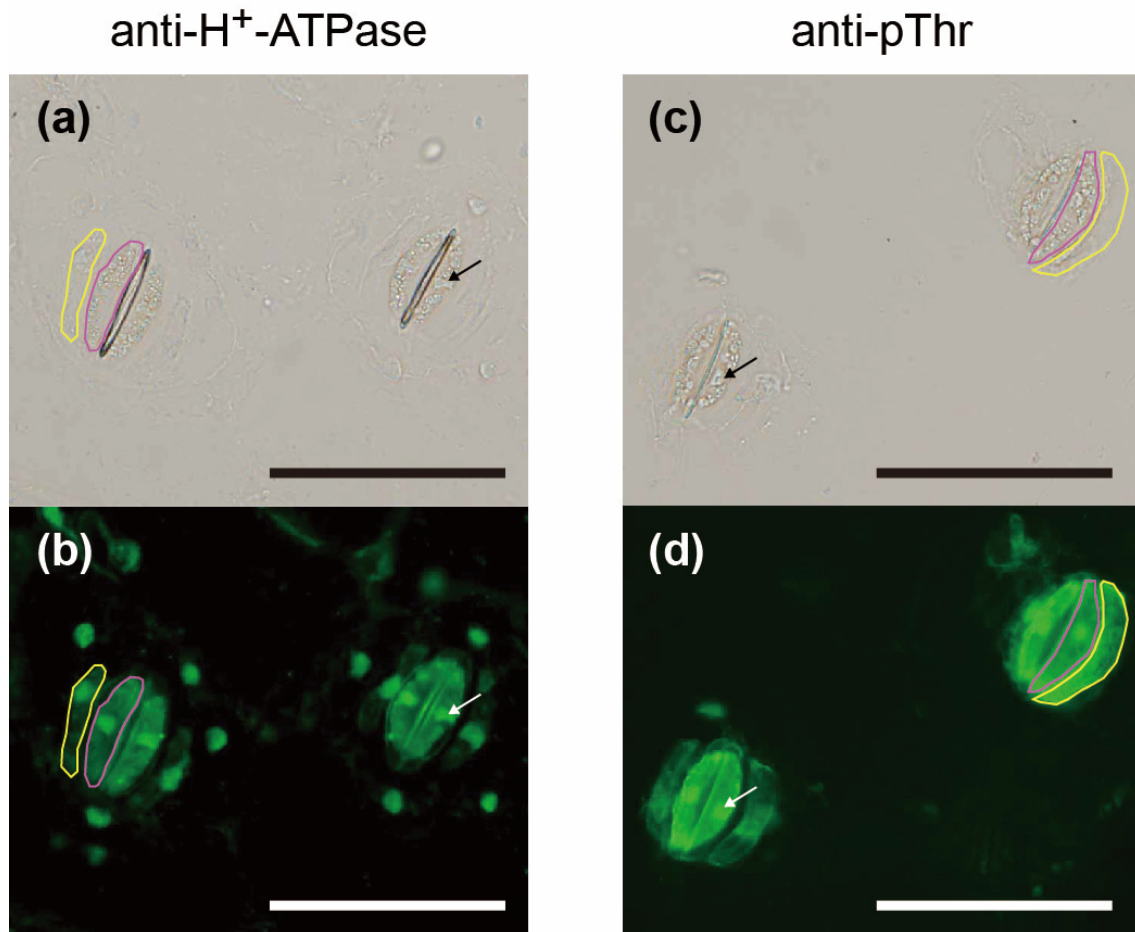


Fig. 5-3. Immunocytochemical detection of the plasma membrane H^+ -ATPase in the epidermal strips of *C. communis*. (a and c) Bright field images; (b and d) Fluorescence images of Alexa Fluor 488. The primary antibodies were anti- H^+ -ATPase (Left) and anti-pThr (Right). For the detection of the phosphorylation of H^+ -ATPase, the epidermal strips were treated with 10 μ M fusicoccin in the dark for 0.5 h (c and d). The perimeters of guard cells are shown with magenta line, and those of subsidiary cells are with yellow line. Black and white arrows indicate nuclei. Bars = 100 μ m.

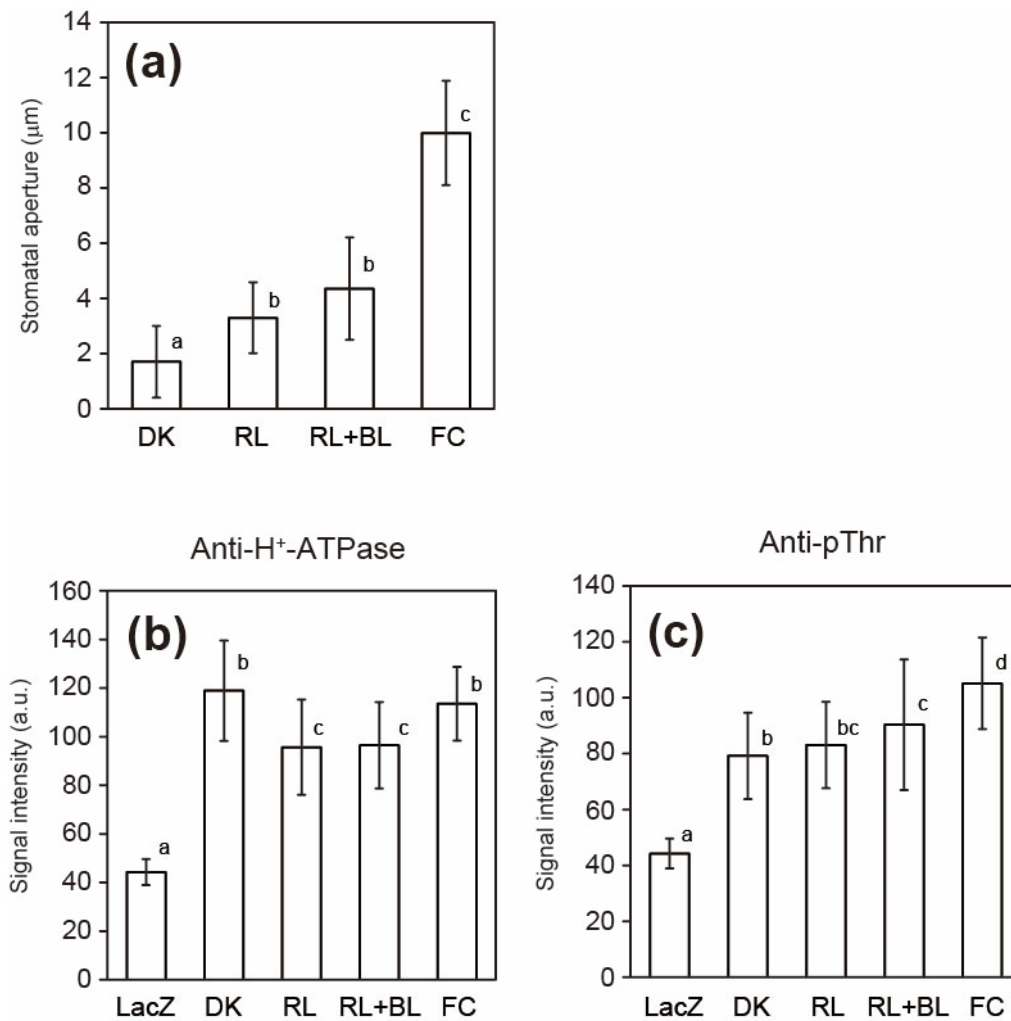


Fig. 5-4. Immunocytochemical detection of the phosphorylation of the plasma membrane H⁺-ATPase in the epidermal strips of *C. communis*. (a) Stomatal aperture of the epidermal strips. CO₂ concentration was maintained at 390 ppm. DK, the epidermal strips were placed in the dark for 2.5 h; RL, the epidermal strips were illuminated with RL (PPFD 500 μmol m⁻² s⁻¹) for 2 h; RL+BL, the epidermal strip were illuminated with BL (PPFD 50 μmol m⁻² s⁻¹) supplemented with RL (PPFD 500 μmol m⁻² s⁻¹) for 2 h, FC; the epidermal strip were treated with 10 μM fusicoccin in the dark for 2.5 h. (b) Immunocytochemical detection of H⁺-ATPase with anti-H⁺-ATPase antibody. LacZ: Instead of the anti-H⁺-ATPase antibody, anti-LacZ antibody was used as the primary antibody. For DK, RL, RL+BL and FC, see above. (c) Immunocytochemical detection of H⁺-ATPase with anti-pThr antibody. Data are the mean ± SD of at least 60 stomata. Different lower case letters denote significant differences in Tukey's multiple comparison test conducted at a significance level of $P < 0.01$.

Chapter 6

General discussion

Conditions to observe the stomatal responses in a physiologically more natural state

There are two types of stomatal movements, known as hydroactive and hydropassive movements. Hydropassive stomatal opening can be induced by drying or high salinity. In particular, isolated epidermes sometimes dry up when watering is inadequate. Mott *et al.* (2008) showed that the stomata in the isolated epidermes could not respond to environmental stimuli, and the result was inconsistent with previous studies since it has been well established that the isolated epidermes respond to light and CO₂ (e.g. Hsiao & Allaway, 1973; Webb *et al.*, 1996). In chapter 2, I developed the method to prevent the epidermal strips of *Commelina communis* from both drying and immersion. In this method, I placed the epidermal strips on the gels containing 30 mM KCl, 1 mM CaCl₂ and 10 mM MES-KOH (pH 6.15). In addition to the adequate watering for the epidermal strips, this method provided another advantage. When the epidermal strips were floated on buffer solution, almost all substomatal cavities were immersed. This method enabled to keep the substomatal cavities air-filled, and I found that stomata, whose substomatal cavities were air-filled, were sensitive to environmental stimuli (Fig. 2-8). I concluded that the method enabled to observe both stomatal responses to light and CO₂ in a physiologically more natural state.

In chapter 2, I compared the stomatal responses between the leaf segments and the epidermal strips placed on the gels. I noticed, however, the disadvantage of this method since the apoplast in the epidermal strips would greatly differ from the one in the leaf segments by the presence of the buffer in the gels. In other words, I concerned that the differences in the stomatal responses between the leaf segments and the epidermal strips were not precisely evaluated. Therefore, I further developed the novel method to re-examine the presence of mesophyll signals in chapter 4. I placed the dark-treated epidermal strips on the mesophyll segments pretreated in the dark or in the light, and compared the stomatal responses between them. In this newly-developed method, the apoplast in the epidermal strips was not disturbed by the buffer, and the precise controlled experiments were made.

Roles of the mesophyll in controlling the stomatal responses

Stomata in the isolated epidermes were less sensitive to environmental stimuli compared with those in leaves (Lee & Bowling, 1992; Olsen *et al.*, 2002; Mott *et al.*, 2008). The illumination to the single stoma was insufficient for the stomatal opening, though, the illumination to the surrounding leaf area induced stomatal opening (Mott *et al.*, 2008). In *Chlorophytum comosum*, mesophyll with active chloroplasts was required for the stomatal opening in red light (Roelfsema *et al.*, 2006). Thus, it has been pointed out that stomatal responses are influenced by mesophyll.

In chapter 2, I placed the epidermal strips on the mesophyll segments of *C. communis* and compared the stomatal responses among the leaf segments, the epidermal strips and the epidermal strips placed on the mesophyll segments. Stomatal opening and closure were accelerated when the epidermal strips were touched to the mesophyll (Table 2-1 and Fig. 2-9). It was suggested that the mesophyll controlled both stomatal opening at low CO₂ and stomatal closure at high CO₂.

As described in the previous section, there was a disadvantage of the method used in chapter 2. In chapter 4, I placed the dark-treated epidermal strips on the mesophyll segments pretreated in the dark or in the light. Stomatal opening was enhanced by the mesophyll segments pretreated in the light at 390 ppm CO₂ and inhibited by the mesophyll segments pretreated at 700 ppm CO₂ (Figs. 4-5 and 7). These results suggested that the mesophyll signals inducing stomatal opening or closure were accumulated in the mesophyll in response to environmental stimuli and the effect of the mesophyll signals lasted for several hours. In summary, I could further confirm the presence of mesophyll signals.

Characteristics of the mesophyll signals

Mesophyll signals have been proposed to be aqueous (Lee & Bowling, 1992, 1993, 1995). Consistent with these studies, metabolites of photosynthesis and chloroplastic ATP, zeaxanthin, NADPH and RuBP have been hypothesized to be the mesophyll signals (Wong *et al.*, 1979; Farquhar & Wong, 1984; Grantz & Schwartz, 1988; Zeiger & Zhu, 1998; Tominaga *et al.*, 2001; Buckley *et al.*, 2003). Contrary to these hypothesis, Mott *et al.* (2013) claimed that the mesophyll signals should be vapor phase ions.

In chapter 3, the polyethylene or cellophane films were inserted between the epidermal

strips and the mesophyll segments. Aqueous substances would move across the cellophane films and not across the polyethylene films. Since the stomatal responses in the epidermal strips were accelerated when the cellophane films were inserted, the mesophyll signals should be aqueous. In order to estimate the molecular size of mesophyll signals, the dialysis membranes were inserted between the epidermal strips and the mesophyll segments. When the MWCO 100–500 D dialysis membranes were inserted, the stomatal opening at 100 ppm CO₂ remained to be induced and the stomatal closure was inhibited especially in white light (Fig. 3-5). Therefore, the range of the molecular size was estimated to be less than 500 D for the stomatal opening and 100 D–1,000 D for the stomatal closure.

In addition to these findings, I analyzed the dependency on photosynthesis in stomatal responses. It has been proposed that the stomatal opening especially in red light are dependent on photosynthesis (e.g. Sharkey & Raschke, 1981; Wang *et al.*, 2011) and while, my study was the first to analyze the dependence on photosynthesis of the stomatal closure. It was shown that the stomatal opening at 100 ppm CO₂ was strongly dependent on mesophyll photosynthesis and this result was consistent with the previous studies (Fig. 2-9 and Fig. 3-3). However, the stomatal closure at 700 ppm CO₂ was hardly dependent on photosynthesis in mesophyll and guard cells (Fig. 2-9 and Fig. 3-3). It was suggested that the mesophyll signals inducing the stomatal opening were different from those inducing the stomatal closure.

Candidates of the mesophyll signals

From the molecular size of the mesophyll signals, proteins were excluded from the candidates. In both stomatal opening and closure, mesophyll signals were less than 1,000 D. In the case that the mesophyll signals are consisted of amino acids, the mesophyll signals could be the peptide including less than 4 amino acids.

In chapter 3, I quantified the metabolites in the epidermal strips to narrow down the candidates of the mesophyll signals. Malate (M.W. 134.1), citrate (M.W. 192.1), fumarate (M.W. 116.1) and *cis*-aconitate (M.W. 174.1) were considered to be the possible mesophyll signals inducing the stomatal opening in RL (Fig. 3-6). The molecular size of these metabolites were within the range of the estimated molecular size (Fig. 3-5). I analyzed the stomatal responses to malate, citrate and fumarate, and it was suggested that only citrate had the potential to induce the stomatal opening (Fig. 3-7). In *Arabidopsis thaliana* and *Nicotiana tabacum*, citrate

accumulated during the dark period and decreased during the light period (Scheible *et al.*, 2000; Watanabe *et al.*, 2014). In contrast, malate and fumarate decreased during the dark period and accumulated in the light period (Scheible *et al.*, 2000; Watanabe *et al.*, 2014). Citrate might accelerate the stomatal opening in the morning to obtain CO₂ for photosynthesis. When the light intensity become weaker around the evening, malate and fumarate accumulated in the leaves might accelerate the stomatal closure to prevent the loss of water. I compared the metabolites in the epidermal strips placed directly on the gels and those touched on the mesophyll segments. As pointed out in chapter 4, there is a possibility that the metabolic activities in the epidermal strips were repressed by the buffer in the gels. Therefore, the results from the present metabolome would be crude.

Among the candidate metabolites of the mesophyll signals, malate and fumarate have been proposed to control stomatal responses. Araújo *et al.* (2011) suggested that malate and fumarate from the mesophyll inhibited the stomatal opening, using the antisense transgenic plants with reduced expression of SDH2-2 in *Solanum lycopersicum*. Consistently with Araújo *et al.* (2011), malate and fumarate induced stomatal closure (Fig. 3-7). Contrary to these findings, Lee *et al.* (2008) showed that the enhanced influx of malate from the apoplast to guard cells induced stomatal opening. All these together, I hypothesize that malate accumulated in the apoplast around guard cells stimulates the stomatal closure and malate accumulated in the guard cells induce the stomatal opening. Hence, I prospect that the stomatal opening would be observed when the malate influx into the guard cells exceeds the malate supply into the apoplast around the guard cells.

ABA (M.W. 264.3) is one of the candidates of the mesophyll signals that might induce stomatal closure. Carbonic anhydrase catalyzes the reversible reaction of $\text{CO}_2 + \text{H}_2\text{O} \leftrightarrow \text{H}^+ + \text{HCO}_3^-$. This enzyme are also present in mesophyll cells (Badger & Price, 1994). When ambient CO₂ concentrations are high, CO₂ concentrations in mesophyll cells inevitably increase. Then, the equilibrium favors the production of H⁺ and HCO₃⁻. Thus, the pH inside the mesophyll cells becomes more acidic. Under these acidic conditions, ABA would exist in its uncharged form (ABAH), which is able to diffuse across the cell membrane (Slovik *et al.*, 1992). Therefore, when CO₂ concentrations are high, ABA would be released from the mesophyll. Thus, ABA moves from the mesophyll to the guard cells, in turn inducing stomatal closure.

In addition to metabolites and hormones, carbohydrates are also considered to be the

substances controlling the stomatal movements (e.g. Outlaw & De Vlieghere-He, 2001; Kang *et al.*, 2007). I have not quantified the carbohydrates yet. The analysis of carbohydrates would be required.

Future prospects

Mesophyll signals must be present in the apoplast of both the mesophyll and the epidermis. Therefore, it would be necessary to collect the apoplastic fluid from the cell walls of the mesophyll. I challenged to construct the bioassay method in which I supposed to detect the mesophyll signals with the observation of stomatal movements. However, the amount of collected apoplastic fluid was too small. For example, I could collect less than 1 μL of the crude apoplastic fluid from an epidermal strip (10 mm \times 10 mm) by centrifugation. When these fluids were applied to the epidermal strips, the stomata did not move. Thus, I challenged to detect the mesophyll signals with the higher sensitivity. As described in chapter 5, I could analyze the phosphorylation levels of the plasma membrane H^+ -ATPase in *C. communis*. The present results suggested that stomata open widely in red light when the mesophyll signals are supplied (Fig. 2-9a, b and c). It is probable that the plasma membrane H^+ -ATPase is phosphorylated by the mesophyll signals in RL.

To analyze the ingredients in the mesophyll apoplastic fluid, I also consider to collect the apoplastic fluid by washing the mesophyll segments in the distilled water. The washing method might be technically easier than the collection of the crude apoplastic fluid. The collected solution is expected to be the mesophyll apoplastic fluid with the contamination of the xylem sap and the cell content from the damaged cells at the edge of the mesophyll segments. When the leaves are illuminated with light at 390 ppm CO_2 , the apoplastic mesophyll signals inducing the stomatal opening would be released from the mesophyll. In contrast, these signals would not be released in the dark. Only the amount of the ingredients in the mesophyll apoplastic fluid is expected to change dependent on the light conditions. Therefore, the candidates of the mesophyll signals would be narrowed down by analyzing the difference between the amount of the metabolites from the light-treated mesophyll and that from the dark-treated mesophyll. Mesophyll signals related to the stomatal closure at high CO_2 would be also estimated in a similar way. After narrowing down the mesophyll signals, it would be required to analyze the stomatal responses to the candidates of the mesophyll signals. For the identification of the

mesophyll signals, it will be also required to measure the concentration of these substances in the guard cell apoplast and ensure the movement of the candidates from the mesophyll to the epidermis.

Conclusions

The aim of this study was to reveal the roles of the mesophyll in controlling stomatal responses. It was confirmed that the mesophyll controlled both stomatal opening and closure in response to CO₂. It was suggested that mesophyll released apoplastic ‘mesophyll signals’ that accelerated the stomatal responses. Mesophyll signals involved in the stomatal responses at low CO₂ were different from those functioning at high CO₂, since the stomatal opening at low CO₂ was strongly dependent on photosynthesis and the stomatal closure was not. The molecular size of mesophyll signals for the stomatal opening was estimated to be less than 500 D, and those for the stomatal closure was 100 D–1,000 D. From the analysis of metabolites, malate, citrate and fumarate were listed as the candidates of mesophyll signals related to stomatal opening in RL. From the analysis of stomatal responses, only citrate had the potential to induce the stomatal opening. For the identification of the mesophyll signals, further studies are required.

References

- Allen GJ, Chu SP, Harrington CL, Schumacher K, Hoffmann T, Tang YY, Grill E, Schroeder JI. 2001. A defined range of guard cell calcium oscillation parameters encodes stomatal movements. *Nature* **411**: 1053–1057.
- Amodeo G, Talbott LD, Zeiger E. 1996. Use of potassium and sucrose by onion guard cells during a daily cycle of osmoregulation. *Plant & Cell Physiology* **37**: 575–579.
- Araújo WL, Nunes-Nesi A, Fernie AR. 2013. On the role of plant mitochondrial metabolism and its impact on photosynthesis in both optimal and sub-optimal growth conditions. *Photosynthesis Research* **119**: 141–156.
- Araújo WL, Nunes-Nesi A, Osorio S, Usadel B, Fuentes D, Nagy R, Balbo I, Lehmann M, Studart-Witkowski C, Tohge T, Martinoia E, Jordana X, DaMatta FM, Fernie AR. 2011. Antisense inhibition of the iron-sulphur subunit of succinate dehydrogenase enhances photosynthesis and growth in tomato via an organic acid-mediated effect on stomatal aperture. *The Plant Cell* **23**: 600–627.
- Asai N, Nakajima N, Tamaoki M, Kamada H, Kondo N. 2000. Role of malate synthesis mediated by phosphoenolpyruvate carboxylase in guard cells in the regulation of stomatal movement. *Plant & Cell Physiology* **41**: 10–15.
- Assmann SM, Simoncini L, Schroeder JI. 1985. Blue light activates electrogenic ion pumping in guard cell protoplasts of *Vicia faba*. *Nature* **318**: 285–287.
- Allaway WG, and Setterfield G. 1972. Ultrastructural observations on guard cells of *Vicia faba* and *Allium porrum*. *Canadian Journal of Botany* **50**: 1405–1413.
- Azoulay-Shemer T, Palomares A, Bagheri A, Israelsson-Nordstrom M, Engineer CB, Bargmann BOR, Stephan AB, Schroeder JI. 2015. Guard cell photosynthesis is critical for stomatal turgor production, yet does not directly mediate CO₂- and ABA-induced stomatal closing. *The Plant Journal* **83**: 567–581.
- Badger M, Price GD. 1994. The role of carbonic anhydrase in photosynthesis. *Annual Review of Plant Physiology and Plant Molecular Biology* **45**: 369–392.
- Bates GW, Rosenthal DM, Sun J, Chattopadhyay M, Peffer E, Yang J, Ort DR, Jones AM. 2012. A comparative study of the *Arabidopsis thaliana* guard-cell transcriptome and its modulation by sucrose. *PLOS ONE* **7**: e49641.

- Boller T, Kende H. 1980.** Regulation of wound ethylene synthesis in plants. *Nature* **286**: 259–260.
- Bowling DJF. 1987.** Measurement of the apoplastic activity of K⁺ and Cl⁻ in the leaf epidermis of *Commelina communis* in relation to stomatal activity. *Journal of Experimental Botany* **38**: 1351–1355.
- Brearley J, Venis MA, Blatt MR. 1997.** The effect of elevated CO₂ concentrations on K⁺ and anion channels of *Vicia faba* L. guard cells. *Planta* **203**: 145–154.
- Brodribb TJ, McAdam SAM. 2011.** Passive origins of stomatal control in vascular plants. *Science* **331**: 582–585.
- Buckley TN, Mott KA, Farquhar GD. 2003.** A hydromechanical and biochemical model of stomatal conductance. *Plant, Cell & Environment* **26**: 1767–1785.
- Busch FA. 2014.** Opinion: The red-light response of stomatal movement is sensed by the redox state of the photosynthetic electron transport chain. *Photosynthesis Research* **119**: 131–140.
- Cardon ZG, Berry J. 1992.** Effects of O₂ and CO₂ concentration on the steady-state fluorescence yield of single guard cell pairs in intact leaf discs of *Tradescantia albiflora*: Evidence for Rubisco-mediated CO₂ fixation and photorespiration in guard cells. *Plant Physiology* **99**: 1238–1244.
- Chater C, Peng K, Movahedi M, Dunn JA, Walker HJ, Liang YK, McLachlan DH, Casson S, Isner JC, Wilson I, Neill SJ, Hedrich R, Gray JE, Hetherington AM. 2015.** Elevated CO₂-induced responses in stomata require ABA and ABA signaling. *Current Biology* **25**: 2709–2716.
- De Angeli A, Zhang J, Meyer S, Martinoia E. 2013.** AtALMT9 is a malate-activated vacuolar chloride channel required for stomatal opening in *Arabidopsis*. *Nature Communications* **4**: 1–10.
- De Silva DLR, Hetherington AM, Mansfield TA. 1985.** Synergism between calcium ions and abscisic acid in preventing stomatal opening. *New Phytologist* **100**: 473–482.
- Desikan R, Last K, Harrett-Williams R, Tagliavia C, Harter K, Hooley R, Hancock JT, Neill SJ. 2006.** Ethylene-induced stomatal closure in *Arabidopsis* occurs via AtrbohF-mediated hydrogen peroxide synthesis. *The Plant Journal* **47**: 907–916.
- Doi M, Shimazaki K. 2008.** The stomata of the fern *Adiantum capillus-veneris* do not respond

- to CO₂ in the dark and open by photosynthesis in guard cells. *Plant Physiology* **147**: 922–930.
- Edwards MC, Smith GN, Bowling DJF. 1988.** Guard cells extrude protons prior to stomatal opening—A study using fluorescence microscopy and pH micro-electrodes. *Journal of Experimental Botany* **39**: 1541–1547.
- Ewert MS, Outlaw WH, Zhang S, Aghoram K, Riddle K. 2000.** Accumulation of an apoplastic solute in the guard-cell wall is sufficient to exert a significant effect on transpiration in *Vicia faba* leaflets. *Plant, Cell & Environment* **23**: 195–203.
- Fabre N, Reiter IM, Becuwe-Linka N, Genty B, Rumeau D. 2007.** Characterization and expression analysis of genes encoding α and β carbonic anhydrases in *Arabidopsis*. *Plant, Cell & Environment* **30**: 617–629.
- Farquhar GD, Wong SC. 1984.** An empirical model of stomatal conductance. *Australian Journal of Plant Physiology* **11**: 191–210.
- Fernie AR, Martinoia E. 2009.** Malate. Jack of all trades or master of a few? *Phytochemistry* **70**: 828–832.
- Fitzsimons PJ, Weyers JDB. 1983.** Separation and purification of protoplast types from *Commelina communis* L. leaf epidermis. *Journal of Experimental Botany* **34**: 55–66.
- Franks PJ, Farquhar GD. 2007.** The mechanical diversity of stomata and its significance in gas-exchange control. *Plant Physiology* **143**: 78–87.
- Gotow K, Taylor S, Zeiger E. 1988.** Photosynthetic carbon fixation in guard cell protoplasts of *Vicia faba* L. *Plant Physiology* **86**: 700–705.
- Grabov A, Blatt MR. 1998.** Membrane voltage initiates Ca²⁺ waves and potentiates Ca²⁺ increases with abscisic acid in stomatal guard cells. *Proceedings of the National Academy of Sciences, U.S.A.* **95**: 4778–4783.
- Granot D, David-Schwartz R, Kelly G. 2013.** Hexose kinases and their role in sugar-sensing and plant development. *Frontiers in Plant Science* **4**: 44.
- Grantz DA, Schwartz A. 1988.** Guard cells of *Commelina communis* L. do not respond metabolically to osmotic stress in isolated epidermis: Implications for stomatal responses to drought and humidity. *Planta* **174**: 166–173.
- Hanstein SM, Felle HH. 2002.** CO₂-triggered chloride release from guard cells in intact fava bean leaves. Kinetics of the onset of stomatal closure. *Plant Physiology* **130**: 940–950.

- Hashimoto M, Negi J, Young J, Israelsson M, Schroeder JI, Iba K. 2006.** *Arabidopsis* HT1 kinase controls stomatal movements in response to CO₂. *Nature Cell Biology* **8**: 391–397.
- Hayashi M, Inoue SI, Takahashi K, Kinoshita T. 2011.** Immunohistochemical detection of blue light-induced phosphorylation of the plasma membrane H⁺-ATPase in stomatal guard cells. *Plant & Cell Physiology* **52**: 1238–1248.
- Hayashi Y, Nakamura S, Takemiya A, Takahashi Y, Shimazaki KI, Kinoshita T. 2010.** Biochemical characterization of in vitro phosphorylation and dephosphorylation of the plasma membrane H⁺-ATPase. *Plant & Cell Physiology* **51**: 1186–1196.
- Hedrich R, Marten I. 1993.** Malate-induced feedback regulation of plasma membrane anion channels could provide a CO₂ sensor to guard cells. *EMBO Journal* **12**: 897–901.
- Hedrich R, Marten I, Lohse G, Dietrich P, Winter H, Lohaus G, Heldt HW. 1994.** Malate-sensitive anion channels enable guard cells to sense changes in the ambient CO₂ concentration. *The Plant Journal* **6**: 741–748.
- Hennessey TL, Freeden AL, Field CB. 1993.** Environmental effects on circadian rhythms in photosynthesis and stomatal opening. *Planta* **189**: 369–376.
- Hipkins MF, Fitzsimons PJ, Weyers JDB. 1983.** The primary processes of photosystem II in purified guard-cell protoplasts and mesophyll-cell protoplasts from *Commelina communis* L. *Planta* **159**: 554–560.
- Hsiao TC, Allaway WG. 1973.** Action spectra for guard cell Rb⁺ uptake and stomatal opening in *Vicia faba*. *Plant Physiology* **51**: 82–88.
- Hu H, Boisson-Dernier A, Israelsson-Nordström M, Böhmer M, Xue S, Ries A, Godoski J, Kuhn JM, Schroeder JI. 2010.** Carbonic anhydrases are upstream regulators of CO₂-controlled stomatal movements in guard cells. *Nature Cell Biology* **12**: 87–93.
- Hu H, Rappel W-J, Occhipinti R, Ries A, Böhmer M, You L, Xiao C, Engineer CB, Boron WF, Schroeder JI. 2015.** Distinct cellular locations of carbonic anhydrases mediate carbon dioxide control of stomatal movements. *Plant Physiology* **169**: 1168–1178.
- Hubbard KE, Siegel RS, Valerio G, Brandt B, Schroeder JI. 2012.** Abscisic acid and CO₂ signalling via calcium sensitivity priming in guard cells, new CDPK mutant phenotypes and a method for improved resolution of stomatal stimulus-response analyses. *Annals of Botany* **109**: 5–17.
- Iino M, Ogawa T, Zeiger E. 1985.** Kinetic properties of the blue-light response of stomata.

Proceedings of the National Academic Sciences, U.S.A. **82**: 8019–8023.

- Jahn T, Fuglsang AT, Olsson A, Brüntrup IM, Collinge DB, Volkmann D, Sommarin M, Palmgren MG, Larsson C. 1997.** The 14-3-3 protein interacts directly with the C-terminal region of the plant plasma membrane H⁺-ATPase. *The Plant Cell* **9**: 1805–1814.
- Kang Y, Outlaw WH, Andersen PC, Fiore GB. 2007.** Guard-cell apoplastic sucrose concentration—a link between leaf photosynthesis and stomatal aperture size in the apoplastic phloem loader *Vicia faba* L. *Plant, Cell & Environment* **30**: 551–558.
- Kelly G, David-Schwartz R, Sade N, Moshelion M, Levi A, Alchanatis V, Granot D. 2012.** The pitfalls of transgenic selection and new roles of *AtHXK1*: a high level of *AtHXK1* expression uncouples hexokinase1-dependent sugar signaling from exogenous sugar. *Plant Physiology* **159**: 47–51.
- Kelly G, Moshelion M, David-Schwartz R, Halperin O, Wallach R, Attia Z, Belausov E, Granot D. 2013.** Hexokinase mediates stomatal closure. *The Plant Journal* **75**: 977–988.
- Kim TH, Böhmer M, Hu H, Nishimura N, Schroeder JI. 2010.** Guard cell signal transduction network: Advances in understanding abscisic acid, CO₂, and Ca²⁺ signaling. *Annual Review of Plant Biology* **61**: 561–591.
- Kinoshita T, Doi M, Suetsugu N, Kagawa T, Wada M, Shimazaki K. 2001.** PHOT1 and PHOT2 mediate blue light regulation of stomatal opening. *Nature* **414**: 656–660.
- Kinoshita T, Shimazaki K. 1999.** Blue light activates the plasma membrane H⁺-ATPase by phosphorylation the C-terminus in stomatal guard cells. *The EMBO Journal* **18**: 5548–5558.
- Kinoshita T, Shimazaki K. 2002.** Biochemical evidence for the requirement of 14-3-3 protein binding in activation of the guard-cell plasma membrane H⁺-ATPase by blue light. *Plant & Cell Physiology* **43**: 1359–1365.
- Klüsener B, Young JJ, Murata Y, Allen GJ, Mori IC, Hugouvieux V, Schroeder JI. 2002.** Convergence of calcium signaling pathways of pathogenic elicitors and abscisic acid in *Arabidopsis* guard cells. *Plant Physiology* **130**: 2152–2163.
- Kollist H, Nuhkat M, Roelfsema MRG. 2014.** Closing gaps: linking elements that control stomatal movement. *New Phytologist* **203**: 44–62.
- Koornneef M, Reuling G, Karssen CM. 1984.** The isolation and characterization of abscisic acid-insensitive mutants of *Arabidopsis thaliana*. *Physiologia Plantarum* **61**: 377–383.

- Kuiper PJC. 1964.** Dependence upon wavelength of stomatal movement in epidermal tissue of *Senecio odoris*. *Plant Physiology* **39**: 952–955.
- Lambers H, Chapin III FS, Pons TL. 2008.** *Plant Physiological Ecology* Second edition. New York, U.S.A.: Springer-Verlag.
- Lawson T, Oxborough K, Morison JIL, Baker NR. 2002.** Responses of photosynthetic electron transport in stomatal guard cells and mesophyll cells in intact leaves to light, CO₂, and humidity. *Plant Physiology* **128**: 52–62.
- Lawson T, Oxborough K, Morison JIL, Baker NR. 2003.** The responses of guard and mesophyll cell photosynthesis to CO₂, O₂, light, and water stress in a range of species are similar. *Journal of Experimental Botany* **54**: 1743–1752.
- Lawson T. 2009.** Guard cell photosynthesis and stomatal function. *New Phytologist* **181**: 13–34.
- Lee J, Bowling DJF. 1992.** Effect of the mesophyll on stomatal opening in *Commelina communis*. *Journal of Experimental Botany* **43**: 951–957.
- Lee J, Bowling DJF. 1993.** The effect of a mesophyll factor on the swelling of guard cell protoplasts of *Commelina communis* L. *Journal of Plant Physiology* **142**: 203–207.
- Lee J, Bowling DJF. 1995.** Influence of the mesophyll on stomatal opening. *Australian Journal of Plant Physiology* **22**: 357–363.
- Lee M, Choi Y, Burla B, Kim YY, Jeon B, Maeshima M, Yoo JY, Martinoia E, Lee Y. 2008.** The ABC transporter AtABCB14 is a malate importer and modulates stomatal response to CO₂. *Nature Cell Biology* **10**: 1217–1223.
- Leymarie J, Vavasseur A, Lascève G. 1998.** CO₂ sensing in stomata of *abi1-1* and *abi2-1* mutants of *Arabidopsis thaliana*. *Plant Physiology and Biochemistry* **36**: 539–543.
- Lu P, Outlaw Jr. WH, Smith BG, Freed GA. 1997.** A new mechanism for the regulation of stomatal aperture size in intact leaves (accumulation of mesophyll-derived sucrose in the guard-cell wall of *Vicia faba*). *Plant Physiology* **114**: 109–118.
- Lu P, Zhang SQ, Outlaw WH, Riddle K. 1995.** Sucrose: a solute that accumulates in the guard-cell apoplast and guard-cell symplast of open stomata. *FEBS letters* **362**: 180–184.
- Lurie S. 1977.** Photochemical properties of guard cell chloroplasts. *Plant Science Letters* **10**: 219–223.
- MacRobbie EAC, Lettau J. 1980a.** Ion content and aperture in ‘isolated’ guard cells of

- Commelina communis* L. *Journal of Membrane Biology* **53**: 199–205.
- Macrobbie EAC, Lettau J. 1980b.** Potassium content and aperture in ‘intact’ stomatal and epidermal cells of *Commelina communis* L. *Journal of Membrane Biology* **56**: 249–256.
- Marten H, Hedrich R, Roelfsema MRG. 2007.** Blue light inhibits guard cell plasma membrane anion channels in a phototropin-dependent manner. *The Plant Journal* **50**: 29–39.
- Marten H, Hyun T, Gomi K, Seo S, Hedrich R, Roelfsema MRG. 2008.** Silencing of *NtMPK4* impairs CO₂-induced stomatal closure, activation of anion channels and cytosolic Ca²⁺ signals in *Nicotiana tabacum* guard cells. *The Plant Journal* **55**: 698–708.
- Martin ES, Meidner H. 1971.** Endogenous stomatal movements in *Tradescantia virginiana*. *New Phytologist* **70**: 923–928.
- Matrosova A, Bogireddi H, Mateo-Peñas A, Hashimoto-Sugimoto M, Iba K, Schroeder JI, Israelsson-Nordström M. 2015.** The HT1 protein kinase is essential for red light-induced stomatal opening and genetically interacts with OST1 in red light and CO₂-induced stomatal movement responses. *New Phytologist* **208**: 1126–1137.
- Mawson BT. 1993.** Regulation of blue-light-induced proton pumping by *Vicia faba* L. guard-cell protoplasts: Energetic contributions by chloroplastic and mitochondrial activities. *Planta* **191**: 293–301.
- McAdam SAM, Brodribb TJ. 2012.** Fern and lycophyte guard cells do not respond to endogenous abscisic acid. *The Plant Cell* **24**: 1510–1521.
- McAinsh MR, Webb AAR, Taylor JE, Hetherington AM. 1995.** Stimulus-induced oscillation in guard cell cytosolic free calcium. *The Plant Cell* **7**: 1207–1219.
- Merilo E, Laanemets K, Hu H, Xue S, Jakobson L, Tulva I, Gonzalez-Guzman M, Rodriguez PL, Schroeder JI, Broschè M, Kollist H. 2013.** PYR/RCAR receptors contribute to ozone-, reduced air humidity-, darkness-, and CO₂-induced stomatal regulation. *Plant Physiology* **162**: 1652–1668.
- Merritt F, Kemper A, Tallman G. 2001.** Inhibitors of ethylene synthesis inhibit auxin-induced stomatal opening in epidermis detached from leaves of *Vicia faba* L. *Plant & Cell Physiology* **42**: 223–230.
- Messinger SM, Buckley TN, Mott KA. 2006.** Evidence for involvement of photosynthetic processes in the stomatal response to CO₂. *Plant Physiology* **140**: 771–778.

- Meyer S, Mumm P, Imes D, Endler A, Weder B, Al-Rasheid KAS, Geiger D, Marten I, Martinoia E, Hedrich R. 2010.** *AtALMT12* represents an R-type anion channel required for stomatal movement in *Arabidopsis* guard cells. *The Plant Journal* **63**: 1054–1062.
- Moore B, Zhou L, Rolland F, Hall Q, Cheng W-H, Liu Y-X, Hwang I, Jones T, Sheen J. 2003.** Role of the *Arabidopsis* glucose sensor *HXK1* in nutrient, light, and hormonal signaling. *Science* **300**: 332–336.
- Moroney J V., Bartlett SG, Samuelsson G. 2001.** Carbonic anhydrases in plants and algae. *Plant, Cell & Environment* **24**: 141–153.
- Mott KA, Sibbersen ED, Shope JC. 2008.** The role of the mesophyll in stomatal responses to light and CO₂. *Plant, Cell & Environment* **31**: 1299–1306.
- Mott KA, Berg DG, Hunt SM, Peak D. 2013.** Is the signal from the mesophyll to the guard cells a vapour-phase ion? *Plant, Cell & Environment* **2**: 1–8.
- Negi J, Matsuda O, Nagasawa T, Oba Y, Takahashi H, Kawai-Yamada M, Uchimiya H, Hashimoto M, Iba K. 2008.** CO₂ regulator SLAC1 and its homologues are essential for anion homeostasis in plant cells. *Nature* **452**: 483–486.
- Nelson SD, Mayo JM. 1975.** The occurrence of functional non-chlorophyllous guard cells in *Paphiopedilum* spp. *Canadian Journal of Botany* **53**: 1–7.
- Oecking C, Piotrowski M, Hagemeyer J, Hagemann K. 1997.** Topology and target interaction of the fusicoccin-binding 14-3-3 homologs of *Commelina communis*. *The Plant Journal* **12**: 441–453.
- Olsen RL, Pratt RB, Gump P, Kemper A, Tallman G. 2002.** Red light activates a chloroplast-dependent ion uptake mechanism for stomatal opening under reduced CO₂ concentrations in *Vicia* spp. *New Phytologist* **153**: 497–508.
- Outlaw WH, Lowry OH. 1977.** Organic acid and potassium accumulation in guard cells during stomatal opening. *Proceedings of the National Academy of Sciences, U.S.A.* **74**: 4434–4438.
- Outlaw WH, Manchester J. 1979.** Guard cell starch concentration quantitatively related to stomatal aperture. *Plant Physiology* **64**: 79–82.
- Outlaw WH, Tarczynski MC, Anderson LC. 1982.** Taxonomic survey for the presence of ribulose-1,5-bisphosphate carboxylase activity in guard cells. *Plant Physiology* **70**: 1218–1220.

- Outlaw WH, De Vlieghere-He X. 2001.** Transpiration rate. an important factor controlling the sucrose content of the guard cell apoplast of broad bean. *Plant Physiology* **126**: 1716–1724.
- Pearson CJ. 1973.** Daily changes in stomatal aperture and in carbohydrates and malate within epidermis and mesophyll of leaves of *Commelina cyanea* and *Vicia faba*. *Australian Journal of Biological Sciences* **28**: 1035–1044.
- Pemadasa MA. 1981.** Abaxial and adaxial stomatal behaviour and responses to fusicoccin on isolated epidermis of *Commelina communis* L. *New Phytologist* **89**: 373–384.
- Raschke K. 1975.** Simultaneous requirement of carbon dioxide and abscisic acid for stomatal closing in *Xanthium strumarium* L. *Planta* **125**: 243–259.
- Raschke K, Dittrich P. 1977.** [¹⁴C]Carbon-dioxide fixation by isolated leaf epidermes with stomata closed or open. *Planta* **134**: 69–75.
- Reckmann U, Scheibe R, Raschke K. 1990.** Rubisco activity in guard cells compared with the solute requirement for stomatal opening. *Plant Physiology* **92**: 246–253.
- Regenberg B, Villalba JM, Lanfermeijer FC, Palmgren MG. 1995.** C-terminal deletion analysis of plant plasma membrane H⁺-ATPase: yeast as a model system for solute transport across the plant plasma membrane. *The Plant Cell* **7**: 1655–1666.
- Roelfsema MRG, Steinmeyer R, Staal M, Hedrich R. 2001.** Single guard cell recordings in intact plants: light-induced hyperpolarization of the plasma membrane. *The Plant Journal* **26**: 1–13.
- Roelfsema MRG, Hanstein S, Felle HH, Hedrich R. 2002.** CO₂ provides an intermediate link in the red light response of guard cells. *The Plant Journal* **32**: 65–75.
- Roelfsema MRG, Konrad KR, Marten H, Psaras GK, Hartung W, Hedrich R. 2006.** Guard cells in albino leaf patches do not respond to photosynthetically active radiation, but are sensitive to blue light, CO₂ and abscisic acid. *Plant, Cell & Environment* **29**: 1595–1605.
- Roelfsema MRG, Prins HBA. 1995.** Effect of abscisic acid on stomatal opening in isolated epidermal strips of *abi* mutants of *Arabidopsis thaliana*. *Physiologia Plantarum* **95**: 373–378.
- Rolland F, Baena-Gonzalez E, Sheen J. 2006.** Sugar sensing and signaling in plants: conserved and novel mechanisms. *Annual Review of Plant Biology* **57**: 675–709.
- Sattelmacher B. 2001.** The apoplast and its significance for plant mineral nutrition. *New*

- Phytologist* **149**: 167–192.
- Sato S, Soga T, Nishioka T, Tomita M. 2004.** Simultaneous determination of the main metabolites in rice leaves using capillary electrophoresis mass spectrometry and capillary electrophoresis diode array detection. *The Plant Journal* **40**: 151–163.
- Sato S, Yanagisawa S. 2010.** Capillary electrophoresis–electrospray ionization–mass spectrometry using fused-silica capillaries to profile anionic metabolites. *Metabolomics* **6**: 529–540.
- Scheible WR, Krapp A, Stitt M. 2000.** Reciprocal diurnal changes of phosphoenolpyruvate carboxylase expression and cytosolic pyruvate kinase, citrate synthase and NADP-isocitrate dehydrogenase expression regulate organic acid metabolism during nitrate assimilation in tobacco leaves. *Plant, Cell and Environment* **23**: 1155–1167.
- Schnabl H. 1980.** CO₂ and malate metabolism in starch-containing and starch-lacking guard-cell protoplasts. *Planta* **149**: 52–58.
- Schnabl H. 1981.** The compartmentation of carboxylating and decarboxylating enzymes in guard cell protoplasts. *Planta* **152**: 307–313.
- Schwartz A, Zeiger E. 1984.** Metabolic energy for stomatal opening. Roles of photophosphorylation and oxidative phosphorylation. *Planta* **161**: 129–136.
- Schwartz A. 1985.** Role of Ca²⁺ and EGTA on stomatal movements in *Commelina communis* L. *Plant Physiology* **79**: 1003–1005.
- Schwartz A, Ilan N, Grantz DA. 1988.** Calcium effects on stomatal movement in *Commelina communis* L. *Plant Physiology* **87**: 583–587.
- Sharkey TD, Raschke K. 1981.** Effect of light quality on stomatal opening in leaves of *Xanthium strumarium* L. *Plant Physiology* **68**: 1170–1174.
- Shimada K, Ogawa T, Shitbata K. 1979.** Isotachophoretic analysis of ions in guard cells of *Vicia faba*. *Physiologia Plantarum* **47**: 173–176.
- Shimazaki K, Iino M, Zeiger E. 1986.** Blue light-dependent proton extrusion by guard-cell protoplasts of *Vicia faba*. *Nature* **319**: 324–326.
- Shimazaki K, Doi M, Assmann SM, Kinoshita T. 2007.** Light regulation of stomatal movement. *Annual Review of Plant Biology* **58**: 219–247.
- Shimazaki K, Zeiger E. 1985.** Cyclic and noncyclic photophosphorylation in isolated guard cell chloroplasts from *Vicia faba* L. *Plant Physiology* **78**: 211–214.

- Sibbersen E, Mott KA. 2010.** Stomatal responses to flooding of the intercellular air spaces suggest a vapor-phase signal between the mesophyll and the guard cell. *Plant Physiology* **153**: 1435–1442.
- Siegel RS, Xue S, Murata Y, Yang Y, Nishimura N, Wang A, Schroeder JI. 2009.** Calcium elevation-dependent and attenuated resting calcium-dependent abscisic acid induction of stomatal closure and abscisic acid-induced enhancement of calcium sensitivities of S-type anion and inward-rectifying K channels in Arabidopsis guard cells. *The Plant Journal* **59**: 207–220.
- Slovik S, Baier M, Hartung W. 1992.** Compartmental distribution and redistribution of abscisic acid in intact leaves. *Planta* **187**: 14–25.
- Stadler R, Bu M, Ache P, Hedrich R, Ivashikina N, Melzer M, Shearson SM, Smith SM, Sauer N, Germany RS. 2003.** Diurnal and light-regulated expression of AtSTP1 in guard cells of Arabidopsis. *Plant Physiology* **133**: 528–537.
- Suetsugu N, Takami T, Ebisu Y, Watanabe H, Iiboshi C, Doi M, Shimazaki KI. 2014.** Guard cell chloroplasts are essential for blue light-dependent stomatal opening in Arabidopsis. *PLOS ONE* **9**: e108374.
- Talbott LD, Zeiger E. 1993.** Sugar and organic acid accumulation in guard cells of *Vicia faba* in response to red and blue light. *Plant Physiology* **102**: 1163–1169.
- Talbott LD, Zeiger E. 1998.** The role of sucrose in guard cell osmoregulation. *Journal of Experimental Botany* **49**: 329–337.
- Tallman G, Zeiger E. 1988.** Light quality and osmoregulation in *Vicia* guard cells. *Plant Physiology* **88**: 887–895.
- Taylor A, Assmann SM. 2001.** Apparent absence of a redox requirement for blue light activation of pump current in broad bean guard cells. *Plant Physiology* **125**: 329–338.
- Tian W, Hou C, Ren Z, Pan Y, Jia J, Zhang H, Bai F, Zhang P, Zhu H, He Y, Luo S, Li L, Luan S. 2015.** A molecular pathway for CO₂ response in *Arabidopsis* guard cells. *Nature Communications* **6**: 6057.
- Tominaga M, Kinoshita T, Shimazaki K. 2001.** Guard-cell chloroplasts provide ATP required for H⁺ pumping in the plasma membrane and stomatal opening. *Plant & Cell Physiology* **42**: 795–802.
- Travis AJ, Mansfield TA. 1979.** Stomatal responses to light and CO₂ are dependent on KCl

- concentration. *Plant, Cell & Environment* **2**: 319–323.
- Ueno K, Kinoshita T, Inoue SI, Emi T, Shimazaki KI. 2005.** Biochemical characterization of plasma membrane H⁺-ATPase activation in guard cell protoplasts of *Arabidopsis thaliana* in response to blue light. *Plant & Cell Physiology* **46**: 955–963.
- Vahisalu T, Kollist H, Wang Y-F, Nishimura N, Chan W-Y, Valerio G, Lamminmäki A, Brosché M, Moldau H, Desikan R, Schroeder JI, Kangasjärvi J. 2008.** SLAC1 is required for plant guard cell S-type anion channel function in stomatal signalling. *Nature* **452**: 487–491.
- Wang S-W, Li Y, Zhang X-L, Yang H-Q, Han X-F, Liu Z-H, Shang Z-L, Asano T, Yoshioka Y, Zhang C-G, Chen Y-L. 2014.** Lacking chloroplasts in guard cells of crumpled leaf attenuates stomatal opening: both guard cell chloroplasts and mesophyll contribute to guard cell ATP levels. *Plant, Cell & Environment* **37**: 2201–2210.
- Wang Y, Noguchi K, Terashima I. 2011.** Photosynthesis-dependent and -independent responses of stomata to blue, red and green monochromatic light: differences between the normally oriented and inverted leaves of sunflower. *Plant & Cell Physiology* **52**: 479–489.
- Watanabe CK, Sato S, Yanagisawa S, Uesono Y, Terashima I, Noguchi K. 2014.** Effects of elevated CO₂ on levels of primary metabolites and transcripts of genes encoding respiratory enzymes and their diurnal patterns in *Arabidopsis thaliana*: possible relationships with respiratory rates. *Plant & Cell Physiology* **55**: 341–357.
- Webb AAR, McAinsh MR, Mansfield TA, Hetherington AM. 1996.** Carbon dioxide induces increases in guard cell cytosolic free calcium. *The Plant Journal* **9**: 297–304.
- Webb AAR, Hetherington AM. 1997.** Convergence of the abscisic acid, CO₂, and extracellular calcium signal transduction pathways in stomatal guard cells. *Plant Physiology* **114**: 1557–1560.
- Weise A, Lalonde S, Kühn C, Frommer WB, Ward JM. 2008.** Introns control expression of sucrose transporter LeSUT1 in trichomes, companion cells and in guard cells. *Plant Molecular Biology* **68**: 251–262.
- Weyers JDB, Fitzsimons PJ, Mansey GM, Martin ES, Guard ES. 1983.** Guard cell protoplasts—Aspects of work with an important new research tool. *Physiologia Plantarum* **58**: 331–339.

- Wille A, Lucas W. 1984.** Ultrastructural and histochemical studies on guard cells. *Planta* **160**: 129–142.
- Willmer CM. 1988.** Stomatal sensing of the environment. *Biological Journal of the Linnean Society* **34**: 204–217.
- Willmer CM, Dittrich P. 1974.** Carbon dioxide fixation by epidermal and mesophyll tissues of *Tulipa* and *Commelina*. *Planta* **117**: 123–132.
- Willmer CM, Fricker MD. 1996.** *Stomata* 2nd edition. London, UK: Chapman & Hall.
- Wong SC, Cowan IR, Farquhar GD. 1979.** Stomatal conductance correlates with photosynthetic capacity. *Nature* **282**: 424–426.
- Xue S, Hu H, Ries A, Merilo E, Kollist H, Schroeder JI. 2011.** Central functions of bicarbonate in S-type anion channel activation and OST1 protein kinase in CO₂ signal transduction in guard cell. *The EMBO Journal* **30**: 1645–1658.
- Young JJ, Mehta S, Israelsson M, Godoski J, Grill E, Schroeder JI. 2006.** CO₂ signaling in guard cells: calcium sensitivity response modulation, a Ca²⁺-independent phase, and CO₂ insensitivity of the *gca2* mutant. *Proceedings of the National Academy of Sciences, U.S.A.* **103**: 7506–7511.
- Zeevaart JAD, Creelman RA. 1988.** Metabolism and physiology of abscisic acid. *Annual Review of Plant Physiology and Plant Molecular Biology* **39**: 439–473.
- Zeiger E. 1983.** The biology of stomatal guard cells. *Annual Review of Plant Physiology* **34**: 441–475.
- Zeiger E, Zhu JX. 1998.** Role of zeaxanthin in blue light photoreception and the modulation of light-CO₂ interactions in guard cells. *Journal of Experimental Botany* **49**: 433–442.

Acknowledgements

I would like to express my sincere gratitude to my advisor Professor Ichiro Terashima (The University of Tokyo) for his invaluable support, continuous guidance and encouragement throughout my study. He taught me the way to develop the novel methods. The skill must be required to overcome the difficult subject in the field where the tools for the analysis are undeveloped. I also express my special thanks to Professor Ko Noguchi (Tokyo University of Pharmacy and Life Sciences) for his valuable discussions and continuous encouragement.

Besides, I am grateful to Professor Hirokazu Tsukaya (The University of Tokyo), Associate Professor Munetaka Sugiyama (The University of Tokyo), Associate Professor Masaki Tateno (The University of Tokyo), and Associate Professor Manabu Yoshida (The University of Tokyo), the committee of my Ph.D. dissertation, for their helpful comments and suggestions.

I am also grateful to a lot of people except the people described above. Associate Professor Shuichi Yanagisawa (The University of Tokyo) permitted me to use CE-MS system in his laboratory. Group Director Hitoshi Sakakibara (RIKEN Plant Science Center) and Ms. Mikiko Kojima (RIKEN Plant Science Center) quantified the plant hormones. Professor Toshinori Kinoshita (Nagoya University) provided the antibodies to detect the plasma membrane H⁺-ATPase and gave the helpful advice. Ms. Maki Hayashi (Nagoya University) instructed the western blotting and the immunostaining method for the plasma membrane H⁺-ATPase in *Arabidopsis thaliana*. Associate Professor Yoshiji Okazaki (Osaka Medical College) instructed the electrophysiological technique to measure the apoplastic pH of guard cells and gave the invaluable advice. Associate Professor Izumi Mori (Okayama University) gave the technical and helpful advice, especially in the analysis of metabolites. Research Assistant Professor Takumi Higaki (The University of Tokyo) gave the technical advice to analyze the results of the immunostaining of guard cells. Mr. Shigemi Otsuka (The University of Tokyo) manufactured the condenser in the microscopic observation system. The members of Prof. Iba's laboratory (Kyushu University), Prof. Shimazaki's laboratory (Kyushu University) and Prof. Kinoshita's laboratory (Nagoya University) spent much time for the discussion and gave the invaluable advice about the stomatal physiology. I am grateful to all the members of Prof. Terashima's laboratory for their support and encouragement. I could spend precious time with them.

Finally, I thank my family in Hiroshima for their heartwarming support during my doctoral course. I could not continue my study without their support.

Takashi Fujita
December 2015, Tokyo, JAPAN